

0165

922
PL ISSN 0028-3894

ASSOCIATION OF POLISH
NEUROPATHOLOGISTS
and
MEDICAL RESEARCH CENTRE
POLISH ACADEMY OF SCIENCES

NEUROPATHOLOGIA POLSKA

348-

VOLUME 30

1992

NUMBER 3-4

WROCLAW · WARSZAWA · KRAKÓW
ZAKŁAD NARODOWY IM. OSSOLIŃSKICH
WYDAWNICTWO POLSKIEJ AKADEMII NAUK

<http://rcin.org.pl>

NEUROPATHOLOGIA POLSKA

QUARTERLY

VOLUME 30

1992

NUMBER 3-4

EDITORIAL COUNCIL

Maria Dąmbska, Jerzy Dymecki, Krystyna Honczarenko, Danuta Maślińska,
Mirosław J. Mossakowski, Halina Weinrauder

EDITORS

Editor-in-Chief: Irmina B. Zelman

Co-editors: Wiesława Biczyskova, Halina Kroh, Mirosław J. Mossakowski, Mieczysław Wender

Secretary: Anna Taraszewska

Technical Secretary: Teresa Miodowska

EDITORIAL OFFICE

Medical Research Centre

ul. Dworkowa 3, 00-784 Warszawa, Poland, Phone: 49-54-10

The typescript of the present issue was delivered to the publisher 28.12.1992 r.



IRENA HAUSMANOWA-PETRUSEWICZ

ROLE OF ELECTROMYOGRAPHY IN THE DIAGNOSIS OF MOTOR NEURON DISORDERS*

Neuromuscular Unit, Medical Research Centre, Polish Academy of Sciences, Warsaw

Programming of electromyographic examination in motor neuron diseases is discussed taking into account application of appropriate techniques. The difficulties of correct interpretation of results are stressed. The stages of disintegration and reintegration of affected motor units are described as well as compensatory changes of surviving motor units. A detailed description of EMG dynamics of amyotrophic lateral sclerosis, late post-polio syndrome and of childhood spinal muscular atrophy is given.

Key words: *motor neuron diseases, electromyography, motor unit, amyotrophic lateral sclerosis, post-polio syndrome, spinal atrophy.*

Electromyography is one of the main laboratory techniques contributing to the diagnosis of motor neuron disorders (MND) (Swash, Schwartz 1982; Mulder 1984; Bebhia, Kelly 1991). At the same time, electromyographic findings, even those received during routine work, are of great importance for our knowledge of motor neuron physiology (Stålberg, Ekstedt 1973; Carleton, Brown 1979; Brown 1984; Stålberg, Sanders 1984; Stålberg et al. 1986). Of course it concerns mainly the quantified electromyography introduced by Buchthal (Buchthal, Pinelli 1953; Erminio et al. 1959). Since this time the basic significance of the parameters he introduced has not changed very much, however, the new techniques including computer-aided ones, permitted to extend the parameters which characterize individual motor units and their population (Stålberg, Ekstedt 1973).

The introduction of new techniques, beside technical progress, means also a possibility of learning about such properties of motor unit potentials (MUPs) which were not measurable by the previous techniques, this adding new data, important both for research and for increasing the diagnostic yield. Some

* Presented at the workshop on Motor Neuron Disorders during International Congress of EMG, Jerusalem, June 1992.

properties of motor units (MUs) are measurable with classic technique and others require special techniques (Dorfman, Kevin 1988).

Examining a case suspected to be a motor neuron disorder, we have to: 1) programming the relevant EMG examination, 2) performing this examination with appropriate techniques, and 3) discuss the interpretation of the results.

The term „motor neuron disease” which is entirely inappropriate as clinical diagnosis, is an ideal term in electromyography – here we do not try to make a nosological diagnosis. Just what we want is to emphasize the affected motor neuron, which is the common denominator of all of these disorders of various clinical features.

From among many so called motor neuron disorders – focal and diffuse (Table 1) only three have been chosen for the following reasons: they are most important in the practice of a clinical electromyographer, on the one hand, and on the other some of these disorders may serve as models of motor unit (MU) disintegration as sequelae of denervation and also of reintegration of the MU as a consequence of reinnervation.

Table 1. Main motoneuron diseases in adult

Amyotrophic lateral sclerosis
Polio
Late post-polio syndrome
Spinal atrophies
Syringomyelia
Jakob-Creutzfeldt disease
Toxic
Post-radiation syndrome

We will discuss: 1) Amyotrophic lateral sclerosis (ALS) – the disease attracting most the attention of neurologists and electromyographers as a model of the progressing process and fast disintegration of the MU with an unstable and short period of reintegration; 2) Late post-polio syndrome as an example of late decompensation of a previously reintegrated MU; 3) Chronic benign spinal muscular atrophy (SMA) as an example of more stabilized remodelling of the MU. Also the differences between this form of SMA and the acute infantile one will be briefly mentioned.

The referring physician asks the electromyographer for confirmation of his clinical diagnosis or its rejection, correction and/or possible new suggestions. Electromyography is a part of neurological examination, therefore it should be involved in all kinds of these answers.

AMYOTROPHIC LATERAL SCLEROSIS (ALS)

- Planning of EMG examination
- Applied methods
- Interpretation of results
- Role of conduction velocity measurement

We have to decide first of the muscles to be tested – usually they should be three, innervated by different, possibly distant motor roots and different nerves. It is recently suggested that if we have, for different reasons, the possibility to test only one muscle in early ALS, it should be the thoracic paraspinal one (Kund et al. 1988).

Then with the use of the most commonly applied concentric needle electrodes for the quantification technique (Daube 1982) we should answer whether:

- 1) is the EMG record abnormal,
- 2) if so, is it neurogenic,
- 3) if so, is it indicative of spinal involvement (using e.g. criteria of Buchthal and Kamieniecka (1982)),
- 4) how severe is the process?
- 5) how rapid is the process?
- 6) which stage of the process are we recording in different muscles?
- 7) what possible compensatory mechanisms are at work? and which complementary techniques should we use to learn the precise fibers distribution within the MU (Stålberg, Ekstedt 1973; Stålberg, Sanders 1984; Stålberg et al. 1986).

In ALS we must assume that we are always missing the real onset of the disease (Lambert 1969; Mulder 1984) – the process is subclinical before wasting and weakness appear, till the loss of 30% or even 50% of MUs occurs. And at this stage the earliest denervation and reinnervation takes place. However, because of uneven intensity of affection of the muscles, we have the opportunity to follow in the course of the disease the process from the very beginning in some later affected muscles (Farago, Hausmanowa-Petrusewicz 1977; Munsat et al. 1988). One of the first signs might be poor recruitment with increased firing rate (even up to 50 c/s). Recruitment is characterized by the ratio of the rate of firing MU to the number of MUs being active. Recruitment frequency (rate of firing of one MU when the next is recruited) and MUs counting would be the appropriate method at this stage (McComas 1977; Daube 1982). In practice, unless for special purpose, they are not very largely used. In practice more easy is evaluation of the interference pattern (IP) by evaluation of the relationship between amplitude and turns (e.g. cloud, banana-shaped clusters) (Stålberg, Sanders 1984; Gilai 1989). Signs indicative of neurogenic character might be observed.

The greatest emphasis is in practice placed on the characteristic of MUPs and reorganization of MUs at different disease stages. There is an informal consensus among electromyographers that the most important parameters are duration, amplitude, complexity and variability (Dorfman, Kevin 1988).

Remodelling passes through three stages: 1) temporary denervation with high, short potentials – the size of MU is decreased, increased fibers density can be already observed; 2) effective compensatory reinnervation with enlargement of the surviving MUs, biopsy shows at this stage the grouping of

muscle fibers; 3) insufficient, ineffective compensatory innervation – that could be due to functional overloading and/or exhaustion of surviving motor neurons – in EMG more complex MUPs, more frequent blocking in some of them are seen. If the motoneuron is unable to maintain this stage, the MUP may become shorter and lower with increased blocking and jitter. In biopsy atrophy of fibers predominates and clinically progression of weakness and atrophy are observed. The detailed study of bioelectrical events at each stage requires, beside concentric needle EMG (CN EMG), complementary techniques like single fiber EMG (SF EMG) and macroelectrode. On potential duration histograms we can identify 5 electrophysiological stages reflecting the above mentioned stages of remodelling (Hecht, Kasatkina 1983; Hecht 1992).

1) The MUPs are mostly short (high or low). The polyphasy at this stage is due to increased synaptic delay and increased dispersion of end-plate zones. Fibrillation potentials also appear.

2) We can observe still greater shifting of the histogram to the left, with quite pronounced presence of fibrillations.

3) The next stage occurring in partial denervation is collateral sprouting from the neighbouring motor neurons; the sprouts attracted by denervated muscle fibers establish new nerve-muscle contacts and then increased MUP duration, amplitude and area appear. The grouping is the anatomical correlate for increased FD and greater MUPs synchronization. These new nerve-muscle contacts are still unstable, and we often observe failures in nerve terminal end-plate contact expressed as increased jitter both at the end-plate level and in the new sprouts along with increased occurrence of blocking. The polyphasy of the MUP at this stage is also due to slow conduction velocity in the newly formed axons (Peyronnard, Charron 1980).

4) If no further denervation occurs in the next stage, increased MUP amplitude, duration, area and FD are observed. It is at this stage that the so called linked (complex) potentials appear (Lang, Partanen 1976; Partanen, Lang 1976). They are attributed to increased temporal dispersion due to the slower conduction velocity (CV) of the new sprouts and/or slow CV in denervated muscle fibers with a low safety margin of transmission across newly formed motor end-plates, which is mostly responsible for increased jitter and increased occurrence of blocking. An obvious shift of the histogram to the right is observed. It is important to stress that increases in MU territory are very limited as compared with the very pronounced increases of FD. Fibrillation potentials at this stage are not frequent. This stage is relatively stable and is to some extent a measure of the effectiveness of the compensatory mechanism available to the motor neuron. The maximal increase of the size of the MU is shown by macro EMG. The morphological correlate of this functional reorganization of the MU is increased grouping, terminal innervation ratio, increased Lester codispersion index, i.e. statistical analysis of fiber typing of the nearest neighbor within the muscle (Lester et al. 1983).

5) In ALS this balance is very unstable and further dynamics of the disease leads to destabilization of the MUs and changes in MUPs parameters. This is related to the progress of the disease process which involves motor neurons, or to the overloading, or aging of motor neurons with enlarged territories, or to other factors responsible for the loss of the MUs capacity to maintain reinnervation. At this stage we see once more an increased number of linked potentials, fibrillations, increased jitter and blocking.

In human neurogenic diseases all the above mentioned stages do not occur as a rule simultaneously in all MUs. Therefore, we are usually picking up different kinds of MUPs. We can record in chronically partially denervated muscle: 1) potentials of normal MUs which can survive and even not send sprouts (Pinelli et al. 1991); 2) MUPs in the process of disintegration; 3) MUPs which were previously normal, but now have increased parameters with signs of instability; 4) MUPs with signs of stabilized reinnervation; 5) previously enlarged MUPs which became destabilized and show signs of destabilized reinnervation (Figs 1–3).

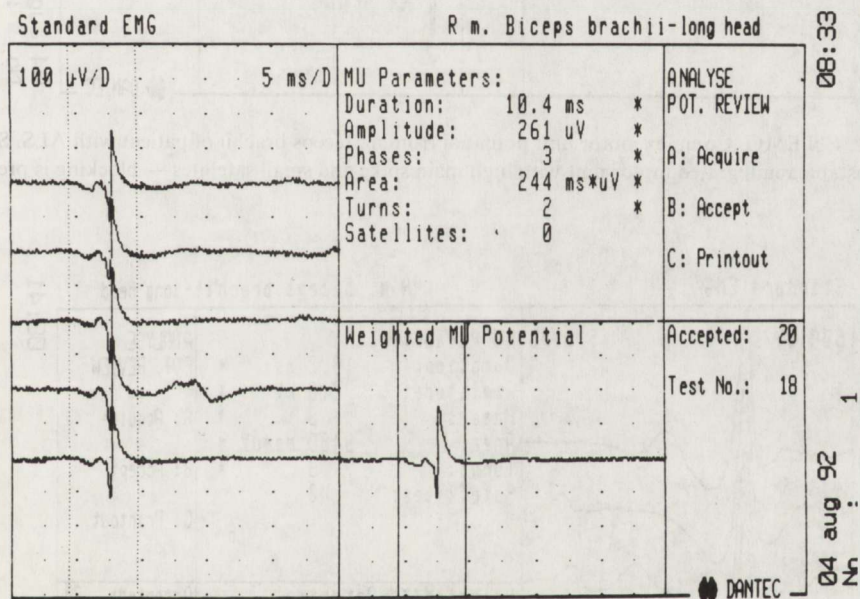


Fig. 1. CN EMG. Motor unit potential from m. biceps brachii of patient with ALS. The stage of disintegrated motor unit, potential is low with reduced area

The CV measurement is an absolutely necessary supplement to EMG examination. In the early stage of the disease the CV is a commonly used differential criterion to distinguish neuropathies from spinal processes. Sensory CV is in ALS normal (we are not taking into account unusual cases). The differentiation from the recently frequently described pure motor neuropathies is more difficult but possible on the basis of focal blocks, pronounced slowing

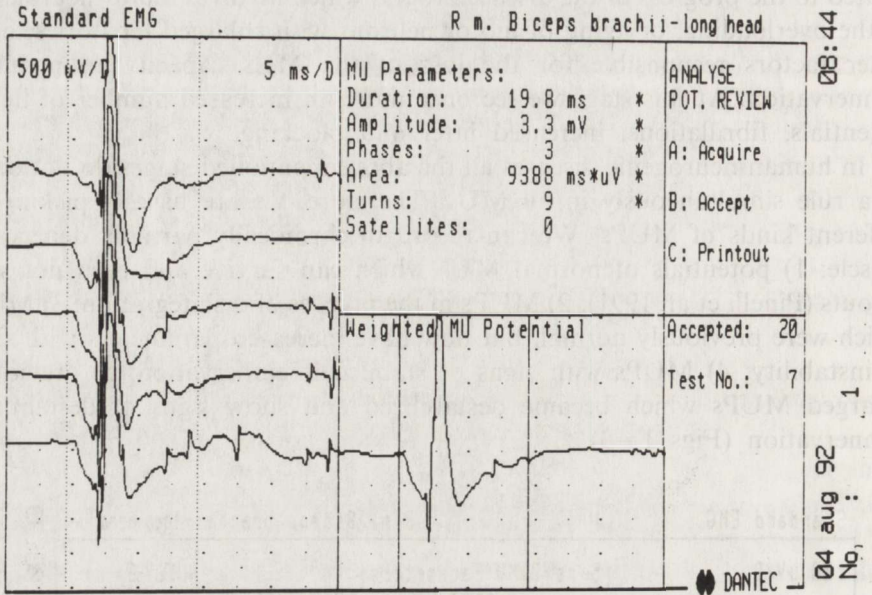


Fig. 2. CN EMG. Complex motor unit potential from m. biceps brachii of patient with ALS. Stage of unstable reintegrated motor unit with high main spike and small satellites — blocking is present

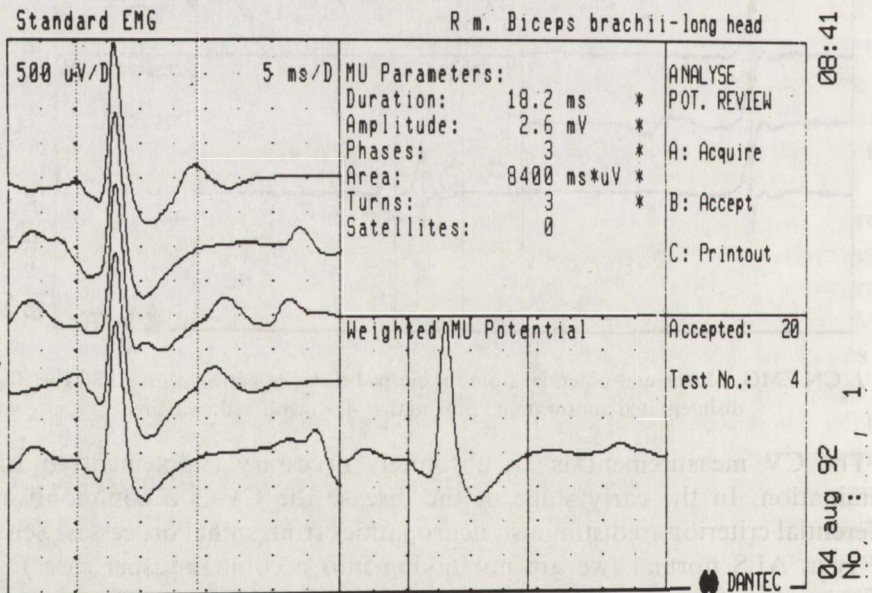


Fig. 3. CN EMG. Reintegrated motor unit from biceps brachii of patient with ALS

in the latter. However, sometimes blocking may happen in ALS as well (Trojaborg – personal communication). In the course of ALS the compound muscle action potential (CMAP) falls in amplitude, this occurs particularly in very severe cases and is rather a poor prognostic sign (Eretkin 1967). We have shown some evidence of selective involvement of slow conducting fibers in ALS (Hausmanowa-Petrusewicz, Kopeć 1973). Because of the variable neuromuscular transmission of new collateral sprouts, often a decreament of CMAP at a slow rate of stimulation occurs (Bernstein, Antel 1981). Among our patients with ALS ten started with an myasthenia-like syndrome and were at certain times misdiagnosed.

LATE POST-POLIO SYNDROME

– Methods

– Interpretation of results

Late polio is a model of apparently accomplished reintegration of the motor unit and after then some relapse of destabilization. It could be assumed that after acute polio the enlarged MUs appear as the result of “successful” reinnervation which might be stabilized. Some factors, however, leading to decompensation may destabilize the MU again. CN EMG reveals high, long MUAPs, decreased number of acting MUs; the application of SF EMG might show increased FD, also increased jitter and blocking – signs of destabilization (Wiechers 1986; Ryniewicz et al. 1990). The following could be an alternative explanation of these phenomena: they could be late signs of destabilization, superimposed on a previously compensated process or we can assume that instability of MUs in patients after polio is something which persists permanently when the disease is clinically finished (Bradley 1987; Ryniewicz et al. 1990). In the late post-polio syndrome, typical relapsing disintegration of apparently reintegrated MUs is observed and we can imagine that repeated reinnervation might be possible giving a still more variable picture of remodelled MU. The reasons for a not reintegrated for long time and thereby unstable MU could be different: 1) delayed recovery due to late sprouting, 2) too large motor neuron territory and inability of the motor neuron to sustain the reinnervation of so many muscle fibers, 3) metabolic limit of motoneuron capacity, causing failure in neuromuscular transmission, 4) scarred motoneuron e.g. by polio.

The delayed sprouts in partially denervated muscle, e.g. after polio might be also related to weak signals from muscle fibers needed to attract sprouting at a normal rate or to an inefficient motoneuron.

The important fact is that in polio the process is only apparently asymmetric and the asymmetry concerns only clinical symptoms. Electrophysiological examination reveals a more spread out process than we used to consider (Maselli et al. 1986). The factors which occur many years after the polio attack may be as follows: loss of peripheral muscle fibers of giant MU,

loss of motoneurons due to some additional factors including a normal aging process with loss of about 1% of MUs per year, and an overloaded or overused motoneuron. Why does it happen quite often in muscles apparently intact during the acute episode of polio? It could be assumed that those muscles are overloaded more than the weak muscles, and therefore their MUs can become destabilized after some time. It is also possible that being much less clinically affected during the acute episode, they have not developed a sufficiently rich innervation (Bradley 1987). At any rate, late polio is an example of: 1) overaccommodating reinnervated MU, 2) overengaged reinnervation, and 3) scarred motoneuron.

It remains an intriguing question, whether after such a relapsing disintegration of the motor unit subsequent reinnervation is possible and what course it may run. Could the partially affected motoneuron at least try to enlarge its territory?

Thus, electromyographic examination in the late polio syndrome has important diagnostic role by characterizing the functional state of MUs and the functional state of muscle fibers distributed within MUs — all the EMG parameters considered jointly are of prognostic importance (Stålberg et al. 1986). Beside diagnostic and prognostic yield, such a quantified examination gives also insight into the pathomechanism of late post-polio muscle atrophy (Wiechers 1986, 1988; Bradley 1987; Ryniewicz et al. 1990).

SPINAL MUSCULAR ATROPHY (SMA)

- Characteristics of model
- Methods
- Interpretation of results
- Chronic forms versus infantile ones

The model of more stabilized, less progressing motor neuron involvement is chronic benign spinal atrophy (type 3 SMA). First of all it is extremely important in clinical practice because, contrary to ALS, usually recognized clinically by even moderately experienced clinicians, the chronic SMA is often misdiagnosed and patients are referred as Becker or limb-girdle dystrophy. The most characteristic EMG signs of SMA are moderate spontaneous activity: fibrillations, fasciculations. Impairment of recruitment (also well demonstrated by “banana” or “clouds”), large (high and long) MUAPs; complex potentials are common, they are usually more stabilized than in ALS (Stålberg et al. 1986). FD is often greatly increased, the macro amplitude is indicative of big-size MU (Desmedt, Borenstein 1977; Hausmanowa-Petrusewicz 1985, 1986; Hausmanowa-Petrusewicz, Karwańska 1986). Motor and sensory conduction are usually normal (Ryniewicz 1977). In very long lasting cases small myopathic potentials appear that are not a part of satellite potentials, but a true result of secondary, myopathic changes (Hausmanowa-Petrusewicz, Karwańska 1986).

The SMA type 1 is an example of the possibility of rearrangement of still developing immature MUs. In immature fibers polyaxonal innervation is seen, it is, however, possible that only one end-plate is functional. In our experience, confirmed by Schmalbruch's (1984) experimental work on immature rats, children with SMA type 1 show no collateral sprouts (Schmalbruch 1992). This would explain the fast progressing malignant course of SMA type 1. There are various possible explanations of this fact: 1) the immature motor neuron could be unable to support additional muscle fibers, 2) immature muscle fibers might be unable to attract sprouts, 3) the muscle fibers may lose this ability before the uninjured motor neuron has matured. The very specific spontaneous activity – motor units firing – might be also an expression of immaturity (Buchthal, Olsen 1970; Hausmanowa-Petrusewicz, Karwańska 1986). In affected children EMG is often decisive in answering the question why the child is floppy.

ROLA ELEKTROMIOGRAFII W DIAGNOSTYCE CHOROÓB NEURONU RUCHOWEGO

Streszczenie

W pracy przedyskutowano programowanie badania elektromiograficznego i elektroneurograficznego w uszkodzeniach dolnego neuronu ruchowego. Uwzględniając zastosowanie różnych technik badawczych podkreślono trudności prawidłowej interpretacji wyników. Opisano różne stadia dezintegracji i reintegracji uszkodzonych jednostek ruchowych, jak również cechy kompensacji w zaoszczędzonych przez procesy chorobowe jednostkach ruchowych. Dokładnie omówiono dynamikę EMG w stwardnieniu zanikowym bocznym, późnym zespole post-polio i w dziecięcym rdzeniowym zaniku mięśni.

REFERENCES

1. Bebhia M, Kelly JJ: Role of electromyography in amyotrophic lateral sclerosis. *Muscle Nerve*, 1991, 14, 1236–1241.
2. Bernstein LP, Antel JP: Motor neuron disease: decremental responses to repetitive stimulation. *Neurology*, 1981, 31, 202–204.
3. Bradley WG: Recent views on amyotrophic lateral sclerosis with emphasis on electrophysiological studies. *Muscle Nerve*, 1987, 10, 490–502.
4. Brown WF: The physiological and technical basis of electromyography. Butterworth, Boston, 1984.
5. Buchthal F, Kamieniecka Z: The diagnostic yield of quantified electromyography and quantified muscle biopsy in neuromuscular disorders. *Muscle Nerve*, 1982, 5, 265–289.
6. Buchthal F, Olsen PZ: Electromyography and muscle biopsy in spinal muscular atrophy. *Brain*, 1970, 43, 15–30.
7. Buchthal F, Pinelli P: Action potentials in muscular atrophy of neurogenic origin. *Neurology*, 1953, 3, 591–603.
8. Carleton SA, Brown WF: Changes in motor unit populations in motor neuron disease. *J Neurol Neurosurg Psych*, 1979, 42, 42–51.
9. Daube JR: EMG in motor neuron disease. AAEE Minimonograph AAEE, Rochester MN, 1982.

10. Desmedt JE, Borenstein S: Interpretation of electromyographical data in spinal muscular atrophy. In: Motor neuron disease. Ed.: FC Rose. Pitman, London, 1977, pp 112–120.
11. Dorfman LJ, Kevin CM: Automatic quantitative electromyography. *Muscle Nerve*, 1988, 11, 804–814.
12. Eretkin C: Sensory and motor conduction in motor neurone disease. *Acta Neurol Scand*, 1967, 45, 499–512.
13. Erminio F, Buchthal F, Rosenfalck P: Motor unit territory and muscle fibers concentration in paresis due to peripheral nerve injury and anterior horn cell involvement. *Neurology*, 1959, 9, 657–671.
14. Farago A, Hausmanowa-Petrusewicz I: The analysis of EMG findings in amyotrophic lateral sclerosis. *EMG Clin Neurophysiol*, 1977, 17, 157–166.
15. Gilai AN: Analysis of turns and amplitude in EMG. In: Computer-aided electromyography and expert system. Ed.: J Desmedt, Elsevier, Amsterdam, 1989, pp 143–160.
16. Hausmanowa-Petrusewicz I: Changes of motor units in neuromuscular diseases. In: Recent achievements in restorative neurology. 2. Progressive neuromuscular diseases. Eds: M Dimitrijevic, BA Kakulas, G Vrbova. Karger, Basel, 1986, pp 139–151.
17. Hausmanowa-Petrusewicz I, Karwańska A: Electromyographic findings in different forms of infantile and juvenile proximal spinal atrophy. *Muscle Nerve*, 1986, 9, 37–46.
18. Hausmanowa-Petrusewicz I, Kopeć J: Possible mechanism of conduction velocity changes in the anterior horn cells involvement. *Electromyography Clin Neurophysiol*, 1973, 13, 357–365.
19. Hausmanowa-Petrusewicz I: Electrophysiological findings in childhood spinal muscular atrophies. *Rev Neurol*, 1985, 144, 710–725.
20. Hecht BM: Morpho-functional organisation of motor units at different stages of compensatory reinnervation (in preparation), 1992.
21. Hecht BM, Kasatkina LF: Electromyographic analysis of different stages of denervation and reinnervation (Rash). *Wiss Z Ernst Moritz-Arndt Univ*, 1983, 32, 27–31.
22. Kund RW, Cornblath DR, Griffin RW: Assessment of thoracic paraspinous muscles in the diagnosis of ALS. *Muscle Nerve*, 1988, 11, 484–492.
23. Lambert EM: Electromyography in amyotrophic lateral sclerosis. In: Motor neuron disease. Eds: FM Norris, LT Kurland. Grune and Stratton, New York, 1969, pp 135–153.
24. Lang H, Partanen V: Satellite potentials and the duration of motor unit potentials. *J Neurol Sci*, 1976, 27, 512–524.
25. Lester JM, Silber DJ, Cohen MH, Hirsch RP, Bradley WG, Brenner JF: The co-dispersion index for the measurements of fiber type distribution pattern. *Muscle Nerve* 1983, 6, 581–587.
26. Maselli RA, Cashman N, Salazar B: Post poliomyelitis muscular atrophy: electrophysiologic and biopsy correlates. AAEE Meeting, Boston, 24–28 September, 1986, abstr 15.
27. McComas AJ: Neuromuscular function and disorders. Butterworth, London, 1977.
28. Mulder DW: Electrodiagnostic techniques, their role in the diagnosis, prognosis and study of etiology of motor neurone disease. *Res Prog in Motor Neurone Disease*. Pitman, London, 1984, pp 99–104.
29. Munsat TL, Andres P, Fenison L, Conlon T, Thibodeau L: The natural history of motoneuron loss in amyotrophic lateral sclerosis. *Neurology*, 1988, 38, 409–412.
30. Partanen J, Lang H: Satellite potentials and the duration of potentials in normal, neuropathic and myopathic muscles. *J Neurol Sci*, 1976, 27, 514–524.
31. Peyronnard JM, Charron L: Muscle reorganization after partial denervation and reinnervation. *Muscle Nerve*, 1980, 3, 509–518.
32. Pinelli P, Pisano F, Ceriani F, Miscio G: EMG evaluation of motor neuron sprouting in amyotrophic lateral sclerosis. *Ital J Neurol*, 1991, 12, 359–367.
33. Ryniewicz B: Motor and sensory conduction velocity in spinal muscular atrophy. *Electromyography Clin Neurophysiol*, 1977, 17, 385–391.

34. Ryniewicz B, Rowińska K, Emeryk B, Hausmanowa-Petrusewicz I: Electrophysiological findings in patients after poliomyelitis. *Electromyography Clin Neurophysiol*, 1990, 30, 423–427.
35. Schmalbruch H: Motoneuron death after sciatic nerve section in newborn rats. *J Comp Neurol*, 1984, 224, 252–285.
36. Schmalbruch H: Denervation of immature muscles: possible clues for the understanding of infantile spinal muscular atrophy Werdnig-Hoffman (personal communication), 1992.
37. Stålberg E, Ekstedt J: Single fibre EMG and micro-physiology of the motor unit in normal and diseased muscle. In: *New developments in electromyography and clinical neurophysiology*. Ed.: JE Desmedt, Karger, Basel, 1973, pp 114–129.
38. Stålberg E, Hilton-Brown P, Rydin E: Capacity of motor neuron to alter its peripheral field. In: *Recent achievements in restorative neurology. 2 Progressive neuromuscular diseases*. Eds: MR Dimitrijevic, BA Kakulas, G Vrbova. Karger, Basel, 1986, pp 237–253.
39. Stålberg E, Sanders DB: The motor unit in amyotrophic lateral sclerosis studied with different neurophysiological techniques. In: *Res Prog in Motor Neurone Disease*. Ed.: CF Rose, Pitman, London, 1984, pp 105–121.
40. Swash M, Schwartz MS: A longitudinal study of changes in motor neuron disease. *J Neurol Sci*, 1982, 56, 185–197.
41. Trojaborg W: personal communication.
42. Wiechers DD: Reinnervation after acute poliomyelitis. AAEE Meeting, Boston, 24–28 September, 1986, abstr 13.
43. Wiechers DD: New concepts of the reinnervated motor unit revealed by vaccine-associated poliomyelitis. *Muscle Nerve*, 1988, 11, 356–364.

Author's address: Neuromuscular Unit, Medical Research Centre, PAsci, 1A Banacha St, Bld D, 02-097 Warsaw, Poland

ANNA FIDZIAŃSKA, HANNA DRAC, ZOFIA GLINKA

INCLUSION BODY MYOSITIS (IBM). MORPHOLOGICAL STUDY

Department of Neurology, School of Medicine and Neuromuscular Unit, Medical Research Centre, Polish Academy of Sciences, Warsaw

Among the chronic idiopathic inflammatory myopathies inclusion body myositis (IBM) has emerged as a clinicopathologic variant. Slowly progressive weakness of the distal and the proximal muscle groups, the presence of rimmed vacuoles with basophilic granules as well as 15–18-nm filamentous inclusions in affected muscle confirm the clinical and histopathological distinction between inclusion body myositis and chronic polymyositis.

Key words: *inclusion body myositis, morphology.*

Inclusion body myositis (IBM) is a distinct form of inflammatory myopathy and differs from polymyositis (PM) and dermatomyositis (DM) by the presence of rimmed vacuoles and filamentous inclusions in the muscle as well as refractoriness to immunosuppressive therapy (Danon et al. 1982; Ringel et al. 1987). Exception to morphological changes, IBM cases may occasionally be misdiagnosed as PM. For this reason, the recognition of this disease is important because it demands a different therapeutic approach and implies a different prognosis than other types of inflammatory myopathy.

In this paper we present morphological changes in the muscle consistent with the diagnosis of IBM.

CASE REPORT

A 52-year-old woman was admitted to the Neurological Department because of progressive painless muscle weakness without spontaneous remission. The patient was healthy until the age of 30 when she started to develop muscle weakness and gait disturbances. Weakness in the legs progressed and at the age of 38 she had increasing difficulty in climbing stairs. Nine years after her first symptoms she noted weakness of the upper limbs. At the age of 47 she was seen at a hospital where polymyositis was diagnosed. She was treated with steroids for 4 months without effect. The weakness of the legs and arms

continued to progress and at the age of 50 she could no longer stand up from the floor without support and was not able to walk on her toes and heels. General physical examination was normal. Neurological abnormalities were limited to the motor system. There was mild proximal wasting of upper limbs, global asymmetric weakness with distal preponderance. There was moderate weakness in the iliopsoas, pelvic girdle and leg muscles. All tendon reflexes were absent. The patient was not able to walk on her heels and toes and change the position from sitting to standing. All sensory modalities were intact. Myotonias and fasciculations were not noted.

The following laboratory tests were normal: complete blood count, urinalysis, blood urea nitrogen, electrolytes, serum protein, cholesterol, uric acid, bilirubin, AspAT, ALAT, immunoglobulins. The serum CK was 24–269 IU, aldolase 39–70 IU. The sedimentation rate was 48–50. EMG showed myopathic changes.

MATERIAL AND METHODS

The quadriceps femoris muscle, taken at biopsy, was studied by light and electron microscopy. One part of the specimen was frozen in isopentane and cooled in liquid nitrogen. Serial frozen sections were stained with hematoxylin and eosin (HE), modified Gomori trichrome, NADH-tetrazolium reductase, succinate dehydrogenase, routine ATP-ase with preincubation at pH 9.6, 4.6, and 4.3, oil red O, PAS and phosphorylase.

The specimen for electron microscopy was fixed in 1% glutaraldehyde in 0.1 M phosphate buffer at pH 7.4, postfixed in 1% osmium tetroxide in the same buffer, dehydrated and embedded in spurr-resin. Semithin sections were stained with toluidine blue for light microscopy. Ultrathin sections double-stained with uranyl acetate and lead citrate were examined in a JEM 1200 electron microscope.

RESULTS

The light microscopic study showed marked variation in fiber size with areas showing atrophic fibers (Fig. 1A), either scattered randomly or grouped in small clusters. Atrophic fibers were usually angular and only occasionally rounded or polygonal. Both histochemical fiber types suffered an equal degree of atrophy. Centrally located nuclei were increased in number. Necrotic fibers and inflammation were not observed. There was a moderate increase in endomysial connective tissue. The most characteristic feature was the presence of single or multiple vacuoles seen in many muscle fibers. The size of vacuoles varied from 1 to 8 μm . Some vacuoles were empty, others contained small

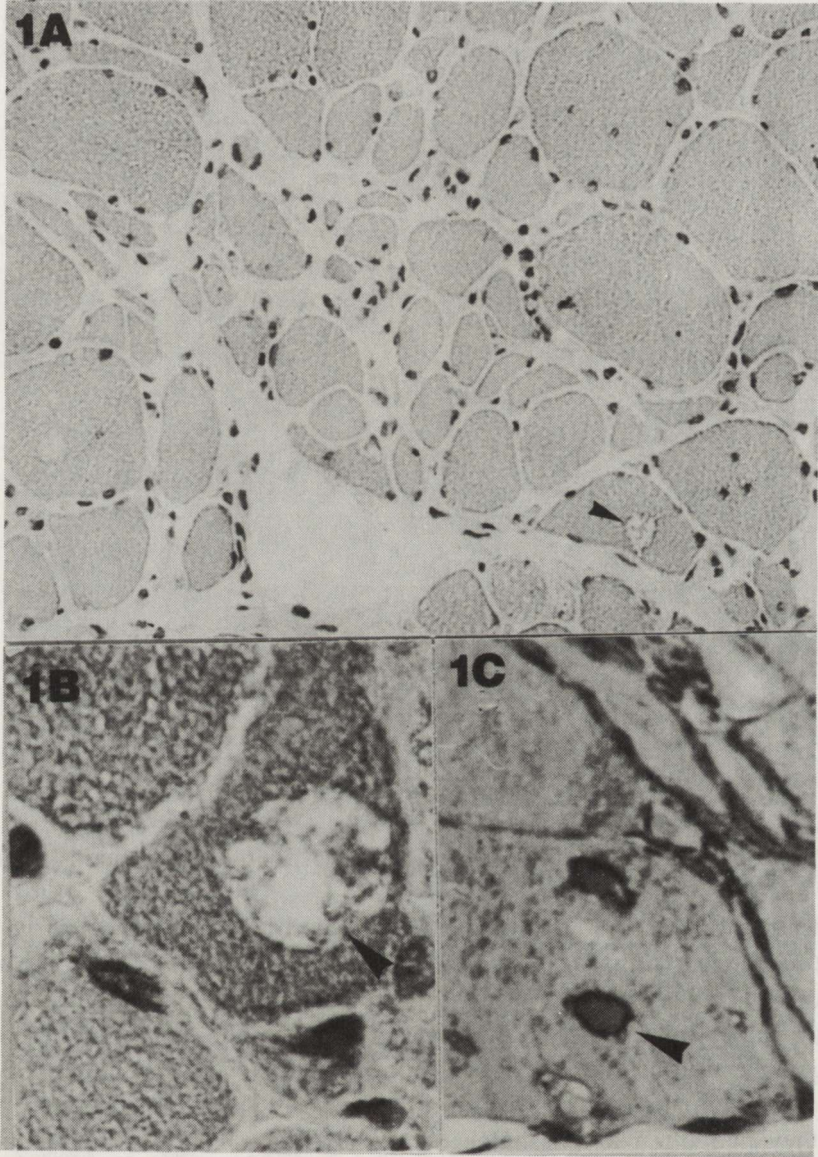


Fig. 1. Quadriceps femoris muscle. *1A.* Muscle fibers show marked variation in the fiber size. In some muscle fibers the presence of vacuoles (arrowhead) is observed. HE. $\times 448$. *1B.* Vacuole contains small basophilic granules (arrowhead). HE. $\times 1120$. *1C.* Homogeneous inclusions (arrowhead). Spurr-resin. $\times 1120$

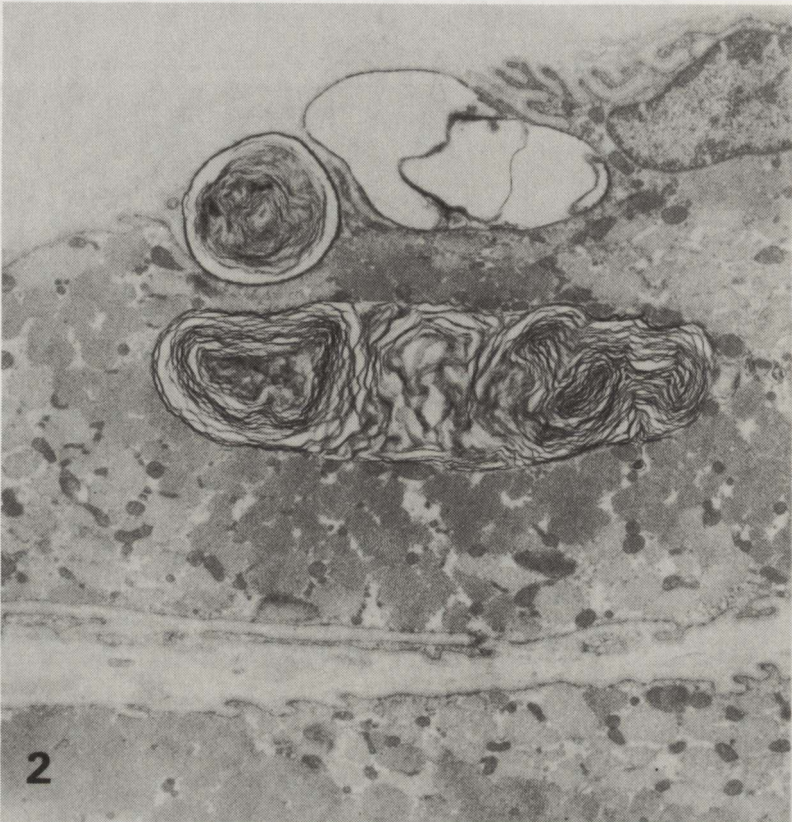


Fig. 2. Conglomeration of membraneous bodies. $\times 600$

basophilic granules (Fig. 1B). In some muscle fibers homogeneous inclusions were observed (Fig. 1C).

Electron microscopic examination showed conglomeration of large membraneous bodies (Fig. 2). They were composed of coiled spiral membrane structures generally situated near the sarcolemma, but occasionally observed deep in the cytoplasm of the muscle cell. Close to the membraneous whorls, a large collection of filaments 15–18 nm in diameter was found (Fig. 3). The abnormal filaments in cross section appeared tubular, in longitudinal projection they had often a crosshatched outline (Fig. 4). Similar filaments were clearly visible within the nuclei (Fig. 5). Abnormally large mitochondria and mitochondria with unusual cristae arrangement as well as crystalloid inclusions were seen only in a few muscle fibers. There was small endomysial foci of lymphocytic infiltration (Fig. 6).

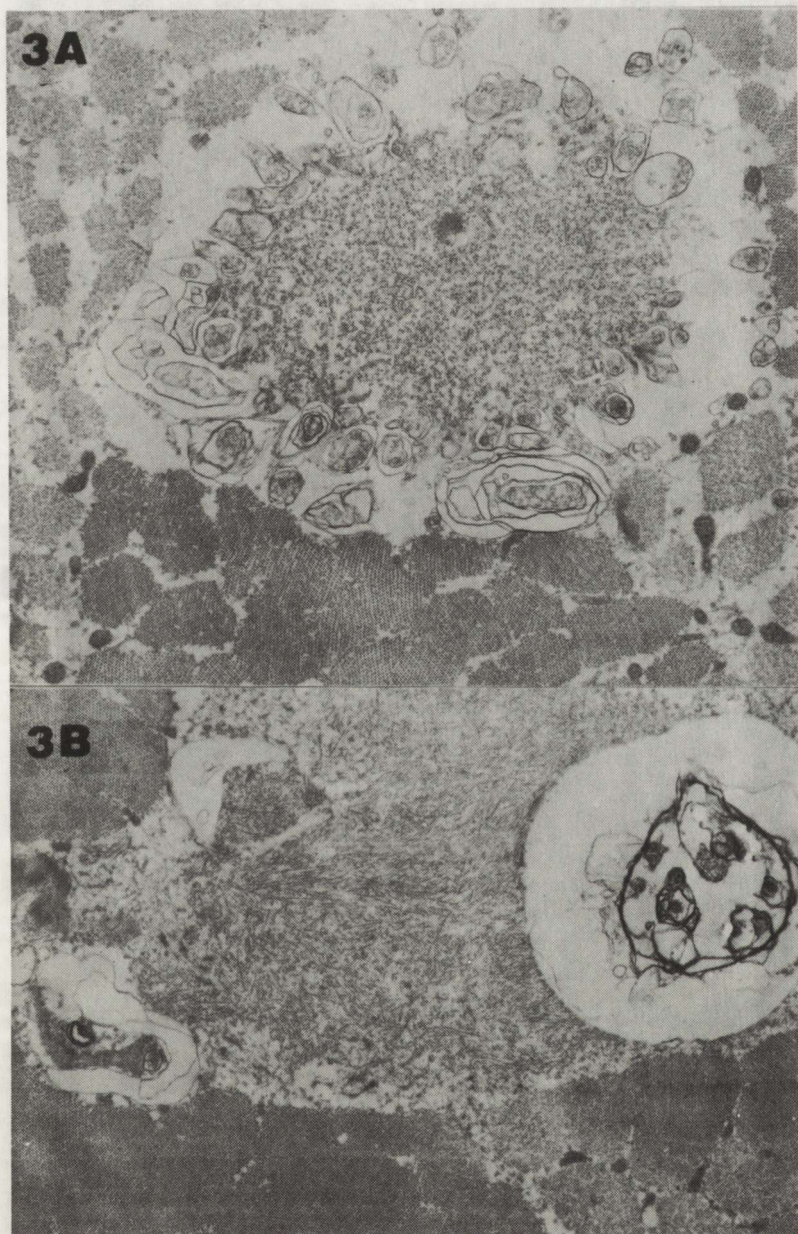


Fig. 3A and 3B. Filamentous inclusions. × 12000



Fig. 4. Higher magnification of filamentous structure. $\times 60\,000$

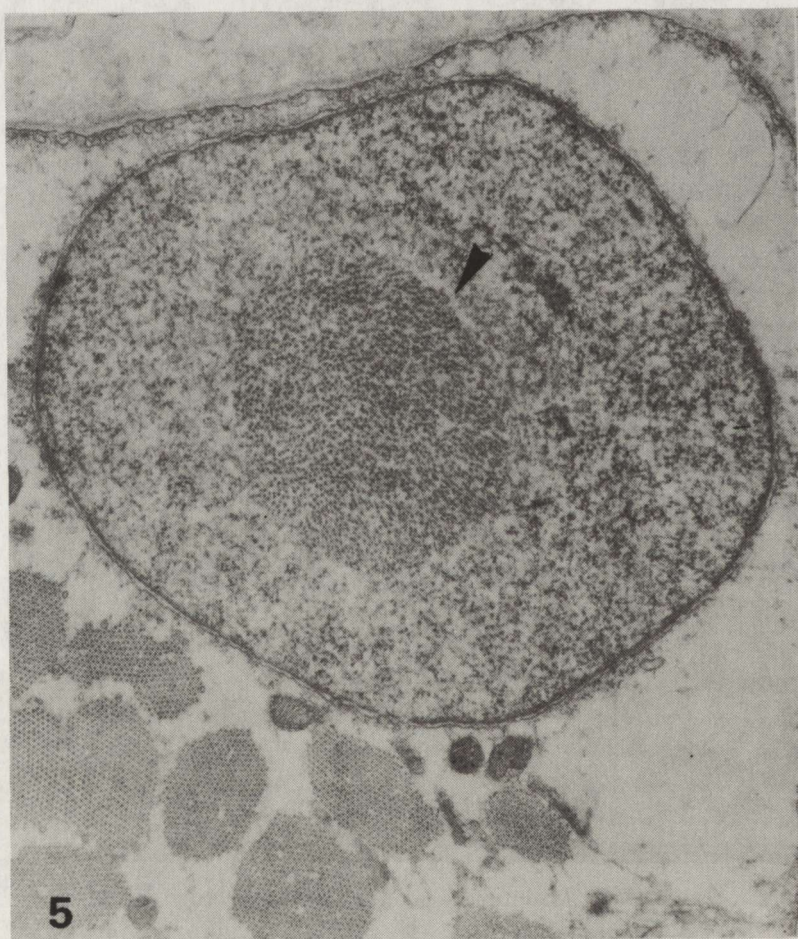


Fig. 5. Nuclear inclusion (arrowhead). $\times 20\,000$

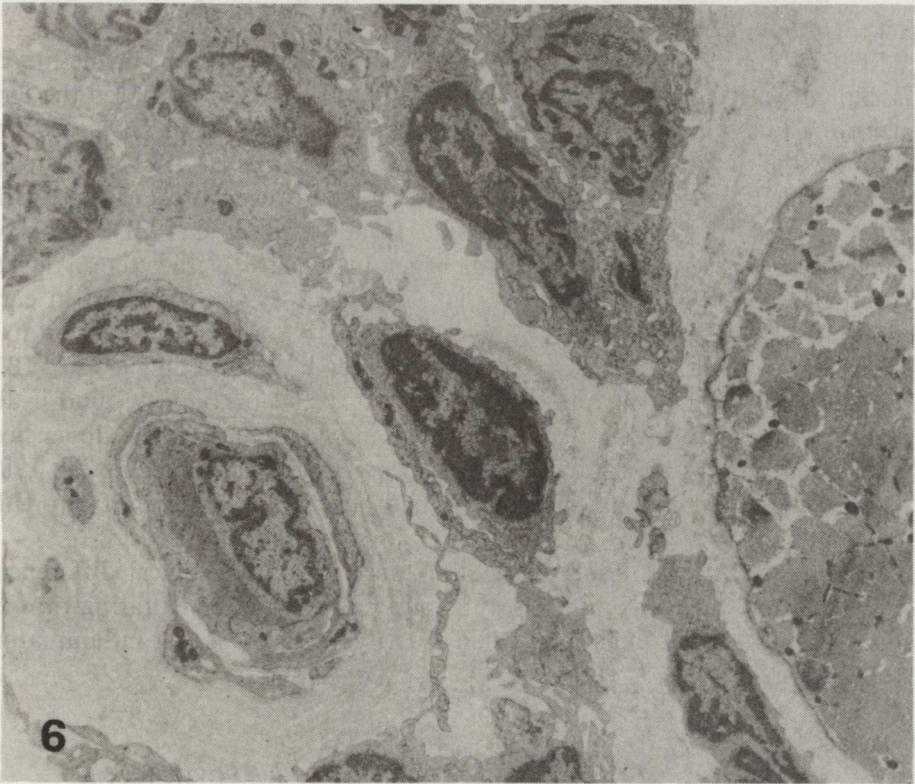


Fig. 6. Lymphocytic infiltration. $\times 5000$

DISCUSSION

The patient here presented was clinically diagnosed as PM, but muscle fibers necrosis and inflammation, one of the common morphological changes in this disease, were not observed. Our case differs significantly from each of the reported examples of PM. The patient was affected late in life and exhibited mainly progressive muscle weakness. The distribution of the weakness was peculiar in that distal muscles were affected in the same mode as the proximal ones. Bulbar muscles were not involved and there were no signs of collagen vascular disease.

Laboratory studies showed no immunologic abnormality and CK was slightly elevated. The degree of necrosis and degenerative changes prominent in PM were not observed in the muscle of our patient and inflammatory exudates were relatively sparse as compared with those occurring in PM. All these differences as well as lack of response to immunosuppression clearly distinguished our case from the typical form of PM. The structural changes found in muscle are entirely consistent with the diagnosis of IBM. Rimmed vacuoles, membrane whorls, cytoplasmic and nuclear inclusions composed

of 15–18-nm filaments are constant pathological finding in this disorder (Jongen et al. 1990).

In 1971 Yunis and Samaha reported sarcoplasmic inclusions in the muscle of a patient with a chronic, benign course of the disease and proposed the term "inclusion body myositis". In 1978 Carpenter et al. added six cases and amplified the original definition of Yunis and Samaha (1971) to further differentiate IBM from idiopathic PM and DM. However, most cases of IBM begin in the sixth or seventh decade of life (Lindenberg et al. 1991), a number of reports have described the disease as beginning as early as the second decade (Yunis, Samaha 1971; Jerusalem et al. 1972; Tome et al. 1981) and in early childhood (Eisen et al. 1983). There are also reports presenting familial myopathies that fulfill the pathological criteria required for a diagnosis of IBM (Cole et al. 1988). The morphological aspect of inclusion bodies found in the muscles recall the nuclear capsid of the paramyxovirus by their dimension, shape, often tubular appearance and transverse periodicity (Julien et al. 1982; Chou 1986). However, paramyxovirus has never been isolated from IBM muscles.

Although IBM and PM usually show distinct morphological differences, the present investigation emphasises the importance of demonstrating rimmed vacuoles and filament inclusions when identifying IBM among inflammatory myopathies.

WTĘTOWE ZAPALENIE MIĘŚNI. BADANIA MORFOLOGICZNE

Streszczenie

Wtrętowe zapalenie mięśni stanowi wariant miopatii zapalnych, odrębny klinicznie i morfologicznie. Narastające osłabienie mięśni ksobnych i odsiebnych, obecność wakuoli z zasadochłoną zawartością oraz obecność filamentarnych wtrętów w uszkodzonym mięśniu różnią wtrętowe zapalenie mięśni od postaci przewlekłej zapalenia.

REFERENCES

1. Carpenter S, Karpati G, Heller I, Eisen AG: Inclusion body myositis: a distinct variety of idiopathic inflammatory myopathy. *Neurology*, 1978, 28, 8–17.
2. Chou SM: Inclusion body myositis: a chronic persistent mumps myositis. *Human Pathol*, 1986, 17, 765–777.
3. Cole AJ, Kuzwiecky R, Karpati G, Carpenter S, Andermann E, Andermann F: Familial myopathy with changes resembling inclusion body myositis and periventricular leucoencephalopathy. *Brain*, 1988, 111, 1025–1037.
4. Danon MJ, Reyes MG, Perurena OH, Masdeu JC, Manaligod JR: Inclusion body myositis. A corticosteroid-resistant idiopathic inflammatory myopathy. *Arch Neurol*, 1982, 39, 760–764.
5. Eisen A, Berry K, Gibson G: Inclusion body myositis (IBM), myopathy or neuropathy? *Neurology*, 1983, 33, 1109–1114.

6. Jeruzalem F, Baumgartner G, Wyler R: Virus-ähnliche Einschlüsse bei chronischen Neuromusculären Prozessen: elektronenmikroskopische Biopsiesbefunde von 2 Fällen. *Arch Psychiat Nervenkrank*, 1972, 215, 148–166.
7. Jongen PJH, Meertens MJHE, Ter Laak HJ, Standhouders AM, Joosten EMG: Inclusion body myositis: diagnostic specificity of basophilic vacuoles and inflammatory inclusions. *J Neurol Sci*, 1990, 98 (suppl), 181.
8. Julien J, Vital CL, Vallat A, Lagueny A, Sapina D: Inclusion body myositis. Clinical, biological and ultrastructural study. *J Neurol Sci*, 1982, 55, 15–24.
9. Lindberg CH, Borg K, Edström L, Hedström A, Oldfors A: Inclusion body myositis and Welander distal myopathy: a clinical, neurophysiological and morphological comparison. *J Neurol Sci*, 1991, 103, 76–81.
10. Ringel SP, Kenny CE, Neville HE, Giorno R, Carry MR: Spectrum of inclusion body myositis. *Arch Neurol*, 1987, 44, 1154–1157.
11. Tome FMS, Fardeau M, Lebon P, Chevally M: Inclusion body myositis. *Acta Neuropathol (Berl)*, 1981, 7, 287–291.
12. Yunis EJ, Samaha FJ: Inclusion body myositis. *Lab Invest*, 1971, 25, 240–248.

Authors' address: Department of Neurology, School of Medicine, 1A Banacha St, 02-097 Warsaw, Poland

ROMAN GADAMSKI, MIROSLAW J. MOSSAKOWSKI

ASYMMETRIC DAMAGE OF THE CA1 SECTOR OF AMMON'S HORN AFTER SHORT-TERM FOREBRAIN ISCHEMIA IN MONGOLIAN GERBILS

Department of Neuropathology, Medical Research Centre, Polish Academy of Sciences, Warsaw

The studies were carried out on 98 three-month-old Mongolian gerbils, submitted to short-term (5 or 7.5 min) forebrain ischemia induced by bilateral ligation of common carotid artery. After 5-day survival animals were sacrificed by transcardiac perfusion with 10% formaldehyde. Paraffin brain sections were stained with cresyl violet and according to Klüver-Barrera method. Pickworth benzidine method was also applied to evaluate hippocampal vascular network.

Varying susceptibility of individual animals to the ischemic incident was found. This was expressed by differences in the intensity and extent of structural lesions of CA1 pyramidal neurons. No abnormalities were found in 41.7% of animals, total neuronal loss in the CA1 sector was observed in 33.3% of cases, while the partial neuronal loss appeared in the remaining 25% of animals. Asymmetric distribution of the neuronal changes observed in 18.4% of cases was a very striking feature. Differences of the angioarchitectonics of CA1 sector as compared with neighbouring parts of Ammon's horn were found. In the pyramidal cell layer very scarce fragments of the blood vessels were present. In adjacent cortical layers (stratum oriens and stratum radiatum) relatively dense capillary network was characterized by appearance of specific vascular loops and tangles localized on the border of stratum pyramidale.

It is supposed that particular spatial arrangement of the vascular network in pyramidal layer of CA1 sector, favouring appearance of local hemodynamic and rheologic abnormalities after temporary brain ischemia, may play an essential pathogenic role in both, selective vulnerability of this neuronal population and individual variations in the intensity and distribution of the neuronal changes.

Key words: *temporary brain ischemia, hippocampus, CA1 neurons, selective vulnerability, vascular factor.*

The problem of selective vulnerability of Ammon's horn pyramidal neurons has a long history as far as its pathogenetic mechanism is concerned. The main lines of the discussion on the subject were established by prominent German neuropathologists: C. and O. Vogts (1925) and W. Spielmeier (1925).

Vogts were linking selective sensitivity of hippocampal pyramidal neurons with their physico-chemical proprieties, using the name of "pathocllisis" to determine their changes induced by pathogenic factors. For Spielmeyer the main pathogenic role was played by vascular factor, indicating special angioarchitectonics in this part of the brain. The extensive studies, carried out in last two decades seem to speak in favour of Vogts pathocllisis concept understood in a modern terms as a complex of metabolic and functional proprieties of the particular groups of pyramidal neurons. The milestones posted along this way were observations indicating different reactions of various Ammon's horn neuronal populations to the same damaging factors, such as for instance, cerebral ischemia (Ito et al. 1975; Kirino 1982) or kainic acid (Nadler et al. 1978), as well as description of the phenomenon called delayed neuronal death, forming a special type of reaction of the pyramidal neurons from Ammon's horn CA1 sector to the short-term forebrain ischemia in Mongolian gerbils (Kirino 1982).

The further studies showed that damage and final breakdown of CA1 pyramidal neurons is preceded by their bioelectric hyperactivity (Suzuki et al. 1983b) with ultrastructural exponents of their metabolic activation (Mossakowski et al. 1989). It has been documented that neuronal hyperactivity is resulting from the influence of excitatory amino acid neurotransmitters, mostly glutamate, followed by intracellular calcium influx, which disturbs essential intracellular metabolic processes leading to irreversible neuronal damage (Drejer et al. 1985; Meldrum et al. 1985). Nociceptive role of excitotoxic action of glutamate in this process, dependent on the specific synaptic organization of the CA1 sector (Collingridge et al. 1983) and an early damage of GABA-ergic interneurons (Gajkowska et al. 1989), was proven in experiments revealing cytoprotective effect on the pyramidal neurons of both glutaminergic deafferentiation of the area (Pulsinelli 1985) and application of specific NMDA receptor blockers (Simon et al. 1984).

This well documented theory, connecting specific reaction of CA1 neurons to the short-lasting ischemic insult with their glutaminergic innervation and calcium-induced metabolic alterations does not explain variability of the symmetry and intensity of neuronal damage observed in Mongolian gerbils after bilateral carotid artery occlusion. The asymmetry of neuronal lesions concerning both their extension and intensity, very seldom mentioned by most of the authors working on this experimental model, was relatively common feature in our material (Mossakowski, Gadamski 1985; 1987a, b).

This inclined us to evaluate this question quantitatively and to search for additional factor or factors which could explain this phenomen. We turned our attention to the Spielmeyer's vascular factor, moreover so as morphometric studies of Imdahl and Hossmann (1986) on capillary perfusion of the CA1 sector of Ammon's horn in Mongolian gerbils in normal and postischemic conditions suggested that protracted postischemic perfusion reduction may possibly play a role of an important factor in maturation of pathological changes.

MATERIAL AND METHODS

Experiments were performed on 98 Mongolian gerbils (*Meriones unguiculatus*), bred in animals quarter of the Medical Research Centre of PASci. Three-month-old male animals weighing ca 75 g were used. Transient forebrain ischemia was induced by bilateral common carotid artery ligation under halothane anesthesia in an open gas system consisting of a mixture of 70% of nitrogen and 30% of oxygen. The carotid arteries were exposed and Heifetz or Vasargile clips were placed on both of them for either 5 or 7.5 minutes. The animals were sacrificed by transcardiac perfusion with 10% neutral formalin 5 days after the ischemic insult, performed under ether anesthesia. The brains were postfixed in the perfusion fluid for 5 days and then cut into coronal blocks. Blocks containing dorsal hippocampus were embedded in paraffin. Sections 10 μm thick were stained with cresyl violet and according to the Klüver-Barrera method.

Morphologic observations were evaluated morphometrically by establishing mean number of pyramidal neurons in a 0.3 mm long segment of CA1 sector of Ammon's horn. The mean value was obtained from the total number of neurons in at least three segments of this length in 3 to 5 subsequent histologic sections from each animal. The results were then compared with mean value of CA1 pyramidal neurons in the reference animals (not subjected to any experimental procedure), which was 44.7 ± 2.5 cells. This value was considered to be 100%.

The morphometric categories used were the same as those applied in our previous studies (Mossakowski, Gadamski 1985; 1987a, b). No morphologic changes were observed when the average number of pyramidal cells was equal to that in the reference animals. Partial neuronal loss was characterized by the presence of varying proportion of the remaining pyramidal neurons. First-degree partial neuronal loss was characterized by 33.0 ± 4.7 cells (73.8%) preserved; second-degree — 23.6 ± 4.1 cells (52.7%) preserved; and third-degree — 15.7 ± 4.3 cells (35.0%) preserved. Total neuronal loss was characterized by replacement of the neuronal layer by proliferating glial cells with either no neurons or one to ten degenerating cells left in the entire CA1 segment.

For evaluation of the vascular network in particular CA1 hippocampal layers, 3 additional animals, not subjected to any experimental procedure, were used. Animals were sacrificed by decapitation under ether anesthesia. Brains were fixed by immersion in 10% neutral formalin and cut in frontal blocks. The blocks containing dorsal hippocampus were cut on freezing microtome. Sixty μm thick free floating sections were stained with benzidine method of Pickworth.

RESULTS

Frequency of morphological alterations of the pyramidal neurons in the CA1 sector was dependent on the duration of the ischemic incident. In the group of animals in which bilateral carotid artery occlusion lasted for 5 min total or

partial loss of pyramidal neurons with accompanying astrocytic proliferation was observed in 50% of cases. The ischemic incident lasting 7.5 min resulted in an increased proportion of damaged animals to 83.3%. Time-dependent differences in the intensity of the neuronal damage were also observed.

The mean data obtained from the whole experimental material comprising animals with 5 and 7.5 min forebrain ischemia were as follows:

– unchanged neuronal population in CA1 sector was observed in 41.7% of cases,

– total loss of CA1 pyramidal neurons was present in 33.3% of animals,

– partial neuronal loss of different degree was found in 25.0% of cases.

In 81.6% of animals with neuronal abnormalities in CA1 sector, the pathological changes were bilateral and symmetrical in their extent and intensity. In the remaining 18.4% asymmetrical distribution of CA1 sector changes was found. Four patterns of these abnormalities were distinguished:

1) entirely normal appearance of CA1 sector on one side with total neuronal loss on the contralateral side (Fig. 1),

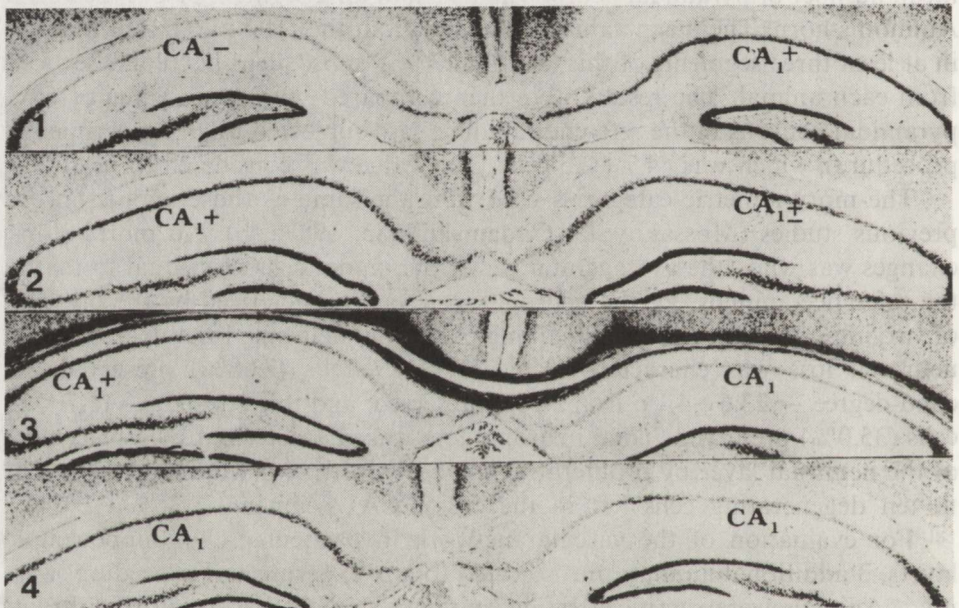


Fig. 1. Exp. animal: 5-min ischemia, 5-day survival. On the left side total loss of CA1 pyramidal neurons (CA₁-) with consecutive glial proliferation. On the right side unchanged neuronal population in the CA1 sector (CA₁+). Cresyl violet. × 60

Fig. 2. Exp. animal: 5-min ischemia, 5-day survival. On the left side entirely normal CA1 sector (CA₁+), on the contralateral side loss of *ca* 50% of pyramidal neurons (CA₁±). Cresyl violet. × 60

Fig. 3. Exp. animal: 7.5-min ischemia, 5-day survival. On the left side lateral half of the CA1 sector with entirely normal pyramidal cell population (CA₁+). Neuronal loss in the medial half and in the entire CA1 sector on the contralateral side. Klüver-Barrera. × 60

Fig. 4. Exp. animal: 7.5-min ischemia, 5-day survival. On the left side only 50% of CA1 sector pyramidal neurons are preserved, on the right side only 30% of neurons with normal morphological appearance. Cresyl violet. × 60

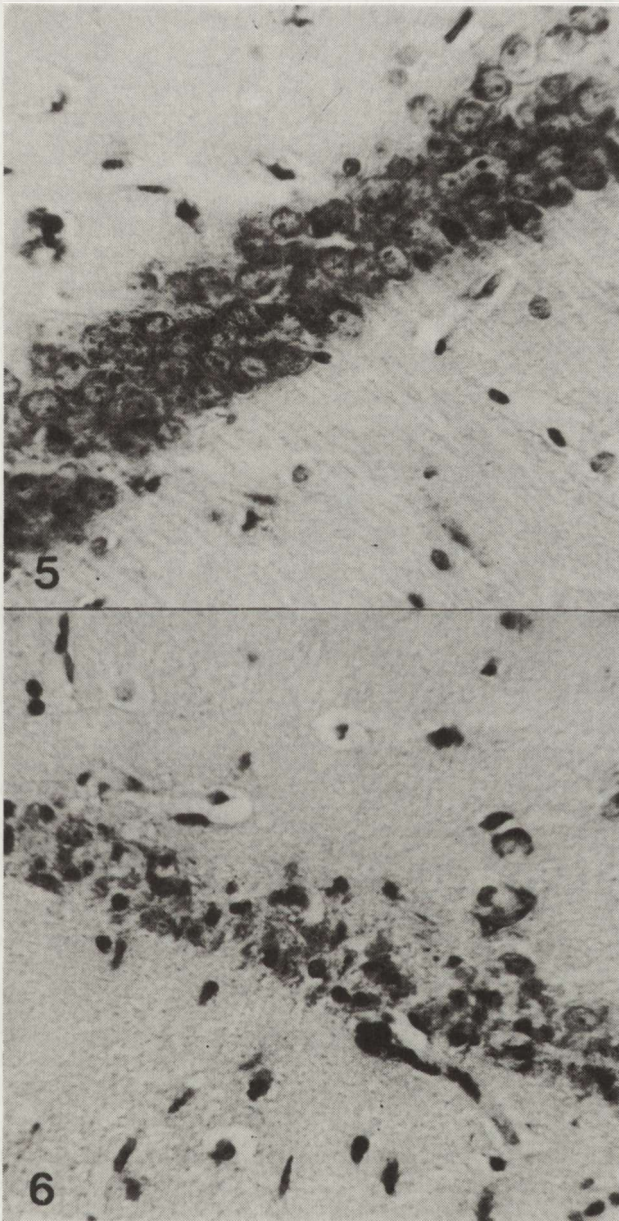


Fig. 5. Exp. animal: 7.5-min ischemia, 5-day survival. Normal population of CA1 sector. Cresyl violet. $\times 400$

Fig. 6. Exp. animal: 5-min ischemia, 5-day survival. Pathological process totally mature: former pyramidal cell layer replaced by proliferating astrocytic glia. Cresyl violet. $\times 400$

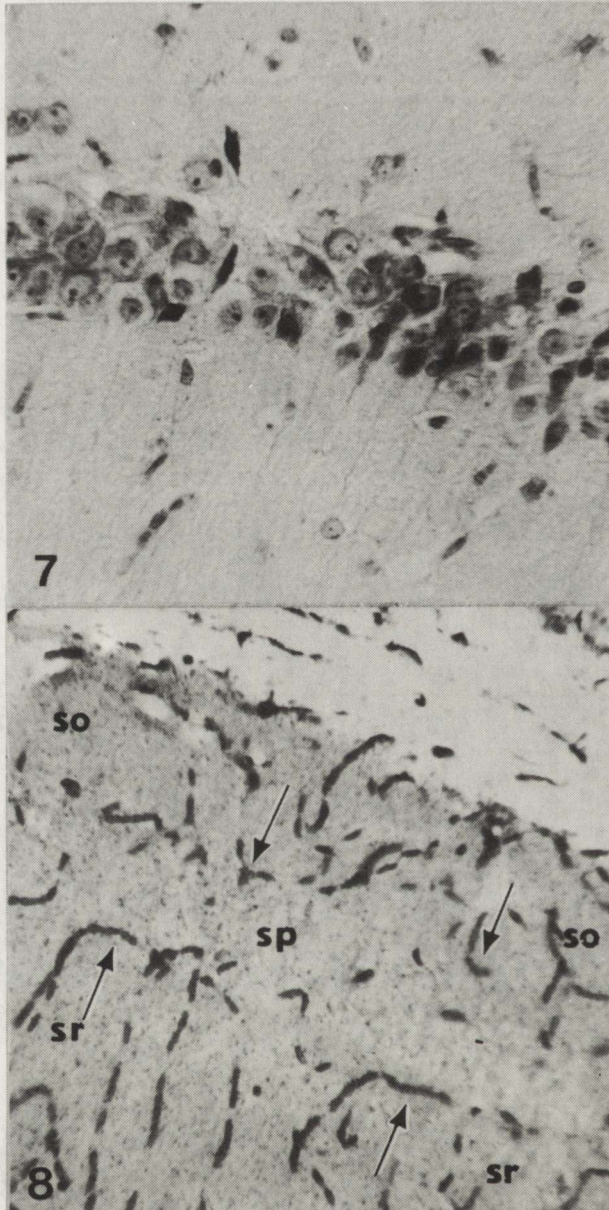


Fig. 7. Exp. animal: 5-min ischemia, 5-day survival. Immature pathological process: between normal pyramidal cells numerous neurons with feature of various types of degeneration. Cresyl violet. $\times 400$

Fig. 8. Control animal. In the vascular network of *stratum oriens* (so) and *stratum radiatum* (sr) on the border of *stratum pyramidale* (sp) characteristic capillary loops (arrow) are visible. Scarce capillaries penetrating *stratum pyramidale*. Pickworth method. $\times 400$

- 2) preserved pyramidal cells of CA1 sector on one side and their partial loss, ranging from 30 to 75% in the opposite hemisphere (Fig. 2),
- 3) total neuronal loss in the medial part of CA1 sector with normal appearance of its lateral half in one hemisphere and either normal or totally damaged neuronal population on the other side (Fig. 3),
- 4) partial, although varying in degree, loss of CA1 pyramidal neurons in both hemispheres (Fig. 4).

The asymmetry of neuronal loss was accompanied in some animals by remarkable variances in maturation rate of the pathological process. Except cases, in which no pathological changes of CA1 sector pyramidal neurons were present (Fig. 5), in most of the animals with the neuronal abnormalities, the pathological process reached full maturation, understood as either total or partial neuronal loss with accompanying astroglial proliferation (Fig. 6), within 5 days after brain ischemia. However, in 20% of these animals maturation of the pathological process seemed to be extended beyond this period, as indicated by differences in morphological picture of CA1 pyramidal neurons. On the background of highly rarefied pyramidal cell population, alongside with normally looking neurons, numerous pyramidal cells with features of degeneration (shrinkage, hyperchromasia, central chromatolysis of different intensity) were present (Fig. 7).

Benzidine staining visualized characteristic structure of hippocampal vascular network. In the CA1 sector it was moderately dense in both cortical layers neighbouring pyramidal cell bodies and strikingly scanty in the pyramidal layer (Fig. 8). Radially oriented vessels of *stratum radiatum* when approaching pyramidal layer banded in a characteristic way forming loops. Identical arrangement of capillaries was typical for *stratum oriens*. In *stratum pyramidale*, containing densely packed cell bodies of pyramidal neurons, only very few fragments of capillaries passing between them were seen. This sharply contrasted with other sectors of Ammon's horn in which relatively dense net of capillaries was observed in less populated pyramidal layers.

DISCUSSION

The results of our studies, contrary to the observation of Suzuki et al. (1983a, b), indicate that damage and loss of the pyramidal neurons in the CA1 sector of Ammon's horn is not a permanent finding in the temporary forebrain ischemia in the Mongolian gerbils. Data presented in this paper, are based on large and sufficient for statistical analysis number of observations to prove a marked variability of individual susceptibility of Mongolian gerbils to the ischemic incident, the phenomenon stressed by us in our earlier papers (Mossakowski, Gadamski 1985; 1987a, b). In the search for explanation of differences in the picture and extent of morphological damage to the CA1 sector neurons, first comes the question whether the operation was correctly performed, above all, whether the temporary closure of the common carotid

arteries was complete. The possibility of such a technical error seems to be excluded by the construction of Heifetz and Vasargil clips. The main argument, however, against reservations of this kind seem to be the asymmetrical lesions observed in our material. In this respect particularly noteworthy are cases in which, after 5 or 7.5 min of ischemia, neuronal loss was limited to the proximal half of the CA1 sector, whereas its distal half and the whole sector on the contralateral side remained intact. This type of asymmetry seems most convincing and ruling out completely any technical incorrectness.

The other factor underlying great differences in our material may result from origin of animals from our own breeding, conducted on the principle of flock not strain, in which the use of a sibling population is rigorously excluded, and only distant relatives are used. It is possible that this way of breeding favours appearance of malformations, characteristic for this species in the intra- and extracerebral vascular network. This may find its reflection in the individually differentiated susceptibility to ischemia.

Our observations seem to indicate that severe damage of the pyramidal neurons should not be exclusively attributed to their special susceptibility to the ischemic incident as generally accepted in the literature, but in addition to the specific angioarchitectonics of CA1 sector. Particularly noteworthy is the dense cell arrangement in this segment, which hardly finds parallel not only in the remaining sectors of Ammon's horn but also in other parts of the CNS. The number of perfusing capillaries is found to be inversely proportional to the density of the neurons. The number of capillaries in the CA1 sector in Mongolian gerbils is 20% lower than in the neighbouring CA3 sector and in the cerebral cortex (Imdahl, Hossmann 1986). Similarly, Weiss et al. (1982) demonstrated on the basis of morphometric analysis, a remarkably lower density of the capillary network in the Ammon's horn in the rats as compared with that in the cerebral cortex. Quantitative differences in vascularization of particular hippocampal segments, demonstrated by Imdahl and Hossmann (1986) are supplemented by the specific configuration of capillaries, as visualized in our benzidine preparations, where they form loops in the hippocampal layers adjacent to pyramidal neurons. Such a configuration of capillaries may be conducive to the turbulence of the morphotic blood elements leading finally to the formation of microthrombi disturbing or totally blocking blood perfusion in the postischemic period. It seems that the microthrombi in these conditions are not transient thrombocyte aggregations, but are of an irreversible nature. This contention was supported by further observations of Imdahl and Hossmann (1986), who demonstrated that reduced volume of circulating blood in the CA1 sector persisted with a tendency to aggravation in time, up to the 7th day after transient forebrain ischemia in Mongolian gerbils.

Assuming the importance of the above mentioned hemodynamic disturbances in the development of morphological abnormalities in the CA1 sector, some additional factors resulting from brain ischemia should be taken into

consideration. These concern mostly the reaction of blood platelets. Drastic reduction of blood supply to the brain due to bilateral ligation of the carotid artery evokes a chain of functional and metabolic reactions, both local and systemic. Autoregulatory mechanisms set up in these pathological conditions result among others, in remarkable changes in the level of numerous biologically active substances such as adenosine, serotonin, catecholamines and others, which besides other consequences, may activate cell membranes of the blood platelets. This in turn, evokes a series of cellular reactions, including calcium ion translocation, changes in the adenyl cyclase activity, resulting in altered cyclic-AMP content as well as changes in the phospholipase activity reflecting on the functional state of the cell membrane, synthesis of prostaglandins and a number of other processes (Detwiler et al. 1978; Fitzpatrick, Gorman 1979; Serutton, Egan 1979). All those changes lead to the formation of thrombocyte aggregates and microthrombi both in the CNS and in other body organs. Hossmann et al. (1980) describing the relatively frequent appearance of microthrombi in various body organs as a consequence of brain ischemia, stressed their exceptional occurrence in the CNS. On the other hand, Pluta et al. (1992) had recently demonstrated the formation of microthrombi in the cerebral blood vessels resulting from global cerebral ischemia of the CNS. They were randomly distributed in various brain structures. Pluta (1992) believes that this pathological process is connected with disturbed functional balance between tromboxan and prostacyclin, reflecting altered relations between platelets and vascular endothelium.

The above mentioned mechanism referring to the hemodynamic and rheologic alterations as a pathogenic factors in the development of the ischemic brain damage, due to their general nature, can not explain by themselves selective involvement of the CA1 sector of Ammon's horn. However, concomitance of scarcity of vascularization and spacial arrangement of vascular network specific for this area, facilitating local hemodynamic disturbances on one hand, and changes in the functional state of thrombocytes on the other, may favor selective damage of the CA1 pyramidal neurons, exposed due to their innervation on the action of excitotoxic amino acid neurotransmitters. The participation of vascular factor seems to explain observed variations in the intensity and extent of cellular lesions. In that context we should admitt that the protective action of indomethacin, prostacyclin and calcium channel blocker – nimodipine against ischemic lesions of CA1 pyramidal neurons, observed in our previous studies (Mossakowski, Gadamski 1985; 1987a, b) can be, at least in part, attributed to the influence of these substances on the hemodynamic and rheologic changes occurring in this area.

Therefore, it seems justified to come back to the old neuropathological discussion concerning the role of metabolic and functional as well as vascular factors in the pathogenesis of the selective vulnerability of CA1 sector. The specific angioarchitectonics of this hippocampal structure facilitating local hemodynamic and rheologic abnormalities may play an important role in this process.

ASYMETRYCZNE USZKODZENIA ODCINKA CA1 ROGU AMONA
PO KRÓTKOTRWAŁYM NIEDOKRWIENIU MÓZGU
U CHOMIKÓW MONGOLSKICH

Streszczenie

Badania przeprowadzono na 98 trzymiesięcznych chomikach mongolskich, u których wywoływano 5- lub 7,5-minutowe niedokrwienie mózgu przez podwiązanie obu tętnic szyjnych. Czas przeżycia zwierząt po niedokrwieniu wynosił 5 dni. Parafinowe skrawki mózgu barwiono fioletem krezylu i wg metody Klüvera-Barrery. Oceniono również metodą benzydynową Pickwortha sieć naczyńową w hipokampie chomików nie poddanych żadnym zabiegom doświadczalnym.

Wykazano znaczne zróżnicowanie osobnicze wrażliwości zwierząt na niedokrwienie mózgu wyrażające się różnicami nasilenia strukturalnych uszkodzeń odcinka CA1 rogu Amona. U 41,7% zwierząt nie stwierdzono w tym obszarze żadnych zmian neuronalnych. Całkowity zanik neuronów CA1 stwierdzono u 25% zwierząt. Na szczególną uwagę zasługiwała niesymetryczność uszkodzeń komórek piramidowych sektora CA1 obserwowana w 18,4% przypadków.

Wykazano różnice angioarchitektoniki odcinka CA1 w porównaniu z sąsiednimi obszarami hipokampa. W warstwie piramidowej sektora CA1 występowały jedynie pojedyncze naczynia krwionośne. W przylegających do komórek piramidowych warstwach granicznej i promienistej tego sektora wykazano obecność charakterystycznych luków i skrętów naczyń położonych na tle stosunkowo gęstej sieci kapilarnej. Były one nagromadzone na pograniczu warstwy komórek piramidowych.

Wysunięto przypuszczenie, iż specyficzne ukształtowanie przestrzenne sieci naczyniowej w sektorze CA1, sprzyjające miejscowym zaburzeniom hemodynamicznym w następstwie przebytego niedokrwienia mózgu, może stanowić istotny czynnik patogenetyczny kształtujący zarówno wybiórczą wrażliwość na niedokrwienie komórek piramidowych tego odcinka, jak i zróżnicowaną intensywność i rozległość uszkodzeń neuronalnych.

REFERENCES

1. Collingridge GL, Kehl SJ, Loo R, McLennan H: Effects of kainic acid and other amino acids on synaptic excitation of rat hippocampus. I. Extracellular analysis. *Exp Brain Res*, 1983, 52, 170–178.
2. Detwiler TC, Charo JF, Feinman RD: Evidence that calcium regulates platelet function. *Thrombos Haemostas*, 1978, 40, 207–211.
3. Drejer J, Benveniste H, Diemer NH, Schousboe A: Cellular origin of ischemia-induced glutamate release from brain tissue *in vivo* and *in vitro*. *J Neurochem*, 1985, 45, 145–151.
4. Fitzpatrick FA, Gorman RR: Regulatory role of cyclic adenosine 3'5'-monophosphate on the platelets cyclooxygenase and platelet function. *Biochem Biophys Acta*, 1979, 582, 44–58.
5. Gajkowska B, Gadamski R, Mossakowski MJ: Influence of short-term ischemia on the ultrastructure of hippocampal gyrus in Mongolian gerbils. II Electron microscopic picture of synapses in early postischemic period (In Polish). *Neuropatol Pol*, 1989, 27, 339–366.
6. Hossmann V, Hossmann K-A, Takagi S: Effect of intravascular platelet aggregation on blood recirculation following prolonged ischemia of the cat. *Brain*, 1980, 222, 159–170.
7. Imdahl A, Hossmann A: Morphometric evaluation of postischemic capillary perfusion in selectively vulnerable areas of gerbil brain. *Brain Res*, 1982, 239, 57–69.
8. Ito U, Spatz M, Walker JT, Jr, Klatzo I: Experimental cerebral ischemia in Mongolian gerbils. I. Light microscopic observations. *Acta Neuropathol (Berl)*, 1975, 32, 209–223.
9. Kirino T: Delayed neuronal death in the gerbil hippocampus following ischemia. *Brain Res*, 1982, 239, 267–271.
10. Meldrum B, Evanös M, Griffiths T, Simon R: Ischaemic brain damage: the role of excitatory activity and of calcium entry. *Br J Anaesthesiol*, 1985, 57, 44–46.

11. Mossakowski MJ, Gadamski R: Influence of indomethacin on ischemic damage of CA1 sector of Ammon's horn in Mongolian gerbils (In Polish). *Neuropatol Pol*, 1985, 23, 493–506.
12. Mossakowski MJ, Gadamski R: Influence of prostacyclin PgI_2 and indomethacin on the ischemic damage of CA1 sector of Ammon's horn in Mongolian gerbils (In Polish). *Neuropatol Pol*, 1987a, 25, 21–34.
13. Mossakowski MJ, Gadamski R: Influence of the calcium channel blocker on the ischemic changes in sector CA1 neurons of Ammon's horn in Mongolian gerbils (In Polish). *Neuropatol Pol*, 1987b, 25, 439–450.
14. Mossakowski MJ, Gajkowska B, Tsitsishvili A: Ultrastructure of neurons from the CA1 sector of Ammon's horn in short-term cerebral ischemia in Mongolian gerbils. *Neuropatol Pol*, 1989, 27, 39–53.
15. Nadler JV, Perry BV, Cotman CW: Preferential vulnerability of hippocampus to intraventricular kainic acid. In: Kainic acid as a tool in neurobiology. Eds: EG McGeer, JW Olney, PL McGeer. Raven Press, New York, 1978, pp 219–237.
16. Pluta R: Trial of prostacyclin application in the prevention of postischemic cerebral damage in rabbits submitted to global cerebral ischemia (In Polish). PhD.-thesis. Medical Research Centre of PASci, Warsaw, 1992, pp 32–36.
17. Pluta R, Lossinsky AS, Mossakowski MJ, Faso L, Wisniewski HM: Reassessment of a new model of complete cerebral ischemia in rats. *Acta Neuropathol (Berl)*, 1992, 83, 1–11.
18. Pulsinelli WA: Deafferentiation of hippocampus protects CA1 pyramidal neurons against ischemic injury. *Stroke*, 1985, 16, 144–146.
19. Scrutton MC, Egan CM: Divalent cation requirements for aggregation of human blood platelets and the role of the anticoagulant. *Thrombos Res*, 1979, 14, 713–727.
20. Simon RP, Swan JH, Griffiths BS: Blockade of N-methyl-D-aspartate receptors may protect against ischemic damage in the brain. *Science*, 1984, 226, 850–852.
21. Suzuki R, Yamaguchi T, Kirino F, Orzi P, Klatzo I: The effects of 5-minute ischemia in Mongolian gerbils. I. Blood-brain barrier, cerebral blood flow, and local cerebral glucose utilization changes. *Acta Neuropathol (Berl)*, 1983a, 60, 207–216.
22. Suzuki R, Yamaguchi T, Choh-Luh Li, Klatzo I: The effects of 5-minute ischemia in Mongolian gerbils. II. Changes of spontaneous neuronal activity in cerebral cortex and CA1 sector of hippocampus. *Acta Neuropathol (Berl)*, 1983b, 60, 217–222.
23. Spielmeyer W: Zur Pathogenese örtlich elektiver Gehirnveränderungen. *Z Ges Neurol Psychiatr*, 1925, 99, 756–776.
24. Vogt C, Vogt O: Der Begriff der Pathoklise. *J Psychol Neurol*, 1925, 31, 245–262.
25. Weiss HR, Buchweitz E, Murtha TJ, Auletta M: Quantitative regional determination of morphometric indices of the total and perfused capillary network in rat brain. *Circ Res*, 1982, 51, 494–503.

Authors' address: Department of Neuropathology, Medical Research Centre, PASci, 3 Dworkowa St, 00-784 Warsaw, Poland

ROMAN GADAMSKI, HALINA KROH

IMMUNOREACTIVITY OF ASTROGLIA IN THE HIPPOCAMPUS OF THE MONGOLIAN GERBIL DURING SHORT SURVIVAL FOLLOWING BRIEF ISCHEMIA

Department of Neuropathology, Medical Research Centre, Polish Academy of Sciences, Warsaw

Mongolian gerbils subjected to 5-min cerebral ischemia by common carotid artery ligation were decapitated after 24, 48, 72 and 96 h of survival to investigate the immunoreactivity of astroglia in the hippocampus. The sections from formalin-fixed, paraffin-embedded brains were stained histologically and with ABC method (Hsu et al. 1981). Control animals (normal and sham-operated) presented positive GFAP immunostaining in corpus callosum, in subventricular regions, in temporal subcortical white matter, in fimbria hippocampi and perivascularly in *stratum lacunosum-moleculare*. Experimental animals, independently of postischemic survival time showed various individual GFAP reactivity. Differences concerning the number and localization of immunoreactive astrocytes in both cerebral hemispheres of the same animal stressed the asymmetry of the reaction. The authors did not observe any accumulation of reactive astrocytes in the area of synaptic terminals of glutaminergic fibers (mossy fibers, Schaffer's collaterals) or in the neighbourhood of CA1 and CA3 sectors. In particular, there was complete lack or only sporadic reactive astrocytes among pyramidal neurons of CA1 and among granular cells of dentate gyrus in all examined animals.

Key words: *brain ischemia, hippocampus, astrocytic reactivity.*

Selective damage to the CA1 sector of Ammon's horn manifested by loss of pyramidal neurons is still the object of keen interest. In spite of multidisciplinary studies on the problem, the base of the selective vulnerability of the hippocampus to brief cerebral ischemia is not yet fully recognized. An essential pathogenic factor is the enhanced bioelectric activity of the CA1 sector pyramidal neurons which appears during the first postischemic day (Suzuki et al. 1983). After-effects in the form of impairment of intracellular calcium homeostasis and blocking of protein synthesis can be the essential reason for cellular death. The responsible factor producing cytotoxic excitation of pyramidal neurons is glutamate release by mossy fiber terminals and Schaffer's

collaterals. Considering the anatomical localization of the synaptic endings of excitatory fibers (mossy fibers, Schaffer's collaterals) the abundant extracellular accumulation of glutamate should take place in CA1 and CA3 sectors of Ammon's horn. This hypothesis might be confirmed by the topography of the immunoreactive astroglia in the hippocampus. Astrocytes are unique elements for the glutamate uptake and capable of being excited by this neurotransmitter via activation of their kainic and quisqualate receptors (Pearce et al. 1986). The cellular excitation might be confirmed by changes in GFAP (glial fibrillary acidic protein) content being in line with the results of Wang et al. (1991), who after injection of N-methyl-D-aspartate (NMDA) into the dorsal hippocampus observed a gradual increase of GFAP content starting on the third experimental day.

The purpose of the study was immunohistochemical evaluation of the dynamics of GFAP reactivity in the early postischemic stage and verification of eventual privileged localization of reactive astrocytes in certain layers of the dorsal hippocampus in Mongolian gerbil.

MATERIAL AND METHODS

The study was performed on 24 Mongolian gerbils from the stock breed in the animal farm of our Institute. The animals (ca. 75 g body weight) were allocated to 5 groups: one control and four experimental groups with a survival of 24, 48, 72 and 96 hours after 5-min cerebral ischemia, produced by bilateral closing of common carotid arteries with Heifetz clips. The procedure was performed under ether anesthesia. The control (2 normal and 2 sham-operated) and experimental animals were sacrificed by decapitation. The brains were fixed in 4% formalin, embedded in paraffin and cut into 10 μ m thick sections. GFAP immunoreactivity was investigated with polyclonal serum (Dacopatts, Copenhagen) solution 1:500, according to avidin-biotin-complex (ABC) method (Hsu et al. 1981).

RESULTS

In animals of both control groups GFAP-positive immunostaining was observed in the subependymal regions of third and lateral ventricles, in corpus callosum, in subcortical temporal white matter, in fimbria hippocampi and *stratum lacunosum moleculare* of hippocampus (Fig. 1).

Experimental group I: 24 h after ischemia the GFAP immunoreaction in 2 animals was not detected. Other 2 animals presented some slightly stained astrocytes in *stratum radiatum* (Fig. 2), whereas one showed intense unilateral astroglial reaction in the hilus and among pyramidal cells of the CA4 sector (Fig. 3).

Group II (48 h survival): Differing topography of positive GFAP immunostaining was characteristic also for animals of this group. One gerbil did

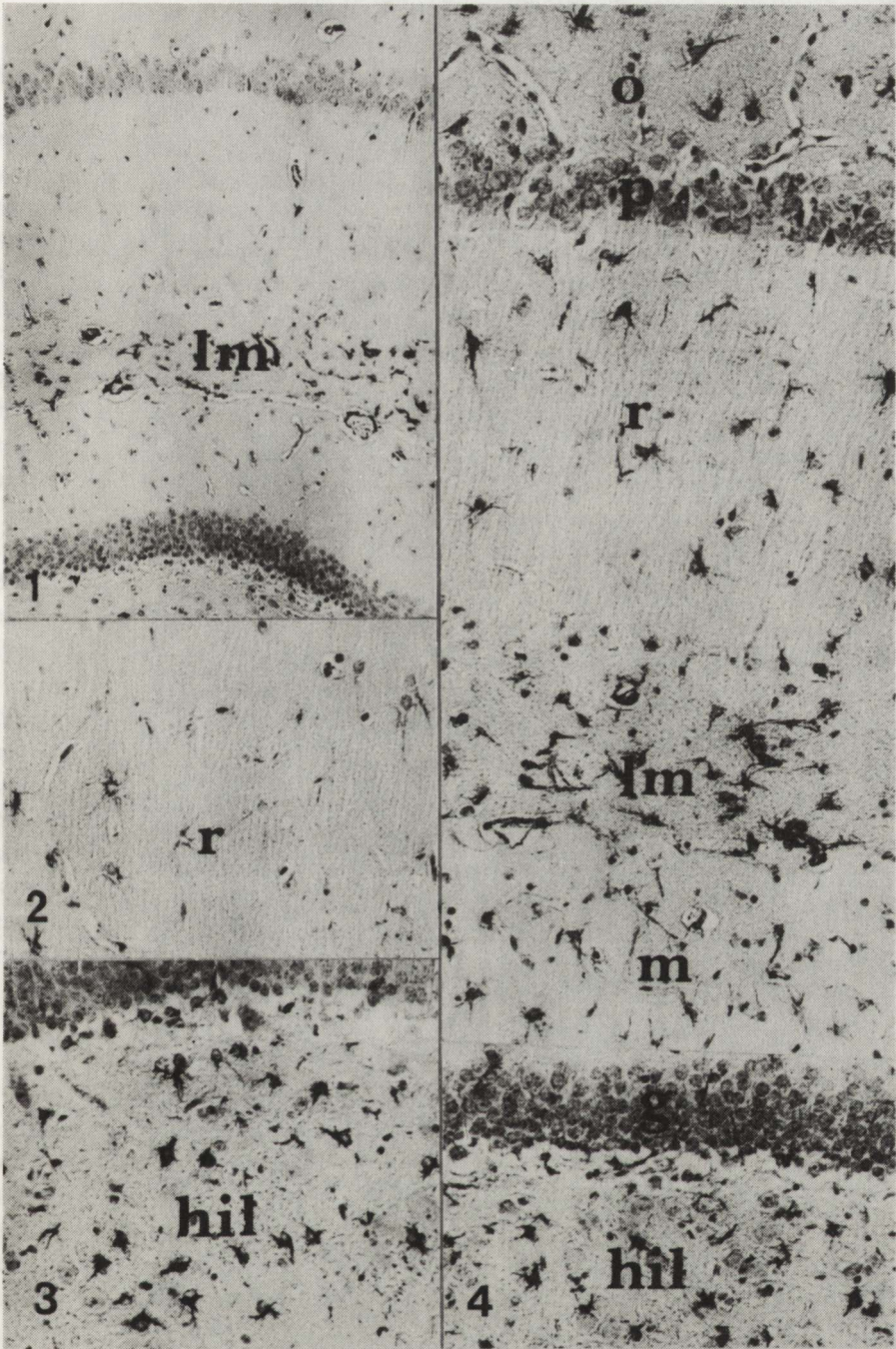


Fig. 1. Shame-operated gerbil. Positive GFAP-reaction in *stratum lacunosum moleculare* (lm). $\times 200$

Fig. 2. Slight GFAP immunostaining of reactive astrocytes in *stratum radiatum* (r.) 24 h postischemic survival. $\times 200$

Fig. 3. Intensive GFAP reaction in *hilus* (hil). 24 h postischemic survival. $\times 200$

Fig. 4. Frontal section of dorsal hippocampus. Reactive astrocytes in all layers except CA1 sector of pyramidal cells (p) and granular cells (g) of dentate gyrus. o — *stratum oriens*, r — *stratum radiatum*, lm — *stratum lacunosum moleculare*, m — *stratum moleculare*, g — *stratum granulosum*, hil — *hilus*. 48 h postischemic survival. $\times 200$

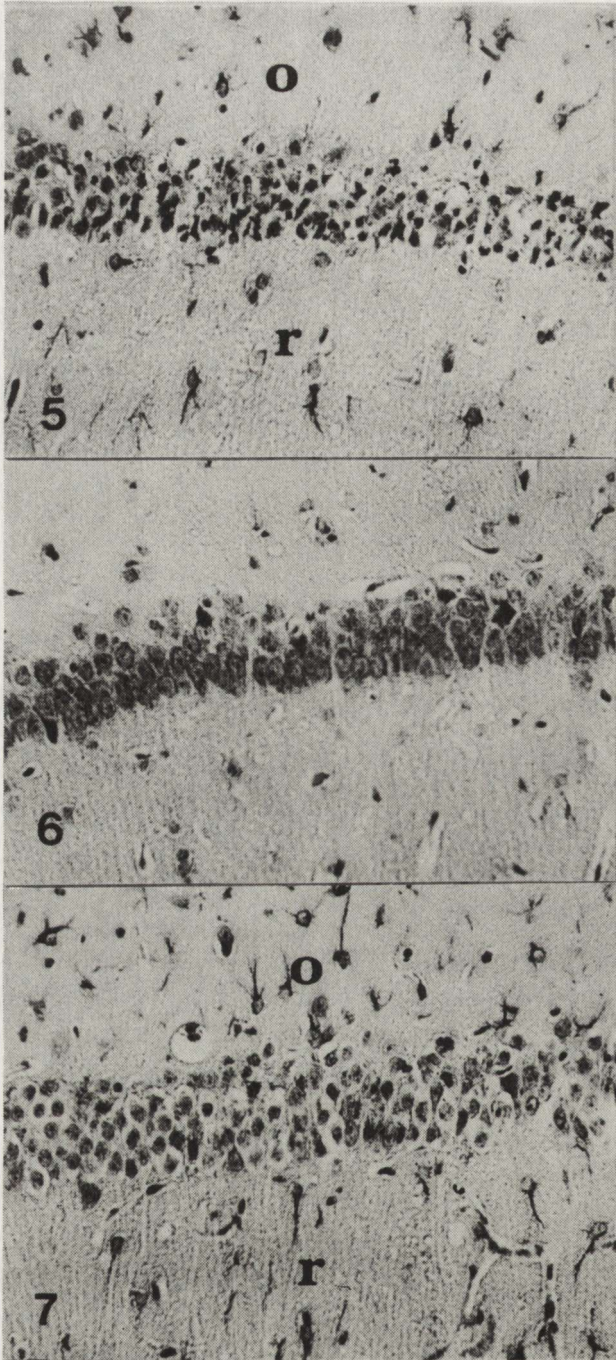


Fig. 5. Unilateral loss of CA1 sector pyramidal neurons. Few reactive astrocytes in *stratum oriens* (o), and *stratum radiatum* (r). 72 h postischemic survival. $\times 200$

Fig. 6. Negative GFAP reaction. 96 h postischemic survival. $\times 200$

Fig. 7. Intensive GFAP reaction in *stratum oriens* (o) and *stratum radiatum* (r). 96 h postischemic survival. $\times 200$

not present any reactive astrocytes in any hippocampal layer. In other 3 animals immunoreactive astroglia was demonstrated in all hippocampal formations. Our attention was attracted by more intense astrocyte immunostaining in deep hippocampal layers, in particular the hilus, *stratum lacunosum moleculare* and *stratum lacunosum*. Only one gerbil displayed full symmetry of astroglial reaction in both hemispheres (Fig. 4). The lack of immunopositive astrocytes among pyramidal cells in CA3 and in the granular cell layers was also bilateral.

Group III (72 h survival): One of the animals of this group presented a very seldom observed early maturation of pathological process (Fig. 5). This phenomenon was expressed by unilateral loss of pyramidal neurons in the CA1 sector. GFAP positive astrocytes were relatively more numerous at the side of the injured neurons than contralaterally. Other animals were characterized by a low intensity of immunostaining in some astrocytes.

Group IV (96 h survival): The GFAP reaction in two animals was not detected (Fig. 6), whereas other 3 presented intensive immunostaining of reactive astrocytes (Fig. 7) in all hippocampal structures except pyramidal cell layer in the CA1 sector.

Summing up the results in all groups it should be stressed that experimental animals, independently of their postischemic survival time, showed marked individual variability of GFAP immunostaining. Besides, there was no tendency of reactive astrocytes to become visualized in definite hippocampal structures. The differences in number and localization of GFAP-positive astroglia in both cerebral hemispheres of the same animal emphasize frequent asymmetry of the reaction. Noteworthy is the total lack or only sporadic reactive astrocytes among pyramidal cells of the CA1 sector and among granular cells of the dentate gyrus in all investigated animals.

DISCUSSION

Our present and previous investigations prove that the time of postischemic maturation of pathologic process and the intensity of morphological damage to the hippocampus is not a constant value (Gadamski, Mossakowski 1992). In numerous cases, in spite of exposure to ischemia, the CA1 sector stained routinely does not differ from control tissue. The pathological process which develops as a result of short-term cerebral ischemia reaches full maturation in the 4th or 5th day of survival and is expressed by the loss of CA1 neurons and in consequence, appearance in their place of a reactive glial cells. However, there are some animals with neuronal changes visible in 72 hours after ischemic incident.

The second difference concerns the number of lost pyramidal cells, and frequent asymmetrical pattern of pathological lesions. The factors responsible for selective neuronal death in the hippocampal CA1 sector have not been fully determined yet. Among the pathogenic factors suggested by the literature, the most widely discussed is the neurotoxic influence of glutamate. In synapto-

somes this amino acid neurotransmitter is accumulated in two basic reservoirs (Sanchez-Prieto, Gonzalez 1988). One of them are the synaptic vesicles from which glutamate can be released by energy-dependent exocytosis (Sanchez-Prieto et al. 1987) or is Ca^{2+} -dependent (Nicholls, Sihra 1986; Nicholls et al. 1987). The other reservoir of glutamate is the cytoplasm from which it can penetrate through cellular membranes into the extracellular space. In conditions of oxygen deficit both the metabolism and release of neurotransmitters changes (Gibson et al. 1975; Erecińska et al. 1984) and results in irreversible neuronal lesions (Sjesjö 1981).

During the sequence of events appearing during ischemia the decrease of the level of high-energy compounds and alterations in the gradient of ions concentrations initiate excessive release of glutamate from its cytoplasmic pool (Sanchez-Prieto, Gonzalez 1988). In the hippocampus one of sites of glutamate release are the mossy fibers originating in the granular cells of the dentate gyrus and forming numerous synaptic contacts with proximal parts of apical dendrites of the CA3 sector pyramidal neurons (Mourre et al. 1989). Another site of glutamate release are Schaffer's collaterals originating in fimbria hippocampi which enter into synaptic contacts with pyramidal neurons of the CA1 sector. Fiber architectonics of glutaminergic pathways allow the assumption that following transient cerebral ischemia the highest extracellular concentration of released glutamate should take place in the CA1 and CA3 sectors. Pyramidal neurons of both sectors should be equally activated by glutamate, whereas activation of their NMDA receptors would provide for high intracellular accumulation of calcium ions, resulting in neuronal death. Considering these phenomena the reason for selective injury to CA1 is still not explained.

Another unusual phenomenon observed by us is the high variability of distribution of GFAP immunoreactive astroglia. In numerous cases transient cerebral ischemia either does not provoke any changes or the immunoreactive astrocytes appear haphazardly in various hippocampal layers. Moreover, due to anatomical conditions the CA1 and CA3 sectors and their closest surrounding should be an area of marked glial immunoreactivity. Pearce et al. (1986) established that astrocytes are capable not only of glutamate uptake, but can be activated by the latter via quisqualate and kainic receptor activation. Occurrence of GFAP-positive astrocytes in the hilus as early as 24 hours after ischemic incident can be explained by early excitation of granular cells, followed by glutamate release from the perforant pathway and mossy fibers.

Some significance in the pathogenesis of ischemia is attributed to zinc, which in normal conditions accumulates in synapses (Frederickson et al. 1983; Frederickson, Danscher 1989), and can, like glutamate, be released during paroxysmal activity (Assaf, Chung 1984; Aniksztejn et al. 1987), after injection of kainic acid (Slowiter, Damiano 1981) or following electric stimulation of the

perforant pathway (Slowiter 1987). Tonder et al. (1990) detected release of zinc also in experimental cerebral ischemia. The authors found intracellular accumulation of zinc in acidophilic neurons, mainly in the hilus, and stress its function in the pathophysiology of seizures and neuronal death. Zinc ions can exert a direct neurotoxic influence (Choi et al. 1988) or interact with glutamate receptors (Peters et al. 1987; Koh, Choi 1988). Early occurrence of reactive astrocytes in the hilus can be connected with the death of some pyramidal neurons in this region. According to Tonder et al. (1990) hilar neurons are very sensitive to ischemia and their early degeneration is connected with an intracellular accumulation of zinc.

In conclusion, we are inclined to believe that:

1. The lack of GFAP reaction, notwithstanding the experienced ischemia, is characteristic for the group of animals in which brief ischemia does not alter the morphology of the CA1 sector.

2. Localization of reactive astrocytes does not correlate topographically with the areas of the hippocampus which following ischemia should accumulate a large glutamate pool extracellularly. Such areas are synaptic terminals of mossy fibers in the CA3 sector and Schaffer's collaterals in CA1.

3. In spite of the anatomically assessed topography of areas which exert their glutamate excitotoxicity on degeneration of pyramidal neurons, the CA3 hippocampal sector is not affected, whereas degenerative changes only influence CA1 sector.

IMMUNOREAKTYWNOŚĆ ASTROGLEJU W HIPOKAMPIE CHOMIKÓW MONGOLSKICH WE WCZESNYCH OKRESACH PO KRÓTKOTRWAŁYM NIEDOKRWIENIU MÓZGU

Streszczenie

Badano immunoreaktywność astrogleju u chomików mongolskich, u których wywołano 5-minutowe niedokrwienie mózgu. Zwierzęta dekapitowano 24, 48, 72 i 96 godzin po niedokrwieniu. U zwierząt kontrolnych dodatni odczyn GFAP obserwowano w spoidle wielkim, pod wyściółką komór bocznych i komory trzeciej, w podkorowej istocie białej okolicy skroniowej, a w hipokampie przynaczyniowo w *stratum lacunosum-moleculare* i w strzępku. U zwierząt doświadczalnych, niezależnie od czasu przeżycia po niedokrwieniu, intensywność odczynu GFAP wykazywała znaczną zmienność osobniczą. Różnice dotyczące ilości oraz lokalizacji immunoreaktywnego astrogleju w obu półkulach mózgu tego samego zwierzęcia podkreślały często spotykany niesymetryczny rozkład zmian strukturalnych. Nie obserwowano liczniejszych odczynowych astrocytów w obszarze zakończeń włókien glutaminergicznych (włókna pierzaste oraz kolaterale Schaffera) w obrębie odcinka CA1 i CA3 rogu Amona lub w ich sąsiedztwie. Na podkreślenie zasługuje całkowity brak odczynu lub tylko sporadyczna obecność immunoreaktywnych astrocytów wśród komórek piramidowych odcinka CA1 oraz wśród komórek ziarnistych zakrętu zębatego u wszystkich badanych zwierząt.

REFERENCES

1. Aniksztejn L, Charton G, Ben-Ari Y: Selective release of endogenous zinc from the hippocampal mossy fibers *in situ*. *Brain Res*, 1987, 404, 58–64.
2. Assaf SY, Chung SH: Release of endogenous Zn^{2+} from brain tissue during activity. *Nature*, 1984, 308, 734–736.
3. Benveniste H, Drejer J, Schousboe A, Diemer N: Elevation of extracellular concentrations of glutamate and aspartate in rat hippocampus during transient cerebral ischemia monitored by intracerebral microdialysis. *J Neurochem*, 1984, 43, 1369–1374.
4. Choi DW, Yokoyama M, Koh J: Zinc neurotoxicity in cortical cell culture, *Neuroscience*, 1988, 24, 67–69.
5. Erecińska M, Nelson D, Wilson OF, Silver IA: Neurotransmitter amino acid in the CNS. Regional changes in amino acid levels in rat brain during ischemia and reperfusion. *Brain Res*, 1984, 304, 9–22.
6. Frederickson CJ, Klitenick MA, Mauton WJ, Kirkpatrick JB: Cytoarchitectonic distribution of zinc in the hippocampus of man and the rat. *Brain Res*, 1983, 273, 335–339.
7. Frederickson CJ, Danscher G: Hippocampal zinc and storage granule pool: localization, physiochemistry and possible functions. In: Nutritional modulation of neural function. Eds: JE Morley, JH Walsh, MB Serman. Academic Press, San Diego, 1989.
8. Gadamski R, Mossakowski MJ: Asymmetric damages of the CA1 sector of Ammon's horn after short-term fore brain ischemia in Mongolian gerbil. *Neuropatol Pol*, 1992, 30, 207–217.
9. Gibson GE, Jope R, Blass JP: Reduced synthesis accompanying impaired oxidation of pyruvic acid in rat brain minces. *Biochem J*, 1975, 148, 17–23.
10. Hsu SM, Raine L, Fanger H: Use of avidin-biotin peroxidase complex (ABC) in immunoperoxidase techniques: a comparison between ABC and unlabelled antibody (PAP) procedures. *J Histochem Cytochem*, 1981, 29, 577–580.
11. Koh JY, Choi DW: Zinc alters excitatory amino acid neurotoxicity on cortical neurons. *J Neurosci*, 1988, 8, 2164–2171.
12. Mourre Ch, Ben-Ari Y, Bernardi H, Fosset M, Lazdunski M: Antidiabetic sulfonylurease: localization of binding sites in the brain and effects on the hyperpolarization induced by anoxia in hippocampal slices. *Brain Res*, 1989, 486, 159–164.
13. Nadler JV, Vaca KW, White WF, Lynch GS, Cotman CW: Aspartate and glutamate as possible transmitters of excitatory hippocampal afferents. *Nature*, 1976, 260, 538–540.
14. Nicholls DG, Sihra TS: Synaptosomes possess an exocytotic pool of glutamate. *Nature*, 1986, 321, 772–773.
15. Nicholls DG, Sihra TS, Sanchez-Prieto J: Calcium dependent and independent release of glutamate from synaptosomes monitored by continuous fluorometry. *J Neurochem*, 1987, 49, 50–57.
16. Pearce B, Albrecht J, Morrow Ch, Murphy S: Astrocyte glutamate receptor activation promotes inositol phospholipid turnover and calcium flux. *Neurosci Lett*, 1986, 72, 335–340.
17. Peters S, Koh J, Choi DW: Zinc selectively blocks the action of N-methyl-D-aspartate on cortical neurons. *Science*, 1987, 236, 589–593.
18. Sánchez-Prieto J, Sihra TS, Nicholls DG: Characterization of the exocytotic release of glutamate from guinea pig cerebral cortical synaptosomes. *J Neurochem*, 1987, 49, 58–64.
19. Sánchez-Prieto J, Gonzalez P: Occurrence of a large Ca^{2+} -independent release of glutamate during anoxia in isolated nerve terminals (synaptosomes). *J Neurochem*, 1988, 50, 1322–1324.
20. Siesjö BK: Cell damage in the brain: a speculative synthesis. *J Cereb Blood Flow Metab*, 1981, 1, 155–185.
21. Sloviter RS, Damiano BP: On the relationship between kainic acid-induced epileptiform activity and hippocampal neuronal damage. *Neuropharmacology*, 1981, 20, 1003–1011.
22. Sloviter RS: Decreased hippocampal inhibition and a selective loss of interneurons in experimental epilepsy. *Science*, 1987, 235, 73–76.

23. Suzuki R, Yamaguchi T, Choh-Luh L, Klatzo I: The effects of 5-minute ischemia in Mongolian gerbils: II Changes of spontaneous neuronal activity in cerebral cortex and CA1 sector of hippocampus. *Acta Neuropathol (Berl)*, 1983, 60, 217–222.
24. Tonder N, Johansson FF, Frederickson CJ, Zimmer J, Diemer NH: Possible role of zinc in the selective degeneration of dentate hilar neurons after cerebral ischemia in the adult rat. *Neurosci Lett*, 1990, 109, 247–252.
25. Wang S, Lees GJ, Rosengren LE, Karlsson JE, Stigbrand T, Hamberger A, Haglid KG: The effect of and N-methyl-D-aspartate lesion in the hippocampus on glial and neuronal marker proteins. *Brain Res*, 1991, 541, 334–341.

Authors' address: Department of Neuropathology, Medical Research Centre, PAsci, 3 Dworkowa St, 00-784 Warsaw, Poland

EWA MATYJA, ELŻBIETA KIDA

HIPPOCAMPAL DAMAGE *IN VITRO* AFTER DIFFERENT PERIODS OF OXYGEN DEPRIVATION

Department of Neuropathology, Medical Research Centre, Polish Academy of Sciences, Warsaw

The dynamics and pattern of postanoxic ultrastructural changes in organotypic culture of rat hippocampus was studied. The experiments were performed on 14-day-old cultures of rat hippocampus exposed to pure nitrogen atmosphere for 10- and 20-minutes and processed for electron microscope 2 and 24 h, 3 and 7 days post anoxia. The earliest changes following 10-min anoxia consisted of marked swelling of mitochondria and Golgi complex of neurons. The presynaptic terminals were preferentially affected. The protoplasmic astrocytes revealed swelling of the cytoplasm whereas the fibrous ones were relatively well preserved. Longer, 20-min anoxia resulted in profound ultrastructural changes even after short survival time. The tissue culture model of anoxia allow to study the direct effect of oxygen deprivation on cell morphology independently of any vascular and/or vasogenic factors.

Key words: *anoxia, rat hippocampus, tissue culture.*

The pathomechanism and morphology of ischemic cell damage have been studied in different models of cerebral ischemia and/or anoxia in numerous clinical and experimental investigations (Choi 1990). Recent studies suggest that vasogenic factors and the no-reflow phenomenon do not play a crucial role in the pathogenesis of neuronal death in ischemic/anoxic stress, as was previously postulated. A variety of other factors are thought to contribute to the development of irreversible ischemic brain damage. The disturbances in brain calcium homeostasis (Deleo et al. 1987; Deshpande et al. 1987; Siesjö, Wieloch 1985; Siesjö, Bengtsson 1989; Simon et al. 1984a), cellular lactic acidosis (Paljarvi 1984; Kraig et al. 1987; Fujiwara et al. 1992), overactivity of the excitatory amino acid transmitter system (Rothman 1984; Beneviste et al. 1984; Simon et al 1984b; Hagberg et al. 1985; Pellegrini-Giampetro et al. 1990) and Na^+ , K^+ -ATPase activity (Nagafuji et al. 1992) are more recently discussed.

Thus, it seemed interesting to study the direct effect of oxygen deprivation on cellular morphology independently of any vascular factors and brain blood

recirculation. This became possible due to the application of a tissue culture model. The aim of our study was to examine the dynamics and pattern of postanoxic ultrastructural changes in the hippocampal formation, a structure characterized by high vulnerability to various noxious factors such as hypoxia/ischemia, epilepsy or neurotoxins *in vivo* (Mouritzen Dam 1980; Perkins, Stone 1985).

MATERIAL AND METHODS

The organotypic cultures of hippocampal formation were prepared from 2-3-day-old Wistar rats. The hippocampus was dissected out under sterile conditions from both cerebral hemispheres, placed in dishes containing Eagle Minimal Essential Medium (MEM) and cut coronally into thin slices. Thin pieces of hippocampal tissue were placed on collagen-coated glass coverslips and put into a Carrel flask. The cultures were kept at 36.5°C in a medium consisting of 25% human serum and 75% MEM supplemented with glucose to a final concentration of 600 mg%, without antibiotics. The medium was renewed twice weekly. On the 14th day *in vitro*, when well differentiated neurons and numerous synaptic contacts were present (Matyja, Kida 1988), selected cultures were exposed to anoxia. They were transferred for 10 or 20 min to a pure nitrogen atmosphere in Carrel flasks adapted for permanent gas flow. Control cultures were grown in standard conditions. After 2 and 24 hours and 3 and 7 days post anoxia both experimental and control cultures were prepared for electron microscope examination. The cultures were rinsed in cacodylate buffer pH 7.2, fixed in 1.5% glutaraldehyde for 1/2 h, postfixated in 2% osmium tetroxide, dehydrated in graded alcohols and embedded in Epon 812. Ultrathin sections were counterstained with uranyl acetate and lead citrate and examined in a JEM 1200 EX electron microscope.

RESULTS

In the electron microscope, control cultures growing in standard conditions showed numerous mature, well preserved neuronal cells, rich in cytoplasmic organelles (Fig. 1). The neuropil was composed of densely packed neuronal and glial processes. Numerous synaptic contacts of various type were present (Fig. 2).

The ultrastructural alterations in the experimental groups of anoxia depended on both the duration of oxygen deprivation and survival time post anoxia.

10-minute anoxia

The earliest neuronal abnormality occurring 2 h post anoxia consisted in severe swelling of mitochondria and Golgi complex. The majority of neurons contained a great amount of enlarged mitochondria with disrupted, short

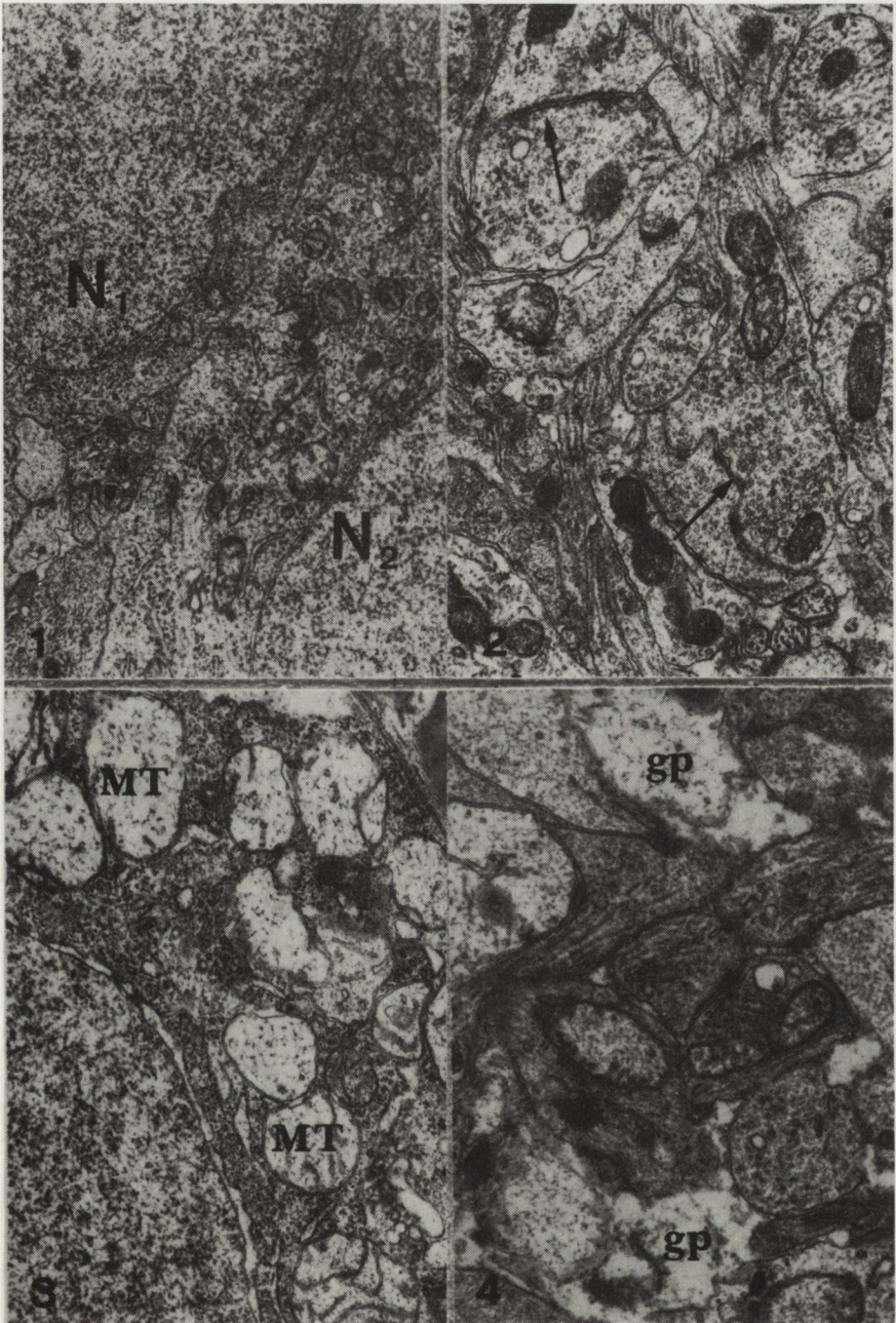


Fig. 1. Control culture of hippocampus 14-day-old *in vitro* (DIV). Two mature neurons (N1, N2). $\times 16000$

Fig. 2. Control culture 14 DIV. Densely packed neuropil with few synaptic contacts (arrows). $\times 16000$

Fig. 3. Culture of hippocampus 14 DIV, 2 hours after 10-minute anoxia. Fragment of neuron containing severely swollen mitochondria (MT). $\times 18600$

Fig. 4. The same culture. Less densely packed neuropil. Some swollen, electron-lucent glial processes (gp). $\times 24000$

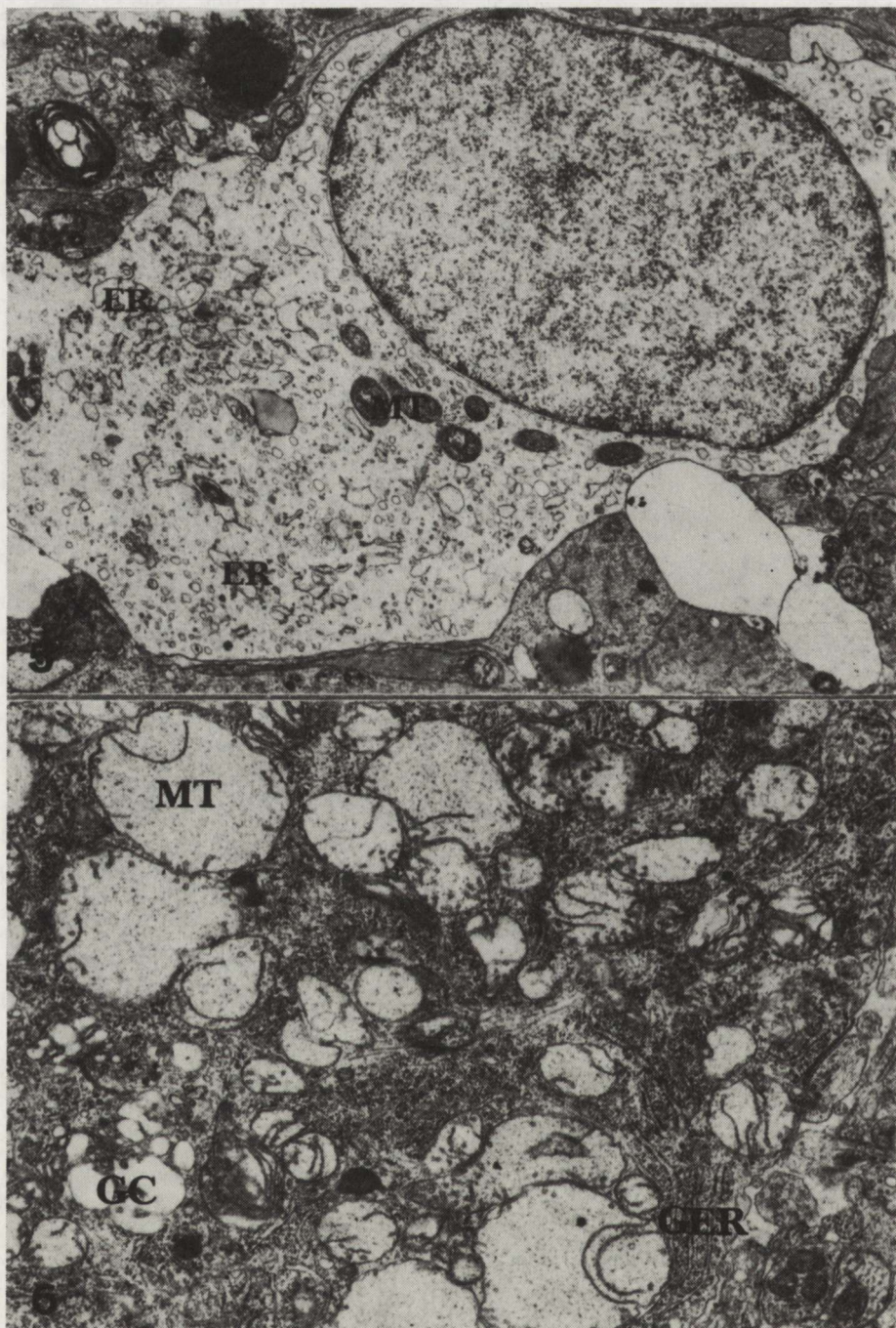


Fig. 5. The same culture. Protoplasmic astrocyte exhibiting swelling of the cytoplasm with dark mitochondria (MT) and dilated channels of endoplasmic reticulum (ER). $\times 12\,500$

Fig. 6. 3 days after 10-minute anoxia. Fragment of neuron displaying severely swollen mitochondria (MT). Well-preserved long channels of granular endoplasmic reticulum (GER) and dilated cisternae of Golgi complex (GC). $\times 15\,000$

cristae and light matrix (Fig. 3). Some mitochondria were less affected and revealed long, irregularly arranged cristae in a relatively electron-lucent matrix. In some neurons cisternae of the Golgi complex were swollen, whereas the channels of granular endoplasmic reticulum apparently were not dilated. The nucleus did not display any abnormalities. The neuropil was less densely packed and among the persisting neuronal processes, some moderately swollen, electron-lucent glial processes could be seen (Fig. 4). Some of the presynaptic boutons were electron-lucent and contained only few synaptic vesicles. The perikarya of protoplasmic astrocytes were markedly swollen and contained dark mitochondria and dilated channels of endoplasmic reticulum (Fig. 5). In the fibrous astrocytes expanded cisternae and vesicles of Golgi apparatus predominated.

The same pattern of ultrastructural alterations was encountered in the cultures examined 24 h post anoxia.

After 3 days, the majority of pyramidal neurons revealed more pronounced morphological changes. The most prominent alterations involved the mitochondria, which were still severely swollen with disrupted cristae and electron-lucent matrix. Some enlarged, swollen mitochondria contained only small fragments of cristae or they seemed entirely empty. The Golgi complex was swollen, but granular endoplasmic reticulum channels were only slightly distended or remained unaffected (Fig. 6). Many large pyramidal neurons exhibited a picture of vacuolar degeneration and contained in the cytoplasm numerous vacuoles and vesicles of various size (Fig. 7). In some of these vacuolized neurons the neurotubules were gathered at the periphery of the cytoplasm. At this time of observation the presynaptic terminals seemed to be preferentially affected. They were often electron-lucent, severely swollen and contained a small amount of synaptic vesicles accumulated close to the presynaptic membrane (Fig. 8). Some axonal boutons contained dark mitochondria and few synaptic vesicles near the synaptic cleft (Fig. 9). The dendritic spines seldom showed ultrastructural abnormalities, whereas post-synaptic large dendrites occasionally exhibited swollen mitochondria or vacuoles. A few axons containing multilaminar or dense bodies could also be seen. The protoplasmic astrocytes and their processes were moderately swollen and sometimes displayed an entirely "empty" cytoplasm containing delicate, floccular material. The fibrillary glial cells were relatively well preserved exhibiting swelling of the periphery of the cytoplasm and slightly dilated channels of granular endoplasmic reticulum. At this stage of postanoxic damage some fibrillary astrocytes were engaged in phagocytosis.

Seven days post anoxia both, relatively well preserved neurons, mainly granular ones, and severely damaged cells were observed. Most affected pyramidal neurons displayed a dark, condensed cytoplasm filled with damaged organelles, vacuoles and dense or multilaminar bodies. There were also many phagocytic cells containing numerous lipid droplets and multivesicular bodies. A lot of fibrillary astrocytes filled with gliofilaments was visible.



Fig. 7. The same culture. Pyramidal neuron exhibiting vacuolar degeneration. Numerous small vacuoles (V), more or less damaged mitochondria (MT) and relatively well preserved channels of GER. $\times 18\ 600$

Fig. 8. The same culture. Enlarged, extremely swollen presynaptic terminal (ax) containing few synaptic vesicles close to the presynaptic membrane (arrow). Unchanged dendritic spine. $\times 24\ 000$

Fig. 9. The same culture. Swollen axonal bouton (ax) containing dark mitochondrion (arrow) and small amount of synaptic vesicles in the vicinity of the synaptic cleft. Apparently normal dendritic spine. $\times 12\ 500$

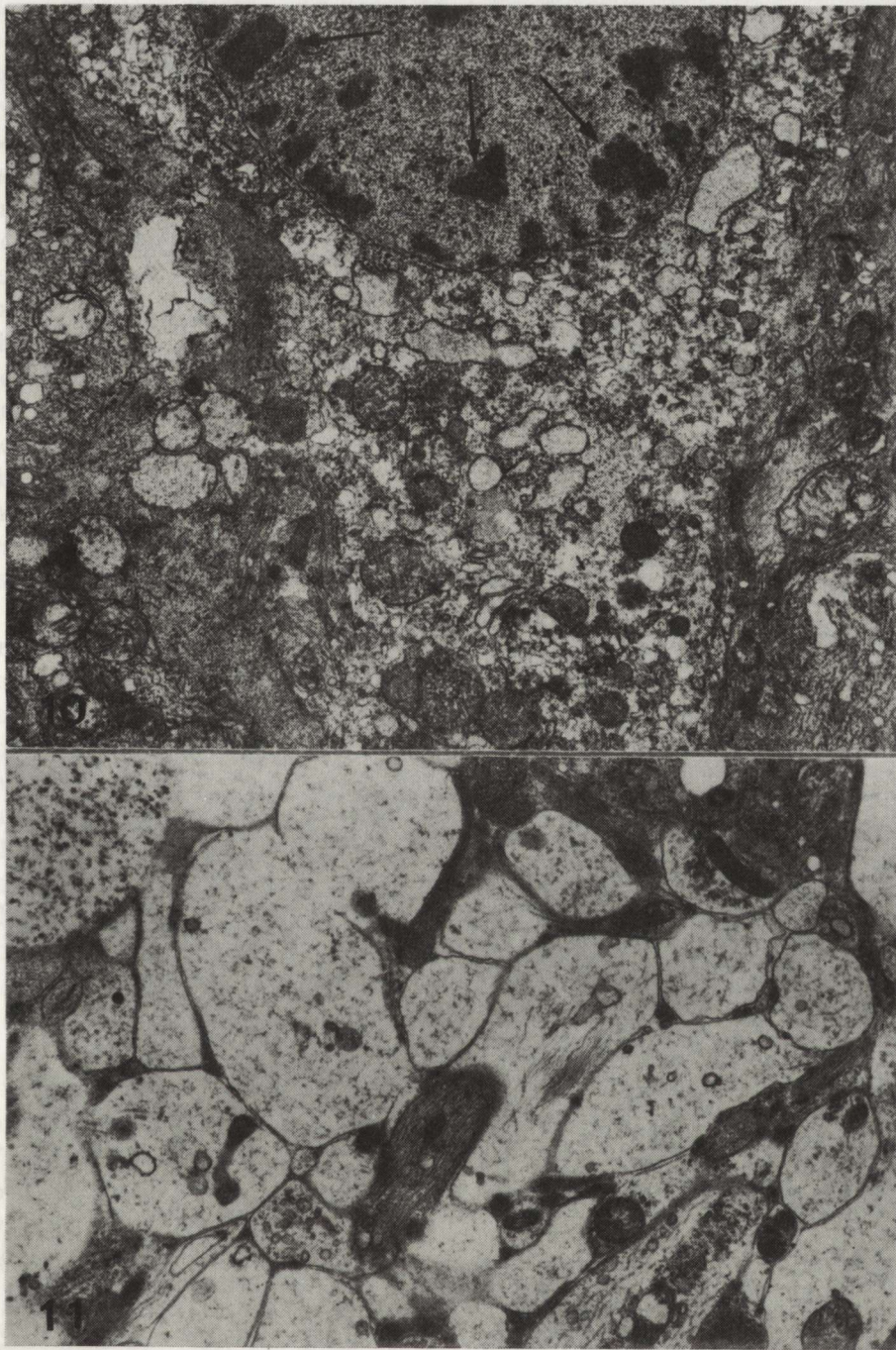


Fig. 10. 24 hours after 20-minute anoxia. Severely damaged neuron. Nucleus showing clumping of the nuclear chromatin (arrows). Cytoplasm filled with damaged organelles. $\times 15000$

Fig. 11. 3 days after 20-minute anoxia. The neuropil exhibits extreme swelling of neuronal and glial processes. $\times 15000$

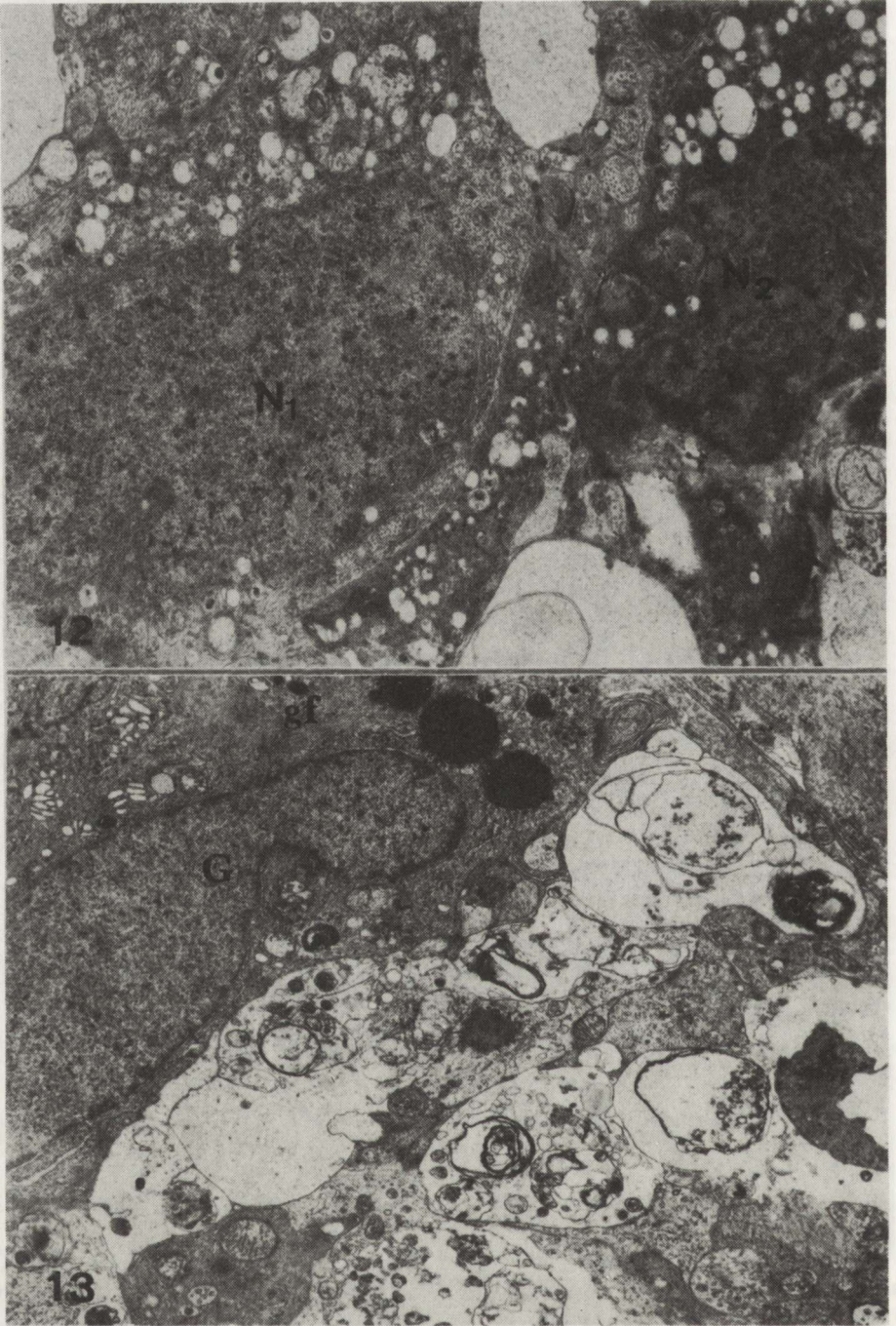


Fig. 12. 7 days after 20-minute anoxia. Two neurons (N1, N2) showing various degree of vacuolar degeneration. $\times 12\ 000$

Fig. 13. The same culture. Degenerated processes containing multilaminar, dense bodies and myelin-like figures. Fibrous astrocyte (G) with lipid droplets and bundles of gliofilaments (gf). $\times 10\ 000$

20-minute anoxia

As early as 2 and 24 h following anoxia the majority of nerve cells showed advanced ultrastructural abnormalities. The mitochondria exhibited various types of changes. Some of them were swollen with dissolution of cristae, whereas others were relatively dark with condensed matrix. Most neurons however, displayed severe swelling of mitochondria manifested by their enlargement, electron lucency of matrix and presence of remnants of cristae adhering to the inner membrane. The channels of granular endoplasmic reticulum were slightly dilated and cisternae of the Golgi complex were usually expanded. More severely damaged neurons exhibited clumping of the nuclear chromatin and degeneration of the organelles (Fig. 10). The neuropil 3 days post anoxia showed extreme swelling of almost all glial and neuronal processes, and synaptic contacts could be detected only occasionally (Fig. 11). Some of the neuronal processes contained dark mitochondria and dilated short channels of granular endoplasmic reticulum. The protoplasmic astrocytes were markedly swollen and displayed cytoplasm almost entirely devoid of organelles. The fibrous astrocytes revealed swelling of the periphery of the cytoplasm as well.

In the following days the majority of pyramidal neurons underwent progressive degenerative changes. Numerous neurons presented a picture of vacuolar degeneration, however, individual nerve cells differed in intensity of vacuolation and condensation of the cytoplasm (Fig. 12). Other neurons were completely disrupted and, apart from total destruction of cytoorganelles, showed nuclear clumping and disruption of the nuclear envelope. The neuropil was composed of numerous enlarged degenerated neuronal processes, some of which contained multilaminar and dense bodies (Fig. 13). In these later stages post anoxia there was an apparent increase in the number of fibrillary glia which showed large cytoplasm containing abundant gliofilaments and dense bodies or lipid droplets and often revealed phagocytic activity.

DISCUSSION

Ultrastructural changes demonstrated in the presently performed tissue culture model of anoxia showed some similarities with the well-known pattern of postischemic cell damage *in vivo*. The earliest prominent ultrastructural abnormalities consisted of severe swelling of mitochondria in the majority of pyramidal neurons. Mitochondria seem to be particularly vulnerable to reduction of the supply of oxygen, as their swelling was seen in both acute and prolonged hypoxia *in vivo* (Yu et al. 1974). It has been postulated for many years that microvacuolization of the cell cytoplasm resulting from swelling of mitochondria and dilatation of endoplasmic reticulum channels, typical for ischemic/anoxic stress, represents the earliest stages of neuronal damage (McGee-Russel et al. 1970; Brown, Brierley 1972, 1973; Brierley et al. 1973; Garcia et al. 1978). However, in *in vitro* study at the early stages of obser-

vation, mitochondrial abnormalities were not accompanied by marked dilatation of endoplasmic reticulum channels. Numerous vacuoles of various size representing enlarged endoplasmic reticulum cisternae could be observed only at later stages post anoxia, moreover, they seemed to originate rather from smooth endoplasmic reticulum. Distinct dilatation of both smooth and granular endoplasmic reticulum channels was seen only in severely affected nerve cells appearing after longer-lasting anoxia and in later stages post oxygen deprivation. Thus, our results seem to suggest that mitochondrial swelling represents the first response of nerve cells to pure oxygen deprivation and is independent of any vascular factors.

Other striking features of postanoxic ultrastructural changes in this study were alterations of synaptic contacts involving predominantly presynaptic terminals. So far the presynaptic alterations were described mainly in prolonged hypoxia (Yu et al. 1974) and various chronic neurological diseases (Kidd 1964; Gonatas et al. 1967). The ultrastructural picture of presynaptic changes in these prolonged hypoxic stages consisted of the formation of multilaminar bodies and vesicular aggregations (Yu et al. 1974). In the present study presynaptic changes were represented by marked swelling of axonal boutons with depletion and disarrangement of synaptic vesicles. A similar type of synaptic degeneration was reported in the distal *stratum radiatum* of the hippocampus CA1 region a short time after complete cerebral ischemia (Ekström, Diemer 1982). It has been also postulated that synaptic activity is the factor mainly responsible for varying sensitivity of tissue to anoxia with mature tissue distinctly more vulnerable (Rothman 1984; Slotkin et al. 1986). Moreover, synaptic terminals were considered as the primary and earlier target in the development of postischemic nerve cell damage (Ekström, Diemer 1982). The presence of numerous well developed synaptic contacts observed in our cultures might, according to this assumption, account for widespread and severe tissue damage. The evidence of presynaptic alterations is in opposition to some experiments suggesting that anoxic/ischemic stress produces selective, primary dendritic damage, resembling the excitotoxic effect (Johansen et al. 1983). Recently, differences in the neurotransmitter regulatory mechanism and participation of excitatory amino acids in the selective vulnerability of particular brain regions to ischemia have been under consideration (Nemoto 1979). The hypothesis of an excitotoxic mechanism of cell death is not eliminated by the morphological evidence of axonal, not dendritic terminals alterations. Primary changes of presynaptic boutons with increased membrane permeability might cause excessive release of excitatory compounds and consequently produce cell damage.

In the process of postischemic neuronal damage the role of glia should also be estimated, especially considering their participation in the metabolism of excitatory amino acid such as glutamate (Martinez-Hernandez et al. 1977; Schousboe et al. 1979; Choi, Rothman 1990). Many ischemic/hypoxic models revealed that neuronal necrosis is associated with structural and metabolic

astrocytes abnormalities (Brown, Brierley 1973). The present study demonstrated that swelling of protoplasmic astrocytes and some abnormalities of their cytoplasmic organelles developing parallel with the early neuronal changes might suggest that this process is independent on neuronal abnormalities. This is in analogy to experiments with excitotoxins, where the character of secondary glial response to neuronal damage was put in question (Singh et al. 1978; Renkawek et al. 1982; Matyja 1986). Moreover, the present study showed that, the evolution and intensity of anoxic cell damage in hippocampal culture are a function of the time of oxygen deprivation and survival time post anoxia.

The similarities between ultrastructural changes in the tissue culture model of anoxia and in many *in vivo* studies allow to conclude that this model is very useful for further experimental work. Its priority is connected with the fact that vascular and vasogenic factors are completely excluded so it becomes possible to study the direct effect of anoxia and the cytoprotective action of different agents against postanoxic cell damage.

USZKODZENIE POANOKSYJNE HIPOKAMPA *IN VITRO*

Streszczenie

Przeprowadzono analizę zmian ultrastrukturalnych rozwijających się pod wpływem anoksji w hodowli organotypowej hipokampa. Model hodowli pozaustrojowej pozwalał na ocenę bezpośredniego wpływu niedotlenienia na elementy komórkowe hipokampa, struktury odznaczającej się szczególną wrażliwością na niedotlenienie.

Badania przeprowadzono na zróżnicowanych 14-dniowych hodowlach hipokampa poddawanych działaniu anoksji przez okres 10 i 20 minut oraz utrwalanych do mikroskopu elektronowego po upływie 2 i 24 godzin oraz 3 i 7 dni.

Najwcześniejsze zmiany neuronalne dotyczące komórek piramidowych polegały na masywnym obrzmieniu mitochondriów prowadzącym do stopniowej wakuolizacji cytoplazmy. Większość kanałów ziarnistej siateczki śródplazmatycznej nie wykazywała zmian. Znamienną cechą było uszkodzenie w obrębie połączeń synaptycznych dotyczące przede wszystkim zakończeń presynaptycznych. Astrocyty protoplazmatyczne wykazywały obrzmienie cytoplazmy oraz mitochondriów, podczas gdy astrocyty włókniste były prawidłowo zachowane.

Zmiany w hodowli tkankowej hipokampa po niedotlenieniu wykazują znaczne podobieństwo do obrazu poanoksyjnych uszkodzeń tkankowych *in vivo*, co pozwala na stosowanie modelu hodowli pozaustrojowej w dalszych badaniach doświadczalnych.

REFERENCES

1. Beneviste H, Drejer J, Shousboe A, Diemer NH: Elevation of extracellular concentrations of glutamate and aspartate in rat hippocampus during transient cerebral ischemia monitored by intracerebral microdialysis. *J Neurochem*, 1984, 43, 1369–1374.
2. Brierley JB, Meldrum BS, Brown A: The threshold and neuropathology of cerebral "anoxic-ischemic" cell change. *Arch Neurol*, 1973, 29, 367–374.
3. Brown AW, Brierley JB: Anoxic-ischemic cell change in rat brain. Light microscopic and fine structural observations. *J Neurol Sci*, 1972, 16, 59–84.

4. Brown AW, Brierley JB: The earliest alterations in rat neurons after anoxia-ischemia. *Acta Neuropathol (Berl)*, 1973, 23, 9–22.
5. Choi DW: Cerebral hypoxia: some new approaches and unanswered questions. *J Neurosci*, 1990, 10, 2493–2501.
6. Choi DW, Rothman SM: The role of glutamate neurotoxicity in hypoxic – ischemic neuronal death. *Ann Rev Neurosci*, 1990, 13, 171–182.
7. Deleo J, Toth L, Schubert P, Rudolphi K, Kreutzberg GW: Ischemia-induced neuronal cell death, calcium accumulation, and glial response in the hippocampus of the Mongolian gerbil and protection by propentofylline (HWA 285). *J Cereb Blood Flow Metab*, 1987, 7, 745–751.
8. Despande JK, Sjesjö BK, Wieloch T: Calcium accumulation and neuronal damage in the rat hippocampus following cerebral ischemia. *J Cereb Blood Flow Metab*, 1987, 7, 89–95.
9. Ekström DKJ, Diemer NH: Complete cerebral ischemia in the rat: an ultrastructural and stereological analysis of the distal *stratum radiatum* in the hippocampal CA1 region. *Neuropathol App Neurol*, 1982, 8, 197–215.
10. Fujiwara N, Abe T, Endoh H, Warashina A, Shimoji K: Changes in intracellular pH of mouse hippocampal slices responding to hypoxia and/or glucose depletion. *Brain Res*, 1992, 572, 335–339.
11. Garcia JH, Lossinsky AS, Kauffman FC, Conger KA: Neuronal ischemia injury: Light microscopy, ultrastructure and biochemistry. *Acta Neuropathol (Berl)*, 1978, 43, 85–95.
12. Gonatas NK, Anderson W, Evangelista J: The contribution of altered synapses in the senile plaque: an electron microscopic study in Alzheimer's dementia. *J Neuropathol Exp Neurol*, 1967, 26, 25–39.
13. Hagberg H, Lehmann A, Sandberg B, Nystrom B, Jacobson I, Hamberger A: Ischemia-induced shift of inhibitory and excitatory amino acids from intra- to extracellular compartments. *J Cereb Blood Flow Metab*, 1985, 5, 413–419.
14. Johansen FF, Jorgensen MB, Diemer NK: Resistens of hippocampal CA1 interneurons to 20-minute transient cerebral ischemia in the rat. *Acta Neuropathol (Berl)*, 1983, 61, 135–140.
15. Kidd M: Alzheimer's disease, an electron microscopical study. *Brain*, 1964, 87, 307–320.
16. Kraig RP, Petito CK, Plum F, Pulsinelli WA: Hydrogen ions kill brain at concentrations reached in ischemia. *J Cereb Blood Flow Metab*, 1987, 7, 379–386.
17. Martinez-Hernandez A, Bell KP, Norenberg MD: Glutamine synthetase: glial localization in brain. *Science*, 1977, 195, 1356–1358.
18. Matyja E: Morphologic evidence of a primary response of glia to kainic acid administration into the rat neostriatum: studied *in vivo* and *in vitro*. *Exp Neurol*, 1986, 92, 609–623.
19. Matyja E, Kida E: Dynamics of rat hippocampus development in organotypic tissue culture. Light and electron-microscopic study. *Neuropatol Pol*, 1988, 26, 431–453.
20. McGee-Russell SM, Brown AW, Brierley JB: A combined light and electron microscopic study of early anoxic-ischemic cell change in the rat brain. *Brain Res*, 1970, 20, 193–200.
21. Mouritzen Dam A: Epilepsy and neuron loss in the hippocampus. *Epilepsia*, 1980, 21, 617–629.
22. Nagafuji T, Koide T, Takato M: Neurochemical correlates of selective neuronal loss following cerebral ischemia: role of decreased Na⁺, K⁺-ATPase activity. *Brain Res*, 1992, 571, 265–271.
23. Nemoto EM: Studies on the pathogenesis of ischemic brain damage and its amelioration by barbiturate therapy. In: *Brain and heart infarct*. Eds: JJ Zülch, W Kauman. Springer, Berlin, 1979, vol II, pp 306–317.
24. Paljarvi L: Brain lactic acidosis and ischemic cell damage: a topographic study with high-resolution light microscopy of early recovery in rat model of severe incomplete ischemia. *Acta Neuropathol (Berl)*, 1984, 64, 89–102.
25. Pellegrini-Giampetro DE, Chericci G, Alesiani M, Carla V, Moroni F: Excitatory amino acid release and free radical formation may cooperate in the genesis of ischemia-induced neuronal damage. *J Neurosci*, 1990, 10, 1035–1041.

26. Perkins MN, Stone TW: Actions of kynurenic acid and quinolinic acid in the rat hippocampus *in vivo*. *Exp Neurol*, 1985, 88, 570–579.
27. Renkawek K, Matyja E, Mossakowski MJ: Glial fibrillary changes induced by kainic acid in organotypic culture of the rat cerebellum. *J Neurol Sci*, 1982, 53, 321–330.
28. Rothman S: Synaptic release of excitatory amino acid neurotransmitter mediates anoxic neuronal death. *J Neurosci*, 1984, 4, 1884–1892.
29. Schousboe A, Svenneby G, Hertz L: Uptake and metabolism of glutamate in astrocytes cultured from dissociated mouse brain hemispheres. *J Neurochem*, 1979, 32, 943–950.
30. Siesjö BK, Bengtsson F: Calcium fluxes, calcium antagonists and calcium related pathology in brain ischemia: a unifying hypothesis. *J Cereb Blood Flow Metabol*, 1989, 9, 127–140.
31. Siesjö K, Wieloch T: Brain ischemia and cellular calcium homeostasis. In: Calcium entry blockers and tissue protection. Ed: T Godfraind. Raven Press, New York, 1985, pp 139–149.
32. Simon RP, Griffiths T, Evans MC, Swan JH, Meldrum BS: Calcium overload in selectively vulnerable neurons of the hippocampus during and after ischemia: and electromicroscopic study in the rat. *J Cereb Blood Flow Metab*, 1984a, 54, 350–361.
33. Simon RP, Swan JH, Griffith T, Meldrum BS: Blockade of N-methyl-D- aspartate receptors may protect against ischemic damage in the brain. *Science*, 1984b, 226, 850–852.
34. Singh VK, McGeer EG, McGeer PL: Changes of (SH) colchicine binding and protein synthesis in rat striatum following kainic acid lesions. *Brain Res*, 1978, 146, 195–199.
35. Slotkin TA, Cowdery TS, Orband L, Pachman S, Whitmore WL: Effects of neonatal hypoxia on brain development in the rat: immediate and long-term biochemical alterations in discrete regions. *Brain Res*, 1986, 374, 63–74.
36. Yu MG, Bakay L, Lee JC: Ultrastructure of the central nervous system after prolonged hypoxia. *Acta Neuropathol (Berl)*, 1974, 22, 222–234.

Authors' address: Department of Neuropathology, Medical Research Centre, PAsci, 3 Dworkowa St, 00-784 Warsaw, Poland

MARIA DAŃBSKA, DANUTA MAŚLIŃSKA, IZABELA KUCHNA

ASTROGLIOSIS IN THE TEMPORAL LOBE OF NEWBORN INFANTS WHO DIED IN THE PERINATAL PERIOD

Laboratory of Developmental Neuropathology, Medical Research Centre, Polish Academy of Sciences, Warsaw

The normal distribution of astrocytes in the temporal lobe of the newborn and that occurring as consequence of perinatal pathology was compared. The astrocytes were revealed by immunohistochemical visualization of glial fibrillary acidic protein (GFAP). The intensity of positive reaction correlates well with the maturation of various white structures. In the group with hypoxic encephalopathy the GFAP-positive reaction was clearly related to the observed neuropathological changes. Intensive reaction in the area of U-fibers confirmed the susceptibility of this region to hypoxic damage. The presence of GFAP-positive cells within Ammon's horn indicates that the degree of reaction depends on the intensity and duration of the lesions.

Key words: *astrocytosis, brain development, perinatal hypoxia.*

Developmental events and pathological changes within the population of glial cells coincide in the maturing central nervous system (CNS) and present diagnostic problems particularly in the perinatal period. At this time, asphyxia of the fetus often occurs and its sequelae require more observations in order to be fully understood (Takashima, Becker 1984; Miller et al. 1986; Zimmer et al. 1991).

The aim of the present study was to compare the normal distribution of astrocytes in the temporal lobe of the newborn at term with the astroglial reaction occurring in this structure as consequence of pathological perinatal process.

MATERIAL AND METHODS

The investigations were performed on the temporal lobe including Ammon's horn of eight infants born at term and two delivered after 36 weeks of pregnancy, who died at birth or during the first week of life. Their brains were neuropathologically examined.

The sections were stained with cresyl violet, hematoxylin-eosin (HE) and according to the Klüver-Barrera method. The appearance of astrocytes and their abnormalities were demonstrated by immunohistochemical visualization of glial fibrillary acidic protein (GFAP), considered as the most sensitive method for study of human post-mortem material (Roessmann, Gambetti 1986). Sections 5 µm thick were deparaffinized and tested with antibodies to GFAP (Amersham). The avidin-biotin-peroxidase complex (ABC) staining technique (Hsu et al. 1982) was applied.

RESULTS

One newborn died because of acute asphyxia during delivery, two were well immediately after birth and their sudden death occurred because of the respiratory distress syndrome and cardiac arrest, respectively. They did not present any symptoms indicating CNS pathology. Neuropathological examination did not reveal any noticeable lesions of the CNS. Those cases constitute the control group.

In all of them GFAP-positive reaction of varying intensity (Table 1A) was observed in various temporal lobe structures. The marginal glia was strongly positive. In the white matter of the central part of the cortical convolutions GFAP-positive reaction was visible (Fig. 1), but in the region of U-fibers it was nearly negative (Fig. 2). The perivascular astrocytes were clearly GFAP-positive, but without hypertrophy of their cell bodies (Fig. 3). The cortex, including the Ammon's horn pyramidal cell layer, was nearly negative. Only single positive cells were found in the vicinity of some blood vessels.

Table 1. GFAP immunoreactivity

	Marginal glia	perivascular	white matter	cortex
A. Control cases				
1	+++	++	+	0
2	+++	++	+	0
3	+++	++	+	0
B. Pathological cases				
4	+++	++	++	++ (focal)
5	+++	++	++ (U-fibers)	++ (layer VI)
6	+++	+++	++	++
7	+++	++	+++	++ (layers III and V)
8	+++	+++	+++	++
9	+++	++	+++ (U-fibers)	++
10	+++	++	+++ (U-fibers)	+++

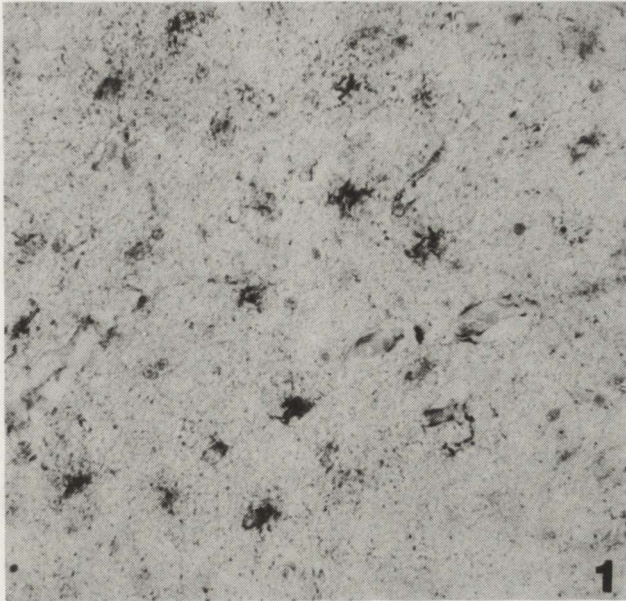


Fig. 1. GFAP-immunoreactive cells in central part of cortical convolution. $\times 200$

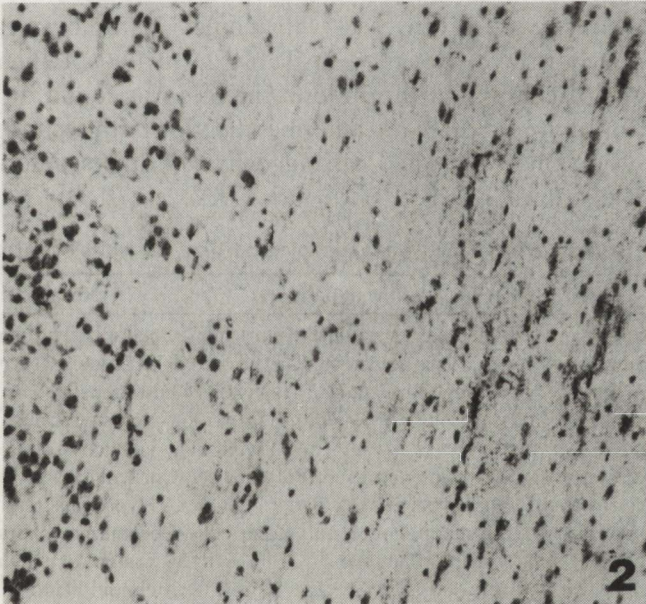


Fig. 2. U-fibers area without GFAP-positive cells. $\times 100$

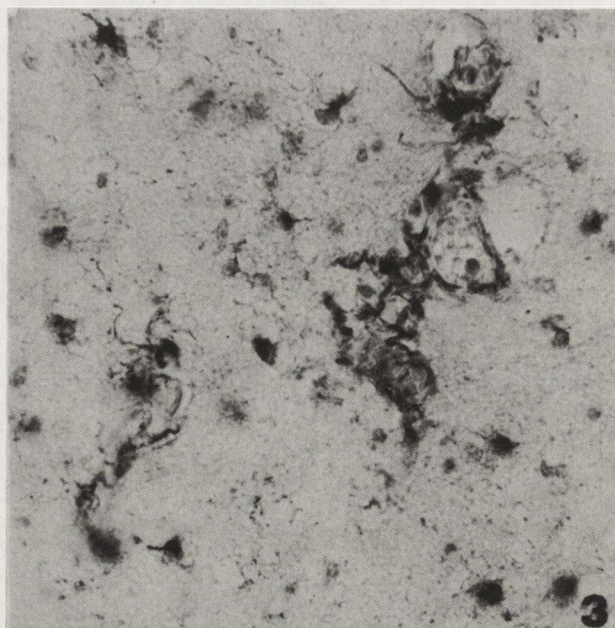


Fig. 3. Perivascular astrocytes without cell bodies hypertrophy. GFAP immunostaining. $\times 200$

Basic data concerning seven cases with clinical pathology leading to the death of the newborn are presented in Table 2. In two of them premature abruption of the placenta with thrombotic changes was found, in three others congenital heart failure, in three intrauterine infection with secondary pneumonia and asphyxia. One fetus died during delivery, others deteriorated after birth very rapidly until death.

Table 2. Basic clinical and neuropathological data of pathological cases

Case No	Age	Clinical data	Neuropathology
4 (23/90)	At term. 2 days	Trilocular heart (single ventricle). Sudden death	Generalized edema. Focal periventricular early necrosis
5 (29/90)	At term. 2 days	Prolonged pregnancy. Asphyxia. APGAR 1. Pneumothorax	Disseminated neuronal lesions. Periventricular hyperplasia of glial cells
6 (19/91)	At term. Dead at birth	Abruptio placentae. Pulmonary hemorrhage	Cortical lesions (layers III and V). Hyperemia and edema
7 (73/90)	At term. 1 day	Intrauterine infection. Recurrent apnea. Pneumonia	Generalized cortical damage. Periventricular early necrosis. Subarachnoid hemorrhage. Meningitis
8 (22/90)	36 weeks. 1 day	Mother's diabetes. APGAR 2. Ventricular septal defect	Disseminated neuronal lesions. Hyperemia
9 (28/90)	36 weeks. 1 day	Intrauterine infection. APGAR 4. Pneumonia	Focal cortical lesions. Hyperemia and edema, mainly periventricular
10 (38/90)	38 weeks. 8 days	Intrauterine infection. RDS	Periventricular leucomalacia. Ammon's horn necrosis. Cerebellar hemorrhage

Neuropathological examination confirmed the changes in the temporal cortex. They presented disseminate neuronal damage, in one case with distinct focal lesions. In Ammon's horn neuronal damage was also disseminated, and only in one of them focal subtotal necrosis was observed. In the white matter, the changes consisted of hyperemia, edema and even features of a very early stage of periventricular necrosis (Fig. 4).



Fig. 4. Early necrotic changes in periventricular white matter. HE. $\times 200$

Table 1B summarizes the intensity of GFAP-positive reactions in pathologic cases. The reaction within marginal glia was similar to that in controls. This parallellism helped to estimate the reaction in other examined areas as clearly more intensive than in the control. In the white matter it seemed increased, particularly in terms of volume and staining intensity of cell bodies and their processes (Fig. 5). The visual pathway surrounding the lateral ventricle did not reveal similar hypertrophy of GFAP-immunoreactive cells. The perivascular glia in this group of cases differed in intensity of GFAP reaction from the controls. The topography of GFAP-positive cells also changed in comparison with controls in the white matter of cerebral convolutions. In four cases the reaction was clearly positive in the region of U-fibers. The cortex with disseminated neuronal lesions revealed several astrocytes dispersed in cell-sparse areas and in the case with focal lesions the GFAP-positive cells were found in the damaged area, particularly around the blood vessels (Fig. 6). In Ammon's horn in all, but one case reaction positive for GFAP was observed in the *alveus* and in *stratum oriens*, but was almost negative in *stratum pyramidale*. In one case with most advanced focal lesions, the GFAP-positive astrocytes were numerous in the area of necrotic changes (Fig. 7) and disseminated in their vicinity.

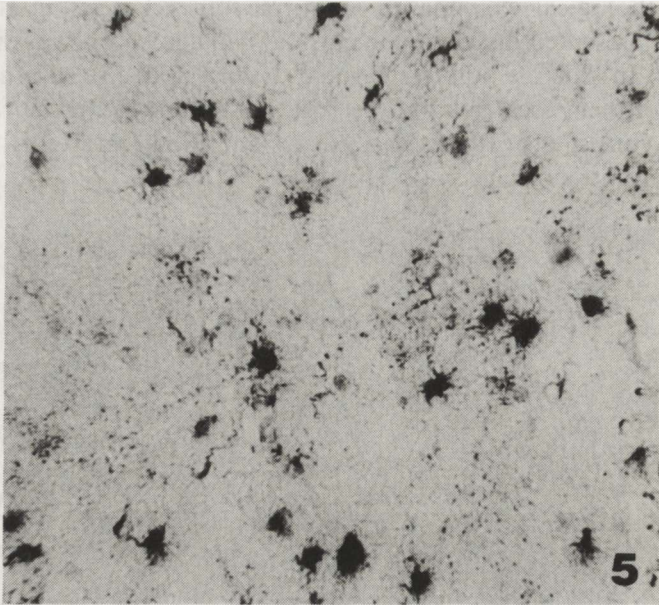


Fig. 5. Intensive GFAP-positive reaction in white matter. $\times 200$

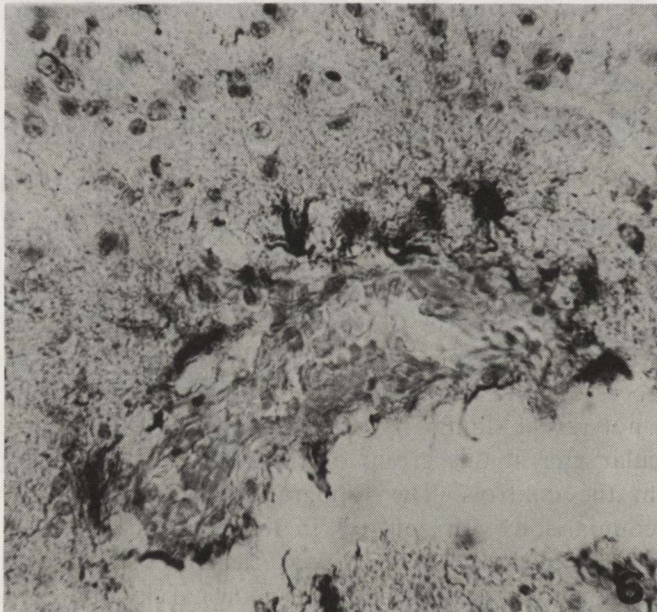


Fig. 6. Perivascular hypertrophic GFAP-immunoreactive astrocytes. $\times 250$

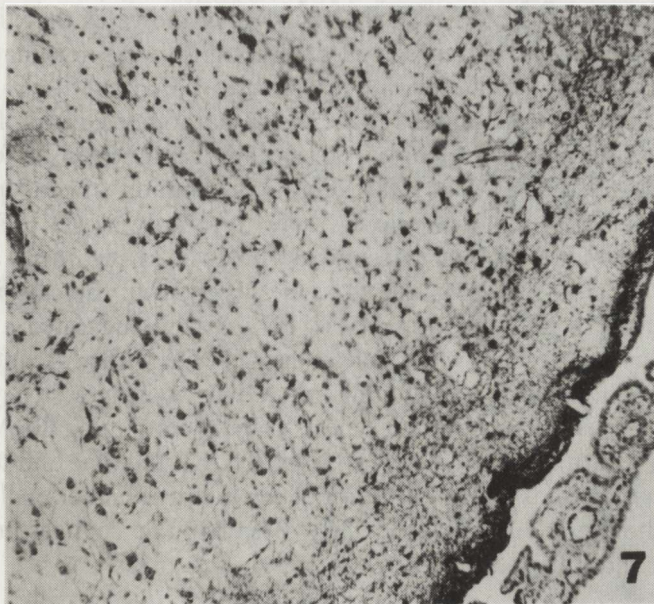


Fig. 7. GFAP-positive astrocytes in the region of necrotic changes in Ammon's horn. $\times 100$

DISCUSSION

The observations of GFAP-positive astroglial cells in control cases are in agreement with previous findings. This type of glia appears in brain hemispheres after 15 weeks of gestational age (Roessmann, Gambetti 1986; Sasaki et al. 1988). The GFAP-positive reaction varies in intensity in different parts of the hemispheres, where it develops with temporal variation (Reske-Nielsen et al. 1987). It was well demonstrated in the white matter of cortical convolutions of our cases, where the area of U-fibers was deprived of this activity, and present in the center, similarly with the observations of Takashima and Becker (1983) that GFAP-positive glia shift from deep to superficial white matter.

The intensive GFAP-immunoreactivity in the pathologic group could be related to the changes observed in those cases. Clinically asphyxia or severe hypoxia appear as principal factors which in all those cases induced the changes in the CNS. Neuropathological examination confirmed the presence of lesions which could be considered as belonging to the large group of perinatal hypoxic encephalopathies. The changes concerning GFAP-positive cells in the deep white matter, although estimated without morphometric evaluation of their number, testify to their hyperplasia and it has been stated by Miyake et al. (1988) that astrogliosis does not always mean increase of the total number of astrocytes. The markedly increasing population of GFAP-positive cells within U-fiber region may be considered as a reaction to hypoxia or other insults (Takashima et al. 1984; Zimmer et al. 1991). It confirms the susceptibility of this structure to hypoxic damage. On the other

hand, less intensive astrogliosis in the visual tract indicates that this structure was not damaged in the observed cases, although the premyelination process was more advanced there than in other observed areas.

Similar as in the white matter, must be the pathomechanism of GFAP-positive cells appearance in the cortex presenting disseminated or focal lesions. Particularly interesting are our observations of Ammon's horn. In cases with pronounced but disseminated lesions, there were only single GFAP-positive cells in the pyramidal cell layer, despite astrocytosis in the *alveus* and *stratum oriens*. The changes seemed similar to those observed in the cat hippocampus after ischemia by Schmidt-Kastner et al. (1990), who suggested a local specificity of astrocytic reaction. Nevertheless, our last case with more intensive focal necrosis of Ammon's horn revealed distinct GFAP-positive astrocytosis in the pyramidal cell layer, confirming that the astrocytes containing GFAP proliferate in Ammon's horn like in other parts of the CNS at the time and to the degree depending on the intensity and duration of the lesion (Zimmer et al. 1991). The perinatal pathology inducing particularly often hypoxic changes in the CNS is one of the conditions leading to this type of changes.

GLEJOZA ASTROCYTARNA W PŁACIE SKRONIOWYM NOWORODKÓW ZMARŁYCH W OKRESIE OKOŁOPORODOWYM

Streszczenie

Porównano występowanie astrocytów w płacie skroniowym noworodków w normie i w następstwie patologii okołoporodowej. Zastosowano immunohistochemiczną reakcję ujawniającą kwaśne glejowe białko włóknikowe (GFAP). Nasilenie odczynów dobrze koreluje z dojrzewaniem struktur istoty białej płata skroniowego. W grupie przypadków obciążonych patologią okołoporodową reakcja GFAP była wyraźnie zgodna z topografią uszkodzeń. Intensywny odczyn w obszarze U-włókien potwierdził wrażliwość tej okolicy na uszkodzenie. Odczyn GFAP w rogu Amona wykazał wyraźną zależność od nasilenia i czasu trwania uszkodzenia.

REFERENCES

1. Hsu SM, Raine L, Fanger H: The use of avidin-biotin complex (ABC) in immunoperoxidase technique. *J Histochem Cytochem*, 1982, 29, 577–580.
2. Miller RH, Abney ER, David S, Constant CF, Lindsay R, Patel R, Stone J, Raff MC: Is reactive gliosis a property of a distinct subpopulation of astrocytes? *J Neurosci*, 1986, 6, 22–29.
3. Miyake T, Kitamura T, Takamatsu T, Fujita S: Quantitative analysis of human astrocytosis. *Acta Neuropathol (Berl)*, 1988, 75, 535–537.
4. Reske-Nielsen E, Oster S, Reinoft I: Astrocytes in the prenatal central nervous system. *Acta Pathol Microbiol Immunol Scand (A)*, 1987, 95, 339–356.
5. Roessmann U, Gambetti T: Astrocytes in the developing human brain. *Acta Neuropathol (Berl)*, 1986, 70, 308–313.
6. Schmidt-Kastner R, Grosse-Ophoff B, Hossmann K-A: Pattern of neuronal vulnerability in the cat hippocampus after one hour of global cerebral ischemia. *Acta Neuropathol (Berl)*, 1990, 79, 444–455.

7. Sasaki A, Hirato J, Nakazato Y, Ishida Y: Immunohistochemical study of the early human fetal brain. *Acta Neuropathol (Berl)*, 1988, 76, 128–134.
8. Takashima S, Becker LE: Developmental changes of glial fibrillary acidic protein in cerebral white matter. *Arch Neurol*, 1983, 40, 14–18.
9. Takashima S, Becker LE, Nishimura M, Tanaka J: Developmental changes of glial fibrillary acidic protein and myelin basic protein in perinatal leukomalacia. *Brain Dev*, 1984, 6, 444–450.
10. Takashima S, Becker LE: Developmental neuropathology in bronchopulmonary dysplasia: alteration of glial fibrillary acidic protein and myelination. *Brain Dev*, 1984, 6, 451–457.
11. Zimmer C, Sampaolo S, Shanker-Sharma H, Cervós-Navarro J: Altered glial fibrillary acidic protein immunoreactivity in rat brain following chronic hypoxia. *Neuroscience*, 1991, 40, 353–361.

Correspondence address: prof. M. Dąbbska, Laboratory of Developmental Neuropathology, Medical Research Centre, PAsci, 3 Pasteura St, 02-093 Warsaw, Poland

JANINA RAFAŁOWSKA¹, DOROTA DZIEWULSKA¹, STANISŁAW KRAJEWSKI²

THE BREAKDOWN PROCESS OF HUMAN BRAIN INFARCTION IN MIDDLE-AGED AND SENILE CASES*

¹ Department of Neurology, School of Medicine, Warsaw ² Department of Neuropathology, Medical Research Centre, Polish Academy of Sciences, Warsaw

The material comprised 15 cases of ischemic brain stroke at the of age 45 to 101 years. Six brain of subjects deceased at the age of 45 to 57 years and 9 brains of those deceased at the age of 80 to 101 years were studied. Phagocytic cell immunoreactivity in both age groups during the first 5 days and on the 11th and 12th were compared. Phagocytic reactivity in cases of patients who died on the 6th, 15th and 35th days after stroke onset was also estimated. Colliquative necrosis with cavitation was observed in middle-aged cases from the 3rd infarction day. In the senile group the beginning of tissue breakdown was noted on the 5th day, but colliquative necrosis with cavitation was found on the 11th infarction day. Senile alterations in the biochemical components in various brain tissue elements are probably the cause of the different course and dynamics of the pathological process.

Key words: aging, brain infarction, breakdown process, immunoreactivity.

Our previous investigations indicated that during the first days of brain infarction in humans, vascular permeability was higher in middle-aged cases than in those who had died in the senile age (Rafałowska et al. 1990). In experimental allergic encephalitis (EAE), penetration of mononuclear cells and serum proteins through small blood vessel walls is the earliest morphological change (Lampert 1965; Kristenson et al. 1976), and an increase of vascular permeability appears parallelly with penetration of mononuclear phagocytes (Simmons et al. 1987). The mechanism of the blood-brain barrier (BBB) injury in these conditions is probably different. Although in both mechanisms hematogenic cells appear at an early stage of the pathological process, but in ischemic brain injury hematogenic polynuclear cells occur in the first stage of necrotic tissue breakdown.

* Investigations supported by the Institute of Psychiatry and Neurology under the Programme No. R. 34.1.

Immunocytochemical evaluation of hematogenic cells participation in the development of morphological changes within the infarcted tissue and age-dependence of those changes constitute the subject of the present studies.

MATERIAL AND METHODS

The material comprised 15 cases with ischemic brain stroke, at an age ranging from 45 to 101 years. Six brains of subjects deceased at the age of 45 to 57 years and 9 brains of those deceased at the age of 80 to 101 years were studied. Phagocytic cells immunoreactivity in both age groups during the first 5 days of infarction and then on the 11th and the 12th day after stroke onset was compared. Furthermore, phagocytic reactivity in cases with longer survival time, on the 6th, 15th, and 35th day of the pathological process, was estimated. In all cases autopsy was performed not later than 24 hours after death. Clinical data, results of autopsy and neuropathological examination have been previously presented (Rafałowska et al. 1990).

Formalin-fixed and paraffin-embedded slices from the infarction area and its surroundings were investigated immunocytochemically. The peroxidase-antiperoxidase (PAP) indirect method of Sternberger et al. (1970) was applied to visualize hematogenic infiltrate markers (McCombie et al. 1985; Cochi, Budka 1987) — alpha-1-antitrypsine and gamma-lysozyme. Immunostaining was performed with polyclonal antibodies (both from Dakopatts) and diaminobenzidine (Sigma) as a chromogen. The sections were counterstained with hematoxylin.

RESULTS

In all the cases except one senile, on the second infarction day immunoreactivity to alpha-1-antitrypsine was noted within the necrotic area. In the senile cases during the first few days of infarction a spongy state was often observed in the necrotic region. The sponginess was more pronounced at the edge of the infarcted zone and was deprived of hematogenic infiltrates. In one senile case, on the 35th infarction day, the nonreactive necrotic area, colliquative necrosis and postcolliquative cavities within the necrotic lesion were found.

On the first and 2nd infarction days, in middle-aged group phagocytes within the perivascular space and necrotic tissue were observed (Fig. 1). In this period in the senile group phagocytes were noted only within blood vessel lumina (Fig. 2). On the 3rd day colliquative necrosis with cavitation in middle aged group appeared (Figs 3–4), whereas in the senile cases phagocytic infiltrates were seen perivascularly and within necrotic tissue (Figs 5–6). In the later period of the pathologic process, the necrotic region in the middle-aged group was manifested by colliquative necrosis with cavitation, while the senile group still showed phagocytic infiltrations and transudates within the infarcted tissue (Figs 7–10). In the subject deceased at the age of

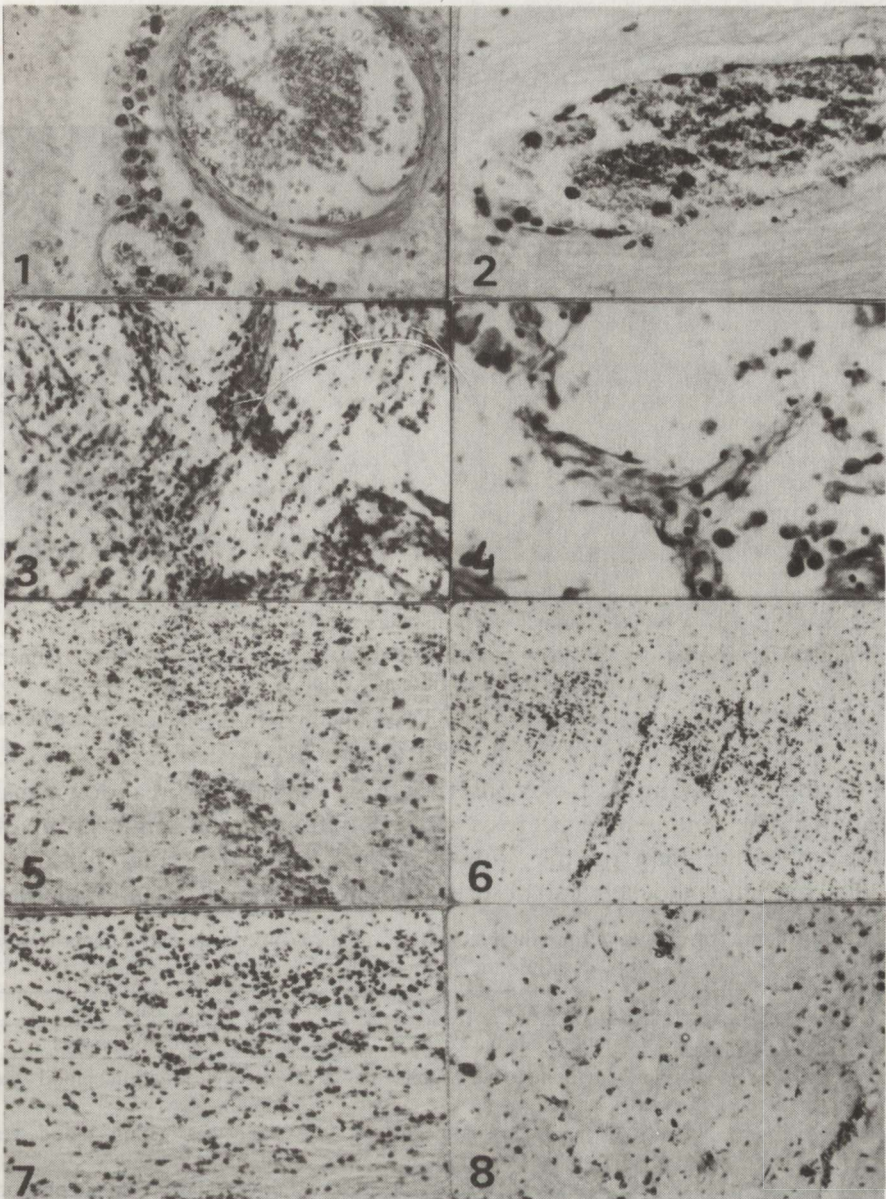


Fig. 1. Patient 57-year-old, 1 day survival. Gamma-lysozyme. Phagocytes within blood vessel and in perivascular tissue. $\times 320$

Fig. 2. Patient 84-year-old, 1 day survival. Gamma-lysozyme. Phagocytes only within blood vessel lumen. $\times 320$

Fig. 3. Patient 49-year-old, 3 days survival. Alpha-1-antitrypsin. Diffuse tissue immunoreactivity and numerous phagocytes within cystic breakdown area. $\times 160$

Fig. 4. Patient 49-year-old, 3 days survival. Gamma-lysozyme. Postcolliquative cavity. $\times 320$

Fig. 5. Patient 88-year-old, 3 days survival. Alpha-1-antitrypsin. Numerous polynuclear cells and smaller number of phagocytes perivascularly and in clusters within tissue. $\times 80$

Fig. 6. Patient 88-year-old, 3 days survival. Gamma-lysozyme. Tissue and perivascular phagocyte infiltrates. $\times 80$

Fig. 7. Patient 55-year-old, 4 days survival. Gamma-lysozyme. Numerous phagocytes within U-fibers area. $\times 160$

Fig. 8. Patient 89-year-old, 4 days survival. Gamma-lysozyme. Single phagocytes dispersed in the tissue. $\times 160$

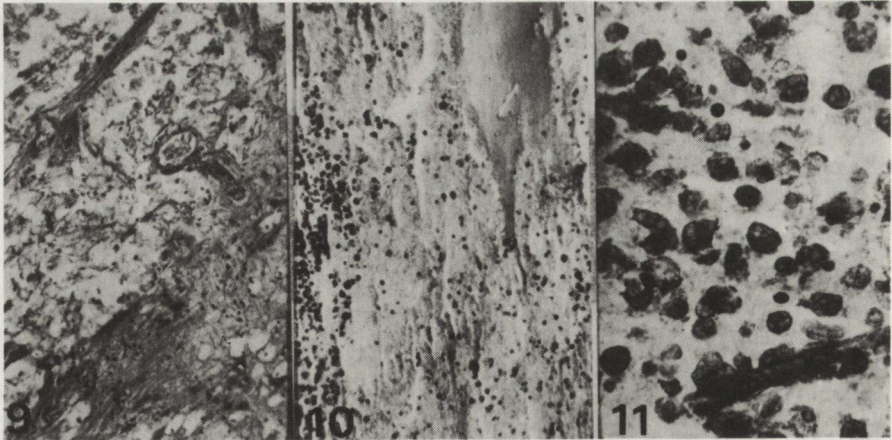


Fig. 9. Patient 45-year-old, 5 days survival. Alpha-1-antitrypsin. Postcolliquative cavity. Not numerous phagocytes. $\times 80$

Fig. 10. Patient 86-year-old, 5 days survival. Alpha-1-antitrypsin. Transudates, numerous phagocytes within infarcted tissue. $\times 160$

Fig. 11. Patient 87-year-old, 15 days survival. Alpha-1-antitrypsin. Colliquative necrosis with numerous phagocytes. $\times 320$

101 on the 6th day after stroke onset there was a lack of breakdown manifestations. The colliquative necrosis and cavitation in the senile group was noted not earlier than on the 15th–35th infarction day (Fig. 11).

Our immunohistochemical observations are summarized in Table 1.

Table 1. Evaluation of phagocyte immunoreactivity to alpha-1-antitrypsin and gamma-lysozyme within the infarction area

Survival time	Middle-aged cases		Senile cases	
	Age	Kind of changes	Age	Kind of changes
1 day	57	Perivascular phagocytes, phagocytes within tissue	84	Phagocytes within blood vessel lumina
2 days	53	Phagocytes within tissue, beginning of breakdown process	80	Phagocytes within blood vessel lumina
3 days	49	Colliquative necrosis with cystic breakdown	88	Perivascular and tissue phagocyte infiltrates
4 days	55	Phagocyte tissue infiltrates, colliquative necrosis, cysts	89	Single phagocytes within tissue
5 days	45	Postcolliquative cavity	86	Phagocyte tissue infiltrates, transudates
6 days			101	Nonreactive necrosis, lack of breakdown manifestations
11 days			87	Colliquative necrosis with cystic breakdown
12 days	50	Perivascular and tissue phagocyte infiltrates, colliquative necrosis, cysts		
15 days			87	Colliquative necrosis with cystic breakdown
35 days			83	Nonreactive and colliquative necrosis with cystic breakdown

DISCUSSION

In our material manifestations of colliquative necrosis with cavities forming in the middle-aged were observed from the 3rd infarction day. In the senile group the beginning of the tissue breakdown was noted on the 5th day of infarction, but colliquative necrosis with cavitation was found on the 11th day after stroke onset.

Evaluation of alpha-1-antitrypsin and gamma-lysozyme revealed diffuse tissue immunoreactivity only in the alpha-1-antitrypsin reaction. It differed in extent and intensity, however, it included necrotic tissue independently of phagocytic reaction intensity. Alpha-1-antitrypsin inhibits proteolytic enzymes activity and indirectly indicates their participation in breakdown of necrotic tissue. It is secreted *in situ* by hematogenic macrophages, but a part of the enzyme is synthesized within the liver. Immunoreactivity of necrotic tissues devoid of phagocytes indicates that this low-molecular weight serum protein penetrates through blood vessel walls. It may testify to the mechanism of the blood-brain barrier (BBB) disturbances.

Evaluation of cell immunoreactivity to alpha-1-antitrypsin and gamma-lysozyme revealed phagocytic reactivity in the infarcted region. Perivascular and disseminated phagocytic infiltrations within the tissue appeared earlier and were more numerous in the middle-aged cases. Therefore, proteolytic processes leading to cystic breakdown of necrotic tissue were more intensive. We do not know whether in senile cases the number of macrophages is smaller or the quantity of proteolytic enzymes and their activity is lower. It can hardly be excluded that the proliferative ability of phagocytes is reduced during bone marrow aging. Aging process may also influence active peptides among which tuftsin is an important phagocytosis-stimulating peptide (Kraus-Berthier et al. 1991). Consequently, it is possible that phagocytic activity in senile humans is less intensive, similarly as the neglected phagocytic function in old animals (Dwilewicz-Trojaczek 1982). Then, all the factors mentioned above, along with a slightly retarded increase of blood vessel permeability (Rafałowska et al. 1990), may lead to extended in time maturation of the necrotic lesion in senile subjects. Our investigations of the senile group indicate that within the first few days of infarction necrosis was manifested by a spongy state without or almost without hematogenic cell reaction. Such a weak cell reaction suggests a similarity to the ischemic morphological changes in the embryonal brain. In that period a weak breakdown process of necrotic lesion by hematogenic phagocytes (Dąbska 1967) may probably be caused by the metabolic immaturity of cells and tissues. It seems that in senile age tissues involution leads to proliferative and enzymatic insufficiency, manifested by significant retardation of the cell reaction. The inflammatory process exponents are weaker in senile cases of multiple sclerosis (Rafałowska et al. 1988), less distinct is the astroglial reaction in senile ischemic brain lesions (Rafałowska et al. 1991). Histological examination of the brain necrotic area also indicates a delayed breakdown of ischemic foci in senile cases

(Barcikowska-Litwin 1984). A changed homeostasis of the senile brain is manifested both by slowing-down of metabolic processes and qualitative (Niebrój-Dobosz et al. 1986; 1988; 1989) and quantitative (Wender et al. 1987) alterations in the biochemical components in various brain tissues. Those alterations are probably the cause of a different course and dynamics of various pathological processes. This has been confirmed both by clinical observations and morphological examination of senile brain cases.

IMMUNOCYTOCHEMICZNA OCENA PROCESU ROZBIÓRKI ZAWAŁU MÓZGU U LUDZI W WIEKU ŚREDNIM I STARCZYM

Streszczenie

Przedmiotem badań były mózgi chorych zmarłych w przebiegu udaru niedokrwiennego. Oceniono 6 przypadków zmarłych w wieku 45–57 lat i 9 przypadków zmarłych w wieku 80–101 lat. W obu grupach wieku porównywano immunoreaktywność komórek żernych w pierwszych pięciu oraz w 11 i 12 dniu zawału, a ponadto oceniono mózgi zmarłych w 6, 15 i 35 dniu choroby. Martwicę rozplywną z tworzeniem się jam stwierdzano w mózgach ludzi w wieku średnim od 3 dnia zawału, natomiast w grupie starszej wczesne przejawy procesu rozbiórki obserwowano w 5 dniu, a martwicę rozplywną z rozpadem jamistym – w 11 dniu zawału. Związane z wiekiem zmiany w składzie biochemicznym różnych elementów strukturalnych mózgu mogą stanowić przyczynę innego przebiegu i dynamiki procesu chorobowego.

REFERENCES

1. Barcikowska-Litwin M: Obraz morfologiczny ogniska rozmiękania mózgowego w wieku starym. *Neuropatol Pol*, 1984, 22, 563–578.
2. Dąmbska M: Martwice a zapalenia w mózгах płodów i noworodków. *Neuropatol Pol*, 1967, 5, 1–33.
3. Dwilewicz-Trojaczek J: Zmiany czynności układu immunologicznego w procesie starzenia się zwierząt. In: *Wybrane zagadnienia immunologii klinicznej*. Eds: Z Kuratowska, A Lutyński, J Dwilewicz-Trojaczek. PZWL, Warszawa, 1982, pp 185–186.
4. Kochi N, Budka H: Contribution of histiocytic cells to sarcomatous development of the gliosarcoma. An immunohistochemical study. *Acta Neuropathol (Berl)*, 1987, 73, 124–130.
5. Kristenson K, Wiśniewski HM, Bornstein MB: About demyelinating properties of humoral antibodies in experimental allergic encephalomyelitis. *Acta Neuropathol (Berl)*, 1976, 36, 307–314.
6. Lampert PW: Demyelination and remyelination in experimental allergic encephalomyelitis. *J Neuropathol Exp Neurol*, 1965, 24, 371–385.
7. McCombe PA, Clark P, Frith JA, Hammound SR, Steward GJ, Pollard JD, McLeod JG: Alpha₁-antitrypsin phenotypes in demyelinating diseases and the allele P, M₃. *Ann Neurol*, 1985, 18, 514–516.
8. Kraus-Berthier L, Ferry G, Combe-Perez V, Vissali M, Remind G, Boutin JA: Approaches to some biochemical mechanisms of action of tuftsin and analogues. *Biochem Pharmacol*, 1991, 1411–1418.
9. Niebrój-Dobosz I, Rafałowska J, Barcikowska-Litwin M: Brain myelin in senile patients with brain infarction. *Neuropatol Pol*, 1986, 24, 351–364.
10. Niebrój-Dobosz I, Rafałowska J, Łukasik M: Do lipid changes influence the density of aging human brain myelin. *Neuropatol Pol*, 1989, 27, 427–436.

11. Niebrój-Dobosz I, Wiśniewska W, Barcikowska-Litwin M: Influence of aging on density of myelin fractions isolated from human brain's white matter. *Neuropatol Pol*, 1988, 26, 19–25.
12. Rafałowska J, Dolińska E, Dziewulska D, Krajewski S: Zaburzenia przepuszczalności bariery krew-mózg w różnych stadiach zawału mózgu u ludzi w wieku średnim i starczym. *Neuropatol Pol*, 1990, 28, 1–17.
13. Rafałowska J, Dolińska E, Dziewulska D, Krajewski S: Astrocytic reactivity in various stages of human brain infarct in middle and senile age. *Neuropatol Pol*, 1991, 29, 181–191.
14. Rafałowska J, Krajewski S, Dolińska E, Barcikowska-Litwin M: W sprawie modyfikacji obrazu histopatologicznego stwardnienia rozsianego w wieku starczym. *Neuropatol Pol*, 1988, 26, 211–224.
15. Simmons RD, Buzbee TM, Linthicum DS, Mandy WJ, Chen G, Wang C: Simultaneous visualization of vascular permeability change and leucocyte egress in the central nervous system during autoimmune encephalomyelitis. *Acta Neuropathol (Berl)*, 1987, 74, 191–193.
16. Sternberger LA, Hardy PM, Jr, Cuculis FF, Meyer MG: The unlabelled antibody enzyme method of immunohistochemistry preparation and properties of soluble antigen-antibody complex (horseradish peroxidase-antiperoxidase) and its use in identification of spirochetes. *J Histochem Cytochem*, 1970, 18, 315–333.
17. Wender M, Adamczewska-Goncerzewicz Z, Stanisławska J, Szczech J, Godlewski A: Pattern of myelin lipids in aging brain. *Neuropatol Pol*, 1987, 25, 235–245.

Authors' address: Department of Neurology, School of Medicine, 1A Banacha St, 02-097 Warsaw, Poland

MIROSLAW RYBA¹, MICHAŁ WALSKI², KRYSZYNA IWAŃSKA³,
KRZYSZTOF GŁOWICKI¹, MAREK PASTUSZKO⁴

THE POSSIBLE ROLE OF ENDOTHELIUM IN PREVENTION OF REBLEEDING IN EXPERIMENTAL SUBARACHNOID HEMORRHAGE (SAH)

¹ Department of Neurophysiology and ² Laboratory of Ultrastructure, Medical Research Centre, Polish Academy of Sciences, Warsaw, ³ Department of Anesthesiology and Intensive Therapy, School of Medicine, Warsaw, ⁴ Department of Neurosurgery, Institute of Surgery, School of Medicine, Warsaw

Experiments were performed on six male cats under nitrous oxide in oxygen anesthesia. Animals were paralysed and artificially ventilated. Subarachnoid hemorrhage (SAH) was produced by basilar artery puncture following clivectomy. After 10 minutes (3 cats) and 60 minutes (3 cats) the basilar artery was dissected and fixed for electronmicroscopic examination.

Ultrastructural examinations revealed in the cytoplasm of the endothelial cells on the side of the vessel lumen, the presence of spherical or flattened cylindrical structures identified as Weibel-Palade bodies. In the endothelium of the proximal segment, 10 and 60 minutes after puncture, the number of these electron-dense bodies increased, and was higher than in the corresponding distal segment. The possible role of the Weibel-Palade bodies in SAH after-effects is discussed.

Key words: *experimental subarachnoid hemorrhage, vasospasm, endothelium, Weibel-Palade bodies.*

Disruption of an intracranial aneurysm is associated with subarachnoid hemorrhage (SAH). Mechanical injury to the brain base artery is one of the experimental models of SAH (Yoshioka et al. 1987). Recent investigations have demonstrated that the neurological state of patients with SAH depends on the amount of extravasated blood (Fisher et al. 1980). Disruption of a brain aneurysm is complicated in more than 30% of cases by a contraction of the cerebral arteries, occurring usually between the third and ninth day after the hemorrhage (Kassel, Boarini 1985). Up to 72 hours after the hemorrhage the most frequent complication is rebleeding, which according to some authors, is in 70% of cases the cause of death (Juvela 1989). This observation justifies search for ways to locally prevent rebleeding.

The results of our earlier investigations indicate that an important role is played in this process by changes occurring in the endothelial cells of cerebral

vessels (Ryba et al., unpublished data) and that the severity of the angiopathic changes due to SAH caused by mechanical damage to the cerebral artery wall decreases with its distance from the lesion site (Yoshioka et al. 1987).

The aim of the study was to follow the distribution of changes in the endothelium with reference to time and distance from the lesion. This problem seems interesting, the more so, since the discovery by Yanagisawa et al. (1988) of an endothelial polypeptide – endothelin, the strongest of all known vasoconstrictors.

MATERIAL AND METHODS

The experiments were performed on six male cats weighing 3.7–4.2 kg. After ketamine injection (20 mg/kg) tracheotomy was performed and the femoral vein was cannulated. After producing muscle atonia (flaccidity) with pancuronium bromide (1 mg i.v.), the animals were ventilated with a mixture of nitrous oxide and oxygen (2:1). Clivectomy was performed transorally. After transection of the dura, the basilar artery was exposed on the segment leading from the vertebral to the posterior cerebral artery. The arterial wall was punctured with a 25 G needle to produce subarachnoid hemorrhage. The puncture was made at the level of branching of the cerebellar posterior inferior artery. After ten (3 cats) and after 60 minutes (3 cats), respectively, the animals were perfused through the ascending aorta with fixative containing 2.5% glutaraldehyde and 2% paraformaldehyde in 0.1 M cacodylate buffer, pH 7.4. After perfusion the fragment of the basilar artery in the immediate vicinity of the puncture (proximal segment) and 10 mm below, that is at the branching of the vertebral arteries were resected. The collected material was fixed in the same solution for 2 hours at 4°C, then postfixated in osmium tetroxide and uranyl acetate, dehydrated in a graded series of ethanol and embedded in Epon 812. Ultrathin sections were stained with uranyl acetate and lead citrate and subsequently examined in a JEM-1200 electron microscope.

RESULTS

Electron microscopic examination of the control material revealed in the cytoplasm of endothelial cells on the side of the vessel lumen, the presence of spherical, or sometimes flattened cylindrical structures (Fig. 1). They were surrounded by a rim of the type of unit membrane (Fig. 2). Their interior was filled with aggregated microtubular material of various electron density.

Ten minutes after the puncture the number of these bodies was higher in the proximal segment (Fig. 3) of the basilar artery than in the distal one (Fig. 4) taken at the same time. Moreover, the enhanced activity of the endothelial cells of the proximal segment as compared with the distal one is noteworthy. It was characterized by a column-like elongation of the cell body and a cytoskeleton well visualized due to aggregation (Fig. 3).

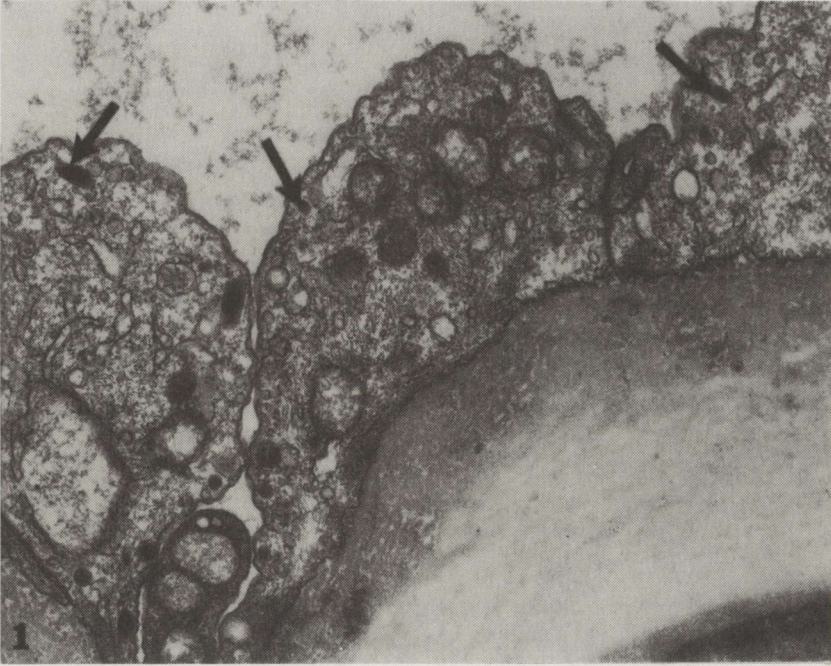


Fig. 1. Control material. In endothelial cells spherical and cylindrical structures (arrows) known as Weibel-Palade bodies are visible. $\times 18\,000$

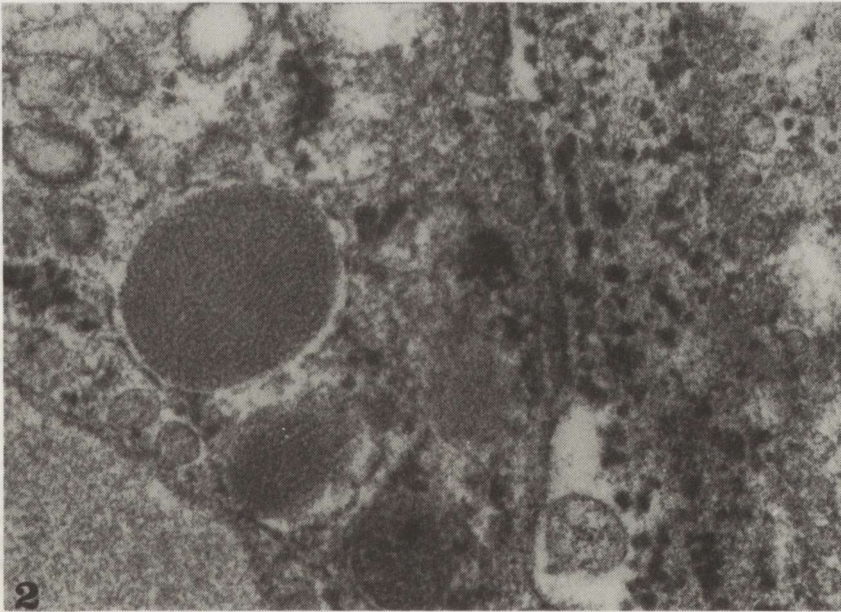


Fig. 2. Fragment of endothelial cell from control vessel. Weibel-Palade body is filled with tubular material and surrounded by double membrane. $\times 110\,000$

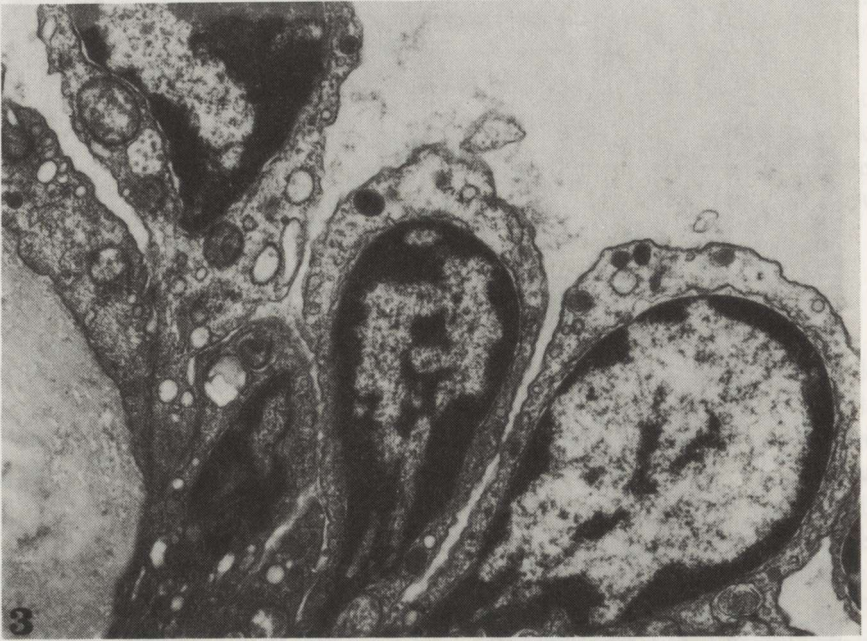


Fig. 3. Proximal segment of basilar artery 10 min after puncture. Close to the plasmatic membranes on the side of the vessel lumen, electron dense bodies of various shape and size are visible. $\times 18\,000$

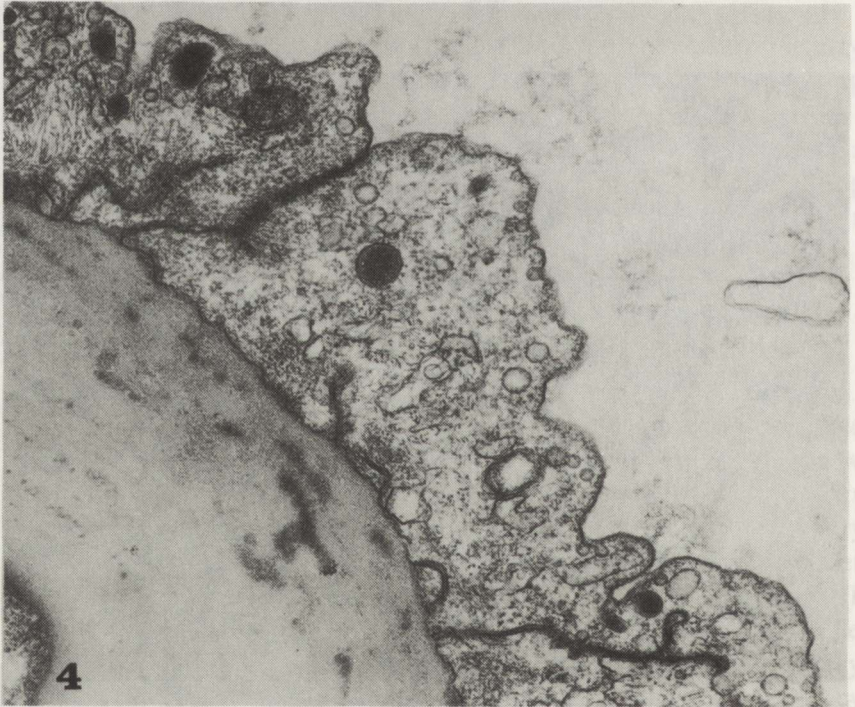


Fig. 4. Distal segment of basilar artery 10 min after puncture. Electron dense bodies of various shape and size in endothelial cells. $\times 18\,000$

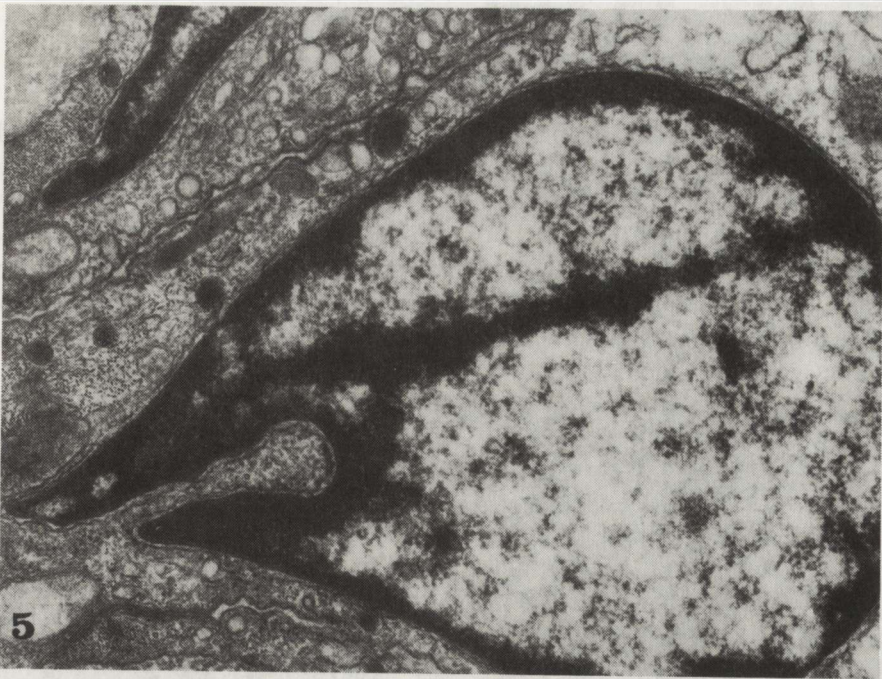


Fig. 5. Proximal segment of basilar artery 60 min after puncture. Numerous vesicular forms of various electron density are seen under the plasmatic membrane of endothelial cell. $\times 22\,000$

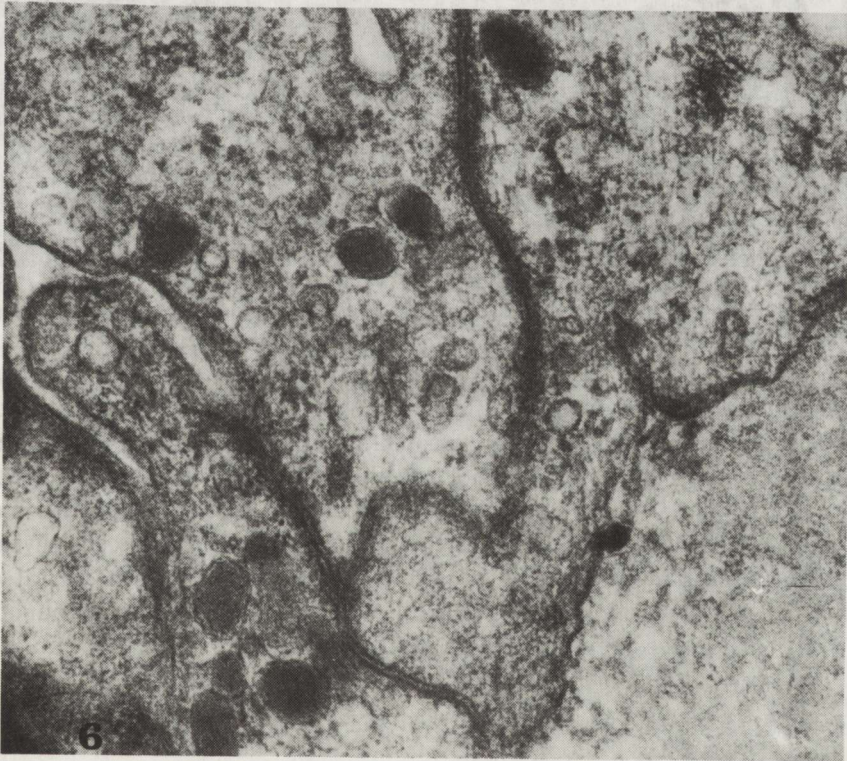


Fig. 6. Distal segment of basilar artery 60 min after puncture. Endothelial cells elongated, junctions between them well preserved. Inside numerous vesicular formations, part of them filled with electron dense material. $\times 24\,000$

Sixty minutes after the puncture the incidence of electron-dense bodies increased in the endothelial cells of both segments. However, their number was higher in the proximal segment than in corresponding distal one (Figs 5 and 6). In the proximal segment features of increased endothelial activity were present represented by an abundance of cellular skeleton elements and of the Golgi apparatus. Fusion of the membrane surrounding the above described electron-dense bodies was observed. This fusion formed a canal filled with the contents of these bodies (Fig. 7).

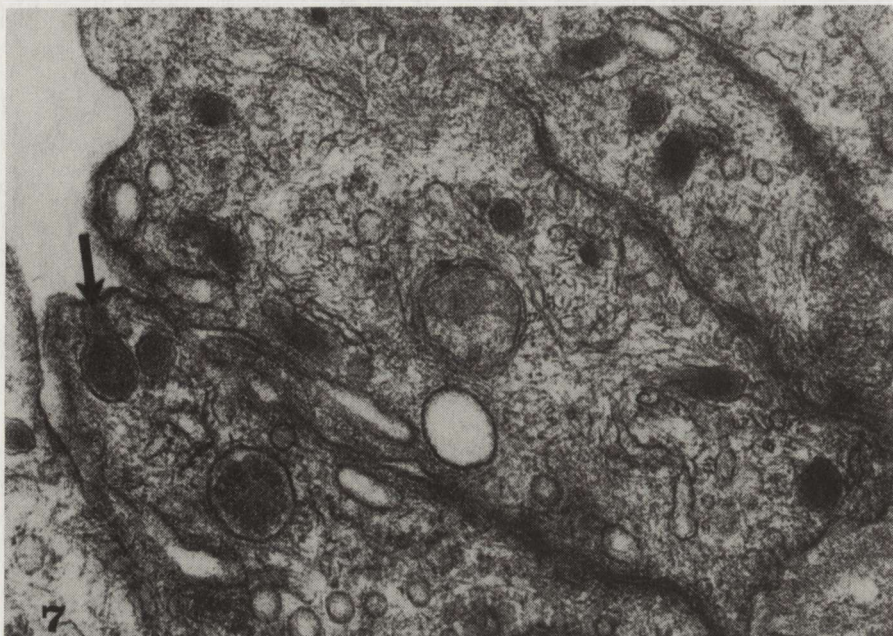


Fig. 7. Proximal segment of basilar artery 60 min after puncture. Numerous electron dense bodies are visible in endothelial cells. One body is connected with the plasmatic membrane of endothelium (arrow.) $\times 24\,000$

On electronmicrographs magnified $\times 20\,000$ the number of dense bodies (identified as Weibel-Palade bodies) was counted on the profiles of endothelial cells. In each group they were counted on 30 profiles of endothelial cells and their mean number were estimated. Quantitative evaluation of the mean number of Weibel-Palade bodies in the cytoplasm of endothelial cells revealed 10 minutes after puncture in the proximal segment 4 and in the distal one 3 bodies per profile of one endothelial cell, whereas 60 minutes after puncture 9 in the proximal segment and 5 in the distal one.

DISCUSSION

In cases of disruption of an intracranial aneurysm arterial blood is extravasated into the subarachnoid space (SAH). The existence of hemostatic mechanisms seems obvious, which acting at the site of rupture of the vessel

wall „plug” the hole. Such a mechanism may be for instance, development of clotting or contraction of the artery. We have attempted in this paper to explain one of these hemostatic mechanisms.

In the cytoplasm of endothelial cells of the basilar artery structural formations were found referred to in the literature as Weibel-Palade bodies (Weibel, Palade 1964). They are morphologically and functionally connected with Golgi apparatus, as ascertained in histochemical investigations on the endothelia of blood and lymphatic vessels (Sengel, Sttoebner 1970; Magari, Ito 1988). Santolaya and Bertini (1970) demonstrated the vasoconstricting activity of extracts of Weibel-Palade bodies from various organs including the brain. This suggests that the Weibel-Palade bodies contain an undefined vasoactive substance which influences the reaction of blood vessels to e.g. mechanical stimuli (Burri, Weibel 1968). In patients with SAH and accompanying vasospasm a rise in the blood endothelin level was noted within the first 24 hours after blood extravasation (Masaoka et al. 1989; Lavesque et al. 1990). Endothelin described for the first time by Yanagisawa et al. (1988) is one of the most potent vasoconstrictors. Its activity may be stimulated by both mechanical and chemical factors such as thrombine, adrenaline and the transforming growth factor-beta. It also may act as an activator of the calcium channels (Masaoka et al. 1989).

If, as a results of vessel lesion, the hemostatic mechanisms come into operation, their morphological manifestations should be more pronounced at the site of the lesion than peripherally. In the present experiments the number of Weibel-Palade bodies was greater at the site of blood vessel puncture than in its peripheral segment and their number increased with time. The literature reports that the vasoconstrictor activity of these granules depends on their amount (Santolaya, Bertini 1970). This suggests that Weibel-Palade bodies accumulated at the site of injury may participate in the mechanism of homeostasis. It is also supposed in experiments with electron microscopic examination (Johannessen 1980) that the secretive granules in the endothelium contain endothelin (Yanagisawa et al. 1988), although *in vitro* tests demonstrated a low vasoconstricting activity of the endothelial lysate (O'Brien et al. 1987). A critical inspection of the present results plus the tentative ascription to the Weibel-Palade bodies of a hemostatic role in SAH, resulting from disruption of an intracranial aneurysm, seem to indicate a contraction of the cerebral artery at the site of injury, and may be of importance in prevention of further blood extravasation. It is suggested that endothelin may play a role in the process. Cytochemical studies of Magari and Ito (1988) revealed that Weibel-Palade bodies do not possess hydrolytic enzymes and glycoproteins of plasmatic membranes, but did not determine finally their composition. According to the authors' opinion, immunocytochemical investigations are needed to ascertain whether Weibel-Palade bodies are endothelin bearers in the endothelium.

DOMNIEMANA ROLA KOMÓREK ŚRÓDBŁONKOWYCH W ZAPOBIEGANIU
DODATKOWEGO KRWAWIENIA W DOŚWIADCZALNYM KRWOTOKU
PODPAJĘCZYNÓWKOWYM

Streszczenie

Doświadczenie przeprowadzono na 6 kotach, u których wywołano krwotok podpajęczynówkowy przez nakłucie tętnicy podstawnej. Po 10 minutach (3 koty) i 60 minutach (3 koty) zwierzęta uśmiercano i pobierano do badania mikroskopowo-elektronowego wycinki z tętnicy podstawnej mózgu w miejscu wkłucia i w odległości 10 mm od uszkodzenia. Wykazano w cytoplazmie komórek śródbłonkowych od strony światła naczynia obecność struktur zidentyfikowanych jako ciała Weibel-Palade. Liczba tych ciał zwiększała się wraz z czasem przeżycia zwierząt i była większa w cytoplazmie komórek śródbłonka w odcinku tętnicy bliższym miejsca jej uszkodzenia. Przedyskutowano możliwość udziału tych struktur w patomechanizmie zaburzeń zapoczątkowanych przez krwotok podpajęczynówkowy.

REFERENCES

1. Bertini F, Santolaya R: A novel type of granules observed in toad endothelial cells and their relationship with blood pressure active factors. *Experientia*, 1970, 26, 522–523.
2. Burri PH, Weibel ER: Beeinflussung einer spezifischen cytoplasmatischen Organelle von Endothelzellen durch Adrenalin. *Z Zellforsch*, 1968, 88, 426–440.
3. Fisher CM, Kistler JP, Davies JM: Relation of cerebral vasospasm to subarachnoid hemorrhage visualized by computerized tomographic scanning. *Neurosurgery*, 1980, 6, 1–9.
4. Johannessen JV: Electron microscopy in human medicine, vol V, McGraw-Hill, New York, 1980.
5. Juvela S: Rebleeding from ruptured intracranial aneurysms. *Surg Neurol*, 1989, 32, 326.
6. Kassel NF, Boarini DJ: Timing of aneurysm surgery. In: *Neurosurgery*. Eds: RH Wilkins, SS Rangachary. McGraw-Hill, New York, 1985.
7. Lavesque H, Sevrain L, Freger P, Tadie M, Courtois H, Creissard P: Raised plasma endothelin in aneurysmal subarachnoid haemorrhage. *Lancet*, 1990, 3, 290.
8. Magari S, Ito Y: Weibel-Palade bodies in endothelial cells of normal thoracic ducts and deep cervical lymphatics in rabbits. *Lymphology*, 1988, 21, 93–98.
9. Masaoka KL, Suzuki R, Hirata Y, Emori T, Marumo F, Hirakawa KL: Raised plasma endothelin in aneurysmal subarachnoid haemorrhage. *Lancet*, 1989, 9, 1402.
10. O'Brien RF, Robbins RJ, McMurtry IF: Endothelial cells in culture produce a vasoconstrictor substance. *J Cell Physiol*, 1987, 132, 263–270.
11. Santolaya RC, Bertini I: Fine structure of endothelial cells of vertebrates. Distribution of dense granules. *Z Anat Entwickl Gesch*, 1970, 131, 148–155.
12. Sengel A, Stoebner P: Golgi origin of tubular inclusions in endothelial cells. *J Cell Biol*, 1980, 40, 223–226.
13. Weibel ER, Palade GE: New cytoplasmic components in arterial endothelia. *J Cell Biol*, 1964, 23, 101–106.
14. Yanagisawa M, Kurihara H, Kimura S, Tomobe Y, Kobayashi M, Mitsui Y, Yazaki Y, Goto K, Masaki T: A novel potent vasoconstrictor peptide produced by vascular endothelial cell. *Nature*, 1988, 132, 411–415.
15. Yoshioka J, Clower BR, Smith RR: The angiopathy of subarachnoid hemorrhage. I. Role of vessel wall catecholamines. *Stroke*, 1987, 15, 288–294.

Correspondence address: dr M. Ryba, Department of Neurophysiology, Medical Research Centre, PAsci, 3 Dworkowa St, 00-784 Warsaw, Poland

ANNA TARASZEWSKA, IRMINA B. ZELMAN

ULTRASTRUCTURAL PATTERN OF BRAIN AGING IN NORMAL RABBIT AND IN PT MUTANT

Department of Neuropathology, Medical Research Centre, Polish Academy of Sciences, Warsaw

The aim of the study was to compare ultrastructural brain changes in aging normal rabbits and in pt mutants with CNS hypomyelination. The study was performed on material of pt and healthy 3- and 4-year-old rabbits and on the control group of adult rabbits aged up to 2 years. Ultrastructural changes in both aging normal and pt rabbits included lipofuscin accumulation in glial and nerve cells, wide extension of astrocytic processes around vessels and in neuropil, thinning of capillary endothelia and their lumen distension, neuroaxonal dystrophy and incidence of degenerated dendrites and synaptic terminals. These changes, especially degeneration of axons and dendrites were much more frequent in the pt mutants than in normal rabbits. Moreover, myelin sheath abnormalities, similar as in younger pt rabbits were a characteristic feature in the aging mutants, whereas, the myelin in aging normal rabbits was well preserved, probably because the white matter changes are rather a later event in senescence. It is concluded, that with the exception of white matter affection in mutants, the age-related changes do not vary much qualitatively between pt and normal rabbit, although they are distinctly enhanced and develop earlier in mutants. Further studies are needed for evaluation of the influence of the aging process on the white matter changes in association with pt mutation and under normal conditions in animals of more advanced age.

Key words: *hypomyelinated pt mutant, rabbit, brain aging.*

Manifestation and time course of brain aging depend on several factors acting during life, including inherited or acquired genetic defects. Mutants with known hereditary traits can be regarded as particularly suitable material for investigation of the influence of some genetic factors on aging processes. The best known example of such conditions in humans is the Down syndrome which is associated with premature brain aging characterized by Alzheimer's type pathological changes (Wiśniewski et al. 1985). The Down syndrome has become a helpful model for studies concerning gene involvement in the pathogenesis of accelerated brain aging of Alzheimer type (Delabar et al. 1990).

The undertaken studies on brain aging in the pt rabbit mutant are justified by previous observations suggesting an accelerated aging process in these

rabbits (Osetowska, Luszawski 1976). The genetic pt trait is X-linked and causes disturbed CNS myelin development and hypomyelination (Zelman, Taraszewska 1984; Taraszewska, Zelman 1986; Domańska-Janik et al. 1986). The affected rabbits are characterized clinically by body tremor and paresis appearing after birth. The symptoms are most pronounced during the period of CNS myelination, then gradually decline beginning from 3-4 months of life. Adult pt rabbits, despite slight spasticity, show complete recovery of motor function, ability for reproduction and survive in good breeding conditions over 5 years. However, in comparison with healthy rabbits, they exhibit phenotypic symptoms of senescence much earlier, even at the age of 3-4 years of life. Neuropathologic examination revealed development also 2 years earlier of unspecific senile brain changes, on the average, in symptomatic pt rabbits (Osetowska, Luszawski 1976).

The aim of the present study was to characterize the ultrastructural feature of early aging brain changes in normal rabbits and to compare them with changes in pt mutants of the same age.

MATERIAL AND METHODS

The study was performed on the material of 5 pt mutants and 3 healthy rabbits aged 3 and 4 years. The animals (2 females and 5 males) exhibited a decrease or loss of reproduction ability, what has been considered as the onset of senile involution in rabbits over 2 years old (Herman 1973; Osetowska, Luszawski 1976). A group of young adult rabbits (13 to 23 months old) was used as comparative material and included 3 pt mutants and 2 healthy normal animals, respectively.

All rabbits were provided by the Breeding Unit of pt mutant stock in Mińsk Mazowiecki and were kept under the same conditions during their life. The pt rabbits used for studies presented the typical symptomatic course of the disease in the first months of life with subsequent improvement at adolescence.

The animals were sacrificed under deep anesthesia (Eunarcon or chloral hydrate i.v.) by intracardiac perfusion with 3.9% glutaraldehyde in 0.4 M phosphate buffer (pH 7.6). The brains and cervical segments of spinal cord were removed after fixation and specimens from frontal cortex, brain stem, cerebellum and dorsal funiculi of spinal cord were taken for EM examination. The material was postfixed in 1% osmium tetroxide, dehydrated in ethanol and propylene oxide and embedded in Epon 812. Semithin sections stained with 1% toluidine blue were used for light microscopic evaluation, then ultrathin sections were cut from selected blocks, stained with uranyl acetate and lead citrate and examined in a JEM 100 B or JEM 100 BX electron microscope.

RESULTS

In the comparative group of young normal animals, the ultrastructural pattern of neuronal and glial cells and of nerve fibers was normal, whereas in pt rabbits the abnormalities of myelinated fibers were a common feature. These



Fig. 1. Pt rabbit 4 1/2-year-old. Spinal cord. Focal distension of myelin sheath by wide layer of cytoplasm displaying degenerative changes and splitting of myelin lamellae. $\times 29\,500$

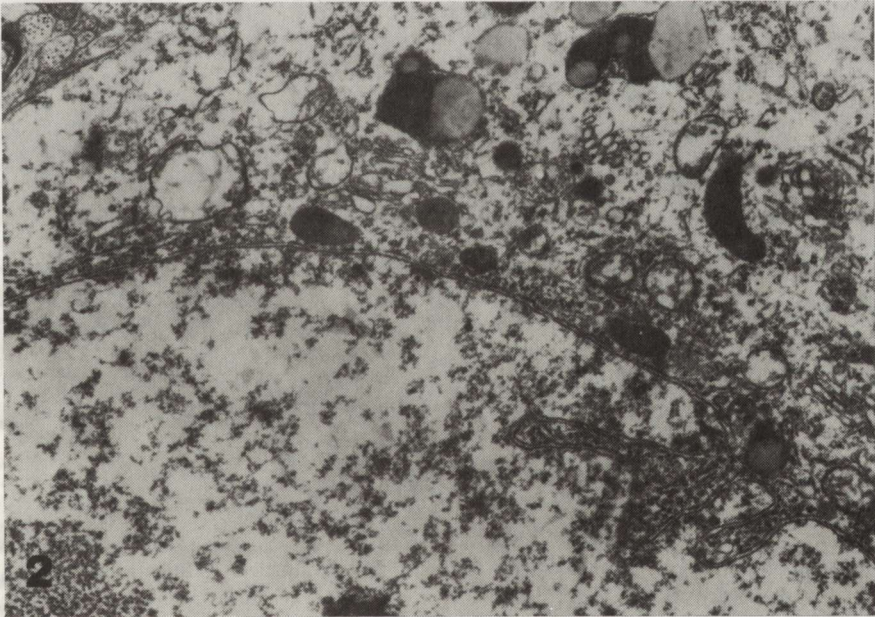


Fig. 2. Pt rabbit 3 1/2-year-old. Frontal cortex. Lipopigment granules, loss of granular endoplasmic reticulum, altered mitochondria and rarefaction of nuclear euchromatin in nerve cell. $\times 15\,300$

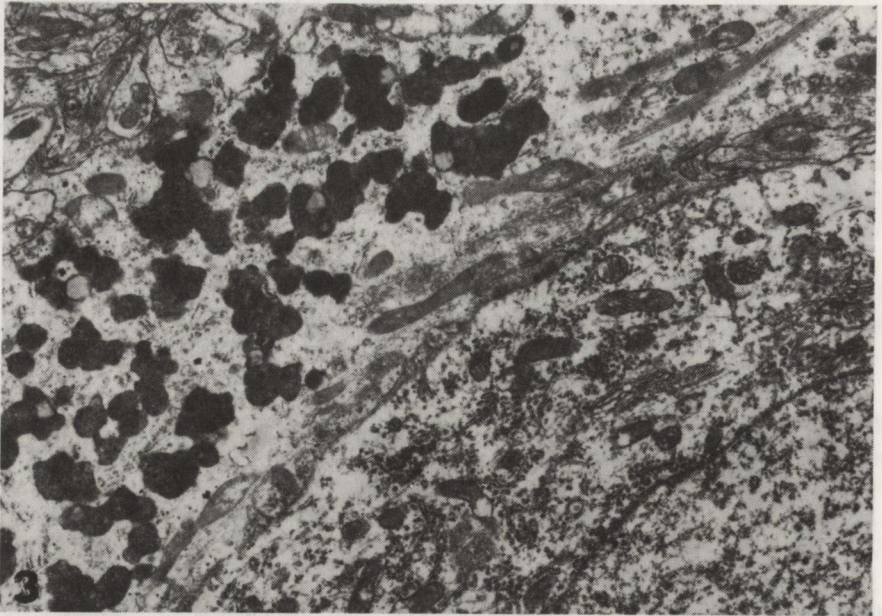


Fig. 3. Normal 4-year-old rabbit. Frontal cortex. Numerous lipopigment granules in cytoplasm of astrocyte alongside of normal nerve cell. $\times 10\,200$

changes were described in detail previously (Taraszewska 1983, 1988). Briefly, they were characterized by a thinning of myelin sheaths, frequent derangement of lamellar myelin structure and some degenerative axonal changes. The same type of myelin sheath abnormalities was seen also in ageing pt rabbits (Fig. 1),

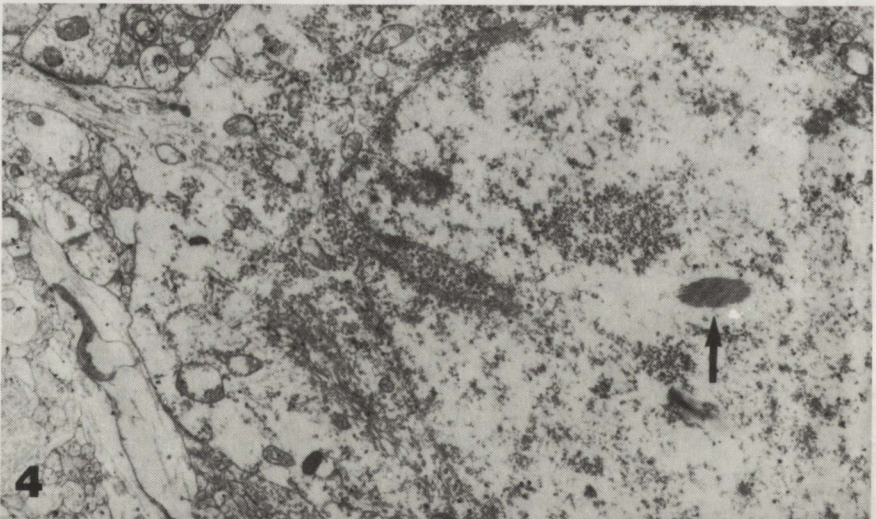


Fig. 4. Pt rabbit 3-year-old. Frontal cortex. In nerve cell intranuclear rod-like fibrillar inclusion (arrow), irregular density of karyoplasm and invagination of nuclear envelope. Paucity of organelles at periphery of cytoplasm. $\times 6\,000$

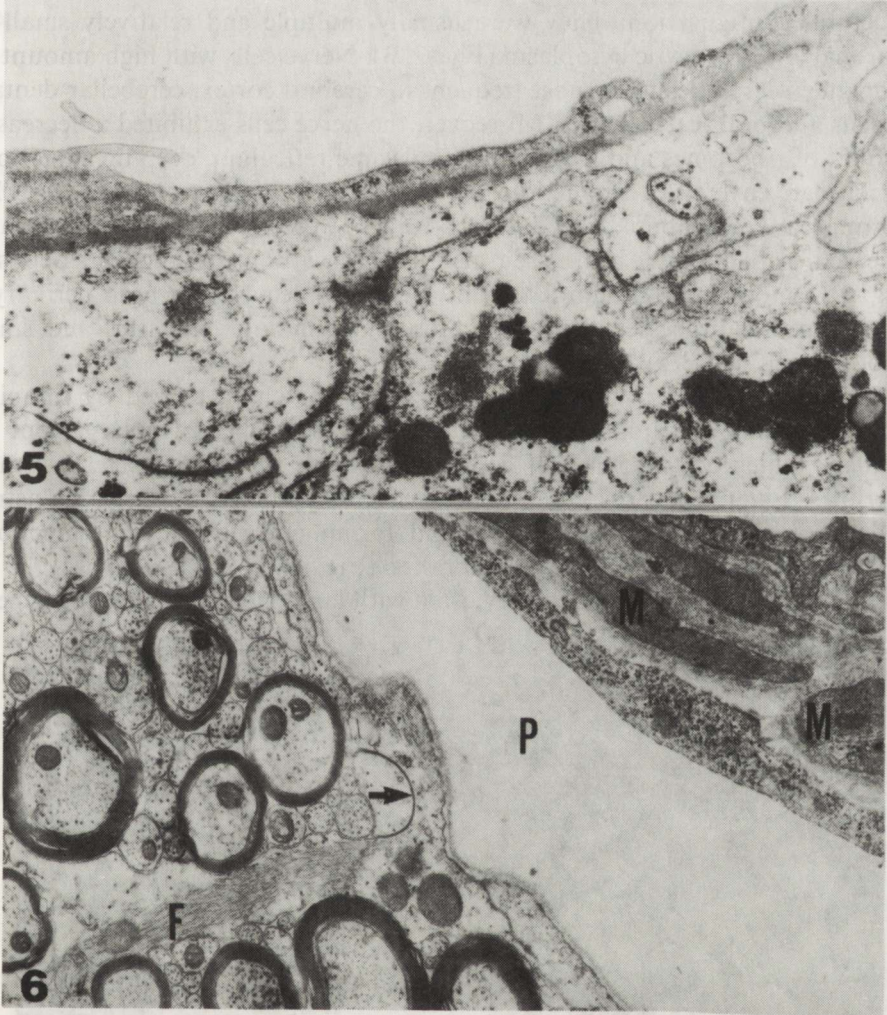


Fig. 5. Normal 4-year-old rabbit. Frontal cortex. Lipopigment granules in large astroglial processes surrounding capillary with distended lumen. $\times 19\,200$

Fig. 6. Normal 4 1/2-year-old rabbit. Brain stem. Fragment of vessel wall with enlarged perivascular space (P) and increase of collagen fibrils between muscle cells (M) in media. Around the vessel astroglial processes with gliofilaments (F) and tight junction between adjoining cell membranes (arrow). $\times 14\,400$

whereas, the ultrastructure of myelin sheaths was well preserved in normal rabbits of the same age.

The main finding in the aging group common to both normal and pt rabbits was the occurrence of lipopigment in the cytoplasm of neuronal, astroglial and microglial cells. In oligodendrocytes, however, lipopigment deposits were found exclusively in pt rabbits.

In the particular cell types lipopigment granules varied in size, number and structural configuration. They were usually multiple and relatively small in neuronal and astrocytic cytoplasm (Figs 2, 3). Nerve cells with high amount of lipopigment granules were most frequent in cerebral cortex, cerebellar dentate nucleus and brain stem nuclei. Moreover, the nerve cells exhibited a decreased amount of ribosomes and granular endoplasmic reticulum, deep invaginations of nuclear envelope, rarefaction of euchromatin and sometimes fibrillar intranuclear inclusions. The latter changes were much more frequently observed in pt rabbits, being seen also in cells without lipopigment deposits (Fig. 4). Lipopigment accumulation in astrocytes occurred in both perikaryal cytoplasm and processes, especially those surrounding capillaries and small blood vessels (Fig. 5).

The ultrastructural pattern of vessel walls was characterized by thinning and elongation of capillary endothelial cells, with marked enlargement of capillary lumen and increase of collagen fibrils in the medial layer of small arterioles. Extended perivascular spaces were surrounded by the large astroglial processes, rich in gliofilaments and forming numerous tight junctions between neighbouring cellular membranes (Fig. 6).

Microglial cells were loaded very often with large mostly single lipopigment



Fig. 7. Pt rabbit 3 1/2-year-old. *Nucleus dentatus*. Great conglomeration of lipopigment in microglial cell cytoplasm. $\times 16\ 300$

depots composed predominantly of coarse lipid droplets and sparse pigment matrix (Fig. 7). Such cells were a frequent finding in both aging rabbit groups.

In oligodendrocytes of pt rabbits an other form of lipopigment was accumulated. It was composed almost exclusively of fine granular pigment matrix displaying at places multilinear structures and clear crystal-like longitudinal clefts (Fig. 8). Lipopigment depots were found in both cytoplasm and processes in the white matter oligodendrocytes as well as in the perikarya of perineuronal satellites (Fig. 9). A characteristic feature of oligodendroglial cells in aging pt rabbits was also large perikaryal cytoplasm with abundance of

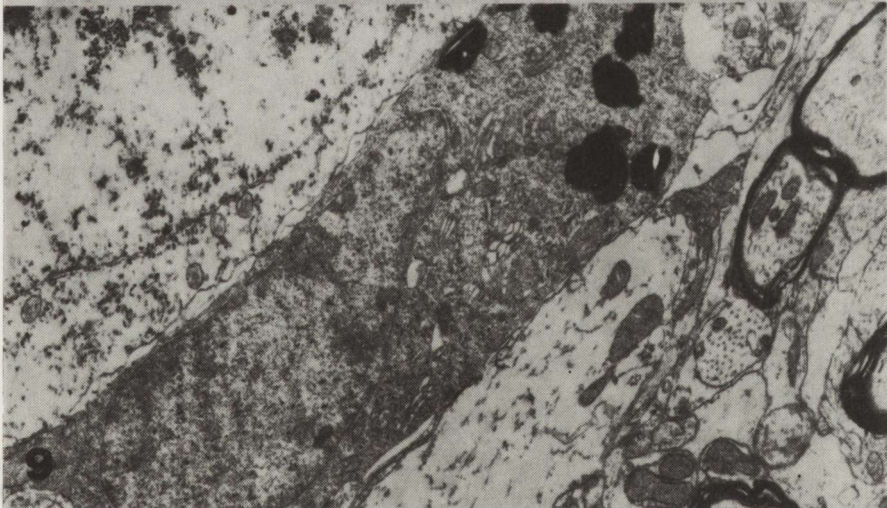
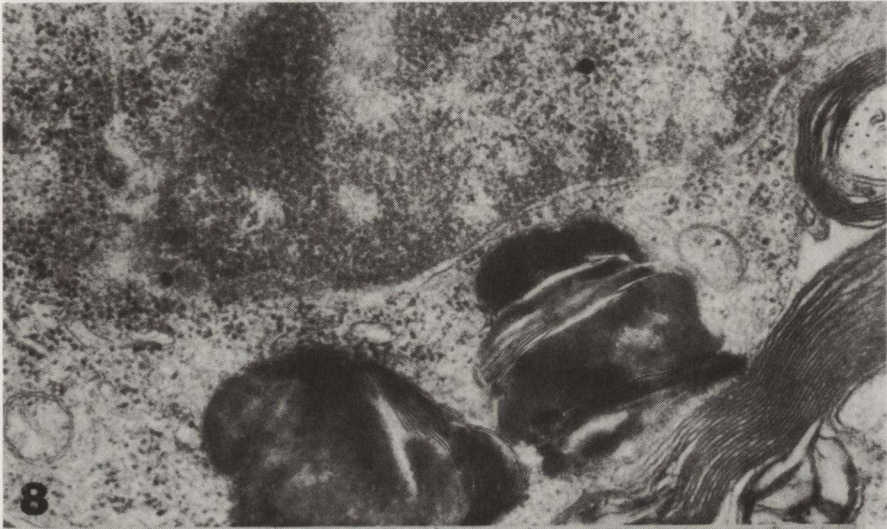


Fig. 8. Pt rabbit 3-year-old. Spinal cord. Electron-dense prismatic depots of pigment matrix with multilamellar structures and linear clear clefts in cytoplasm of oligodendrocyte. In adjacent myelin sheaths loosening of lamellar structure. $\times 32000$

Fig. 9. Pt rabbit 4 1/2-year-old. Brain stem. In cytoplasm of perineuronal satellite oligodendrocyte lipopigment granules of the same appearance as in Fig. 8. $\times 9600$

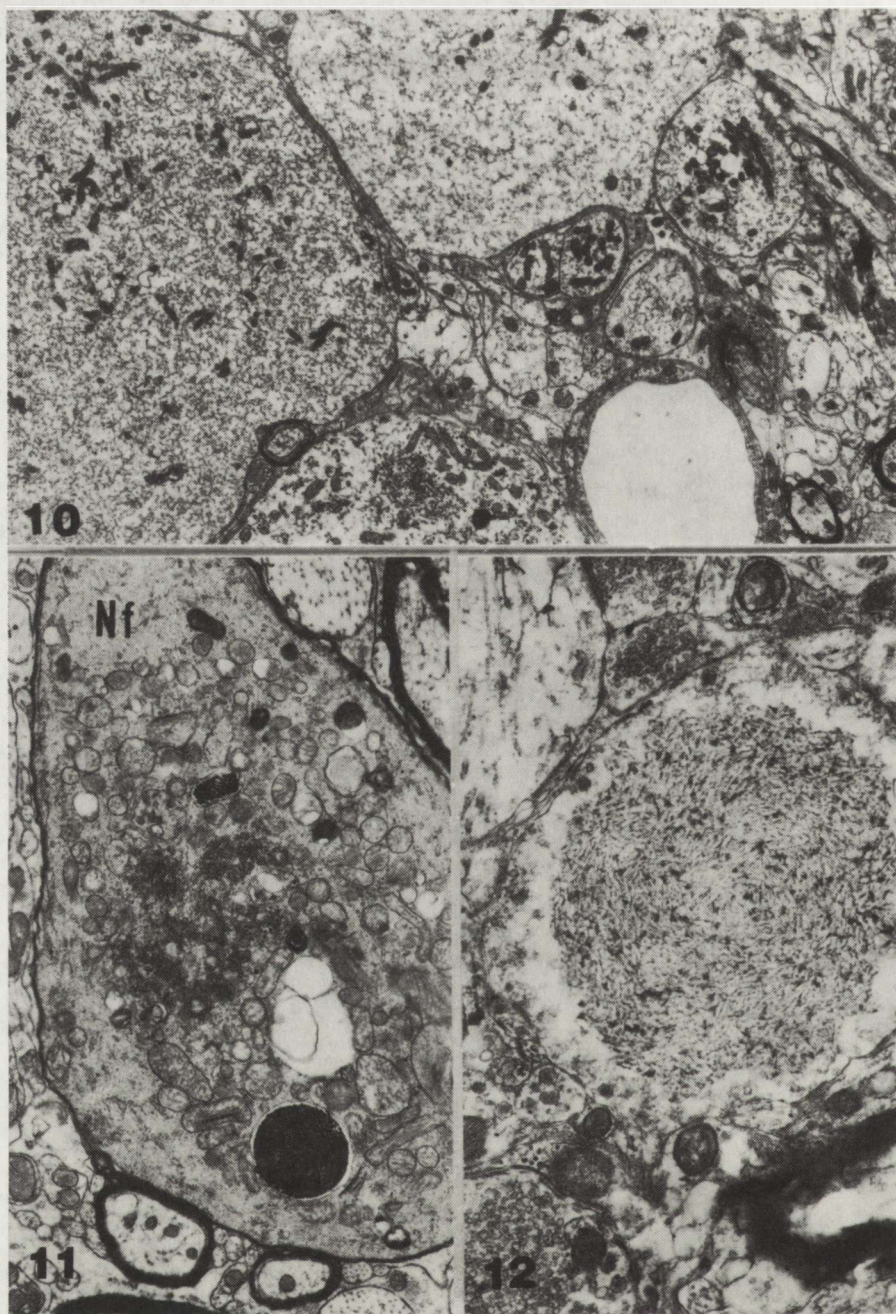


Fig. 10. Pt rabbit 4 1/2-year-old. *Nucleus gracilis*. Large spheroids contain agglomeration of smooth tubular and vesicular structures, small mitochondria and dispersed floccular material. $\times 15000$

Fig. 11. Pt rabbit 4 1/2-year-old. *Nucleus gracilis*. Axonal swelling filled with densely packed neurofilaments (NF), mitochondria, smooth tubular structures, agglomeration of glycogen granules and surrounded by thin myelin sheath. $\times 9700$

Fig. 12. Normal 4-year-old rabbit. Brain stem. Intraaxonal "Lafora" body-like fibrillar inclusion. Some synaptic terminals contain dense bodies. $\times 19000$

free ribosomes and microtubules and prominent cytoplasmic processes adjoining myelin sheaths.

Another common finding in both normal and pt rabbits aged over 3 years was the occurrence of dystrophic axons with variable ultrastructural pattern (Figs 10, 11, 12). Enlarged altered axons and enormous spheroids were particularly numerous in nuclei of dorsal funiculi and less frequent in the white

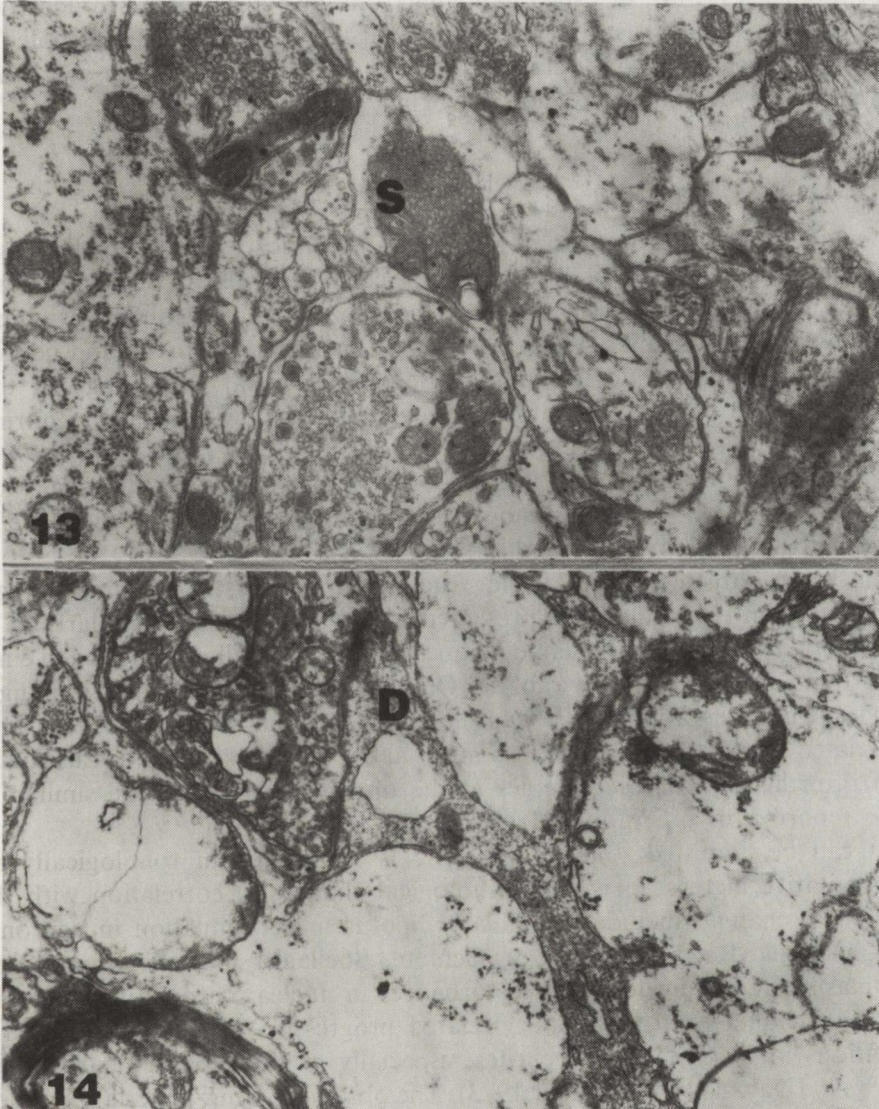


Fig. 13. Normal 4-year-old rabbit. Brain stem. Electron-dense degeneration of axonal terminal with densely packed synaptic vesicles (S). $\times 15000$

Fig. 14. Pt rabbit 3 1/2-year-old. *Nucleus dentatus*. Degenerated dendrite (D) with increased electron density and microvacuolation, surrounded by enlarged swollen astroglial processes. Presynaptic ending is also damaged. $\times 19000$

matter of spinal cord, in brain stem and cerebellum. They revealed highly heterogeneous intrinsic structure corresponding to all the types of dystrophic axons described in the literature (Lampert 1967; Jellinger 1973; Leonhardt 1976; Saito 1980; Yoshikawa et al. 1985). Besides dystrophic axons, dark degenerated axons and synaptic terminals (Fig. 13) were much more frequently encountered in pt rabbits than in normal ones. Moreover, electron-dense vacuolar degeneration of dendrites appeared particularly often in the material of pt rabbits (Fig. 14), in which many dendrites displayed increased density of microtubules, numerous multivesicular bodies, electron-lucent vacuoles or segmental swelling of cytoplasm and loss of organelles. They were also surrounded by enlarged swollen astroglial processes (Fig. 14).

DISCUSSION

A wide range of neurogerontological studies indicate that brain changes in the course of a normal biological aging process are similar in different animal species (Miquel et al. 1983). However, the majority of old animals examined did not exhibit Alzheimer type pathology (neurofibrillary tangles and neuritic plaques) so characteristic for human brain aging, what might suggest, that these changes constitute a separate pathogenic process with regard to normal biological senescence or can be species specific (Unterbeck et al. 1990). Incidence of senile plaques is known only in senile dog (Osetowska 1966; Taraszewska et al. 1971) and in monkey (Wiśniewski, Terry 1973), therefore, in animals with a relatively long life span.

In the available literature, a fine structural characteristics of aging changes in rabbit brain is lacking. The presented results indicate, that similarly as in several other small animals, senile plaques and neurofibrillary tangles have not been found in the examined rabbits. Our results support also previous light microscopic observations, that symptomatic pt mutants undergo the same age-related qualitative changes as normal rabbits (Osetowska, Luszawski 1976). Furthermore, these changes at the ultrastructural level are similar to those reported in other animal species.

It can be admitted, that brain aging is manifested morphologically by a quantitative increase of some pathological changes in correlation with the age. These changes include particularly lipofuscin accumulation in neuronal and glial cells (Reichel et al. 1968; Schlote, Boellaard 1983), ribosomal and endoplasmic reticulum loss and disturbances in nuclear chromatin pattern in neurons (Miquel et al. 1983), age-related progressive increase of structural alterations in dendrites and neurites, especially of the type of neuroaxonal dystrophy (Dayan 1971; Jellinger 1973). The observed in our material extended capillary lumen, thinning and elongation of endothelial cells resemble the previously described blood vessel changes in the brains of mice and rats, regarded as an effect compensatory to endothelial cell loss (Burns et al. 1983).

The above mentioned abnormalities in the ultrastructural pattern of nerve

cell cytoplasm and nuclei and degenerative changes of dendrites and axons were found to be remarkably more frequent in the pt mutants than in normal rabbits. These observations suggest, that the age-related changes of nerve cells develop earlier and are more advanced in the pt mutant in comparison with those in normal rabbits. Moreover, the high incidence of numerous lipopigment granules only in pt rabbit oligodendrocytes indicates that these cells in mutants are also earlier subjected to aging process. The ultrastructural pattern of lipopigment depots in pt rabbit oligodendrocytes does not differ from those observed in oligodendroglia of other old animals or in humans (Vaughn, Peters 1974; Schlote, Boellaard 1983). Sturrock (1980) observed, that oligodendrocytes in the white matter of mice reveal lipopigment accumulation earlier than in gray matter, what according to this author may be related to their higher metabolic activity.

In the pt mutant, accumulation of lipopigment in oligodendrocytes of both white and gray matter may indicate accelerated aging processes of these cells in association with their intrinsic pt-linked metabolic changes. Domańska-Janik et al. (1987) demonstrated, that synthesis of myelin constituents by oligodendroglial cells in pt rabbit brain is preserved and even enhanced, thus the disturbed myelination is probably caused by inhibited utilization or increased elimination of already synthesized myelin-related compounds. The ultrastructural pattern of oligodendroglia characterized by large perikaryal cytoplasm and processes rich in free ribosomes and microtubules could be also relevant to its metabolic activation, similarly as in young pt rabbits (Taraszewska, Zelman 1987).

We noted that changes in ultrastructure of myelin sheaths do not vary much between adult and aging pt rabbits. In normal rabbits, however, myelin sheaths and myelinated fibers were well preserved, presumably, because the age-related myelin changes could be a feature of older age than that of the examined animals. Further research on animals in more advanced age are needed to compare the changes in white matter during normal aging and those in association with pt mutation.

ULTRASTRUKTURALNY OBRAZ STARZENIA SIĘ MÓZGU U NORMALNEGO KRÓLIKA I U MUTANTA pt

Streszczenie

Porównano rozwój zmian starczych w mózgu królika normalnego i mutanta pt, u którego dziedziczne zaburzenia procesu mielinizacji ośrodkowego układu nerwowego ulegają częściowemu wyrównaniu w wieku dorosłym. Badanie wykonano na królikach pt i zdrowych w wieku od 3 do 5 lat i na grupie kontrolnej młodych królików w wieku poniżej 2 lat.

Do zmian charakteryzujących mózgi królików starzejących się należało występowanie lipofuscyny w komórkach glejowych i nerwowych, rozrost wypustek astrocytarnych w neuropilu i wokół naczyń, spłaszczenie śródbłonnów i włóknienie błony śródkowej naczyń, dystrofia neuroaksonalna, rozsiane zmiany zwyrodnieniowe w synapsach i dendrytach. Ultrastrukturalny

obraz tych zmian był jednakowy u królików zdrowych i pt, ale u mutantów ich nasilenie było większe, zwłaszcza zwyrodnienie aksonów i dendrytów obserwowano znacznie częściej. Dodatkowo u królików pt występowały zmiany w osłonkach i włóknach mielinowych związane z nieprawidłowościami mieliny, charakteryzującymi tego mutanta. Ultrastrukturalny obraz tych zmian był podobny jak u dorosłych młodych królików pt. Natomiast u zdrowych królików mielina była dobrze zachowana, co przypuszczalnie wiąże się ze zbyt wczesnym okresem inwolucyjnego wieku badanych zwierząt.

Stwierdzono, że mutacja pt nasila zmiany odzwierciedlające proces starzenia się mózgu, ale nie zmienia ich podstawowego charakteru w badanym przedziale wieku.

Badania u zwierząt w późnym wieku starczym są konieczne dla pełnej oceny wpływu mutacji pt na przebieg procesu starzenia się mózgu oraz określenia wpływu wieku na obraz mieliny u normalnych królików i mutantów pt.

REFERENCES

1. Burns EM, Kruckeberg TW, Gaetamo PK, Shulman LM: Morphological changes in cerebral capillaries with age. In: Brain Aging: Neuropathology and Neuropharmacology. Eds: J Cervós-Navarro, H-J Sarkander, Raven Press, New York, 1983, pp 115–132.
2. Dayan AD: Comparative neuropathology of ageing: studies on the brain of 47 species of vertebrates. Brain, 1971, 94, 31–42.
3. Delabar JM, Blouin JL, Rahmani Z, Créan-Goldberg N, Chettouh Z, Nicole A, Bruel A, Le Blois MC, Sinet PM: Down syndrome: a model for the study of Alzheimer's disease and aging. In: Early Markers in Parkinson's and Alzheimer's Diseases. Eds: P Dostert, P Reiderer, MS Benedetti, R Roneueci, Springer, Wien, New York, 1990, pp 165–179.
4. Domańska-Janik K, Wikiel H, Zelman IB, Strosznajder J: Brain lipids of a myelin-deficient rabbit mutant during development. Neurochem Patol, 1986, 4, 135–151.
5. Domańska-Janik K, Gajkowska B, Strosznajder J, Zalewska T: Metabolic studies on dysmyelinating mutant pt rabbit brain *in vitro*. Neurochem Patol, 1987, 7, 233–249.
6. Herman W: Hodowla królików. PWRL, Warszawa, 1973.
7. Jellinger K: Neuroaxonal dystrophy: its natural history and related disorders. In: Progress in Neuropathology. Ed: HM Zimmerman. Grune and Stratton, New York, 1973, v 2, pp 129–180.
8. Lampert PW: A comparative electron microscopic study of reactive, regenerating and dystrophic terminal axons. J Neuropathol Exp Neurol, 1967, 28, 353–370.
9. Leonhardt H: Axonal spheroids in the spinal cord of normal rabbits. Cell Tissue Res, 1976, 174, 99–108.
10. Miquel J, Johnson JE Jr, Cervós-Navarro J: Comparison of CNS aging in humans and experimental animals. In: Brain Aging: Neuropathology and Neuropharmacology. Eds: J Cervós-Navarro, H-J Sarkander. Raven Press, New York, 1983, pp. 231–258.
11. Osetowska E: Zmiany morfologiczne w mózgach starczych psów. Neuropatol Pol, 1966, 1, 97–110.
12. Osetowska E, Luszawski F: Zmiany starcze w mózgu królika zdrowego i w mózgu królika pt. Neuropatol Pol, 1976, 14, 253–264.
13. Reichel W, Hollander J, Clark JH, Strehler BL: Lipofuscin pigment accumulation as a function of age and distribution in rodent brain. J. Gerontol, 1968, 23, 71–78.
14. Saito K: Spheroid and altered axons in the spinal gray matter of the normal cat. An electron-microscopic study. Acta Neuropathol (Berl), 1980, 52, 213–222.
15. Schlote W, Boellaard JW: Role of lipopigment during aging of nerve and glial cells in the human central nervous system. In: Brain Aging: Neuropathology and Neuropharmacology. Eds: J Cervós-Navarro, H-J Sarkander, Raven Press, New York, 1983, pp 27–74.
16. Sturrock RR: A comparative quantitative and morphological study of aging in the mouse neostriatum, indusium griseum and anterior commissure. Neuropatol Appl Neurobiol, 1980, 6, 51–68.

17. Taraszewska A: Ocena zaburzeń w tworzeniu osłonek mielinowych u królika pt na podstawie badań rdzenia kręgowego w mikroskopie elektronowym. *Neuropatol Pol*, 1983, 21, 327–342.
18. Taraszewska A: Ultrastructure of axons in disturbed CNS myelination in pt rabbit. *Neuropatol Pol*, 1988, 26, 385–402.
19. Taraszewska A, Lewicka-Wysocka H, Nozdryn-Plotnicki B: Analiza neuropatologiczna zmian u psów starczych z nowotworami narządów wewnętrznych. *Neuropatol Pol*, 1971, 9, 219–230.
20. Taraszewska A, Zelman IB: Morfometryczna ocena procesu mielinizacji w mózgu królika pt. II. Spoidło wielkie. *Neuropatol Pol*, 1986, 24, 443–454.
21. Taraszewska A, Zelman IB: Electron microscopic study of glia in pt rabbit during myelination. *Neuropatol Pol*, 1987, 25, 351–368.
22. Unterbeck A, Baynay RM, Scangos G, Wirak DO: Transgenic mouse models of amyloidosis in Alzheimer's disease. *Rev Biol Res Aging*, 1990, 4, 139–162.
23. Wiśniewski HM, Terry RD: Reexamination on the pathogenesis of the senile plaques. In: *Progress in Neuropathology*. Ed: HM Zimmerman. Grune and Stratton, New York, 1973, v 2, pp 1–26.
24. Wiśniewski KE, Dalton AJ, McLachlan C, We GY, Wiśniewski HM: Alzheimer's disease in Down's syndrome: Clinicopathologic studies. *Neurology*, 1985, 35, 957–961.
25. Vaughn DW, Peters A: Neuroglial cells in the cerebral cortex of rats from young adulthood to old age. *J Neurocytol*, 1974, 3, 405–429.
26. Yoshikawa H, Tarui S, Hashimoto PH: Diminished retrograde transport causes axonal dystrophy in the nucleus gracilis. Electron- and light-microscopic study. *Acta Neuropathol (Berl)*, 1985, 68, 93–100.
27. Zelman IB, Taraszewska A: Patologia mieliny u królika pt. *Neuropatol Pol*, 1984, 22, 205–218.

Authors' address: Department of Neuropathology, Medical Research Centre, PASci, 3 Dworkowa St, 00-784 Warsaw, Poland

MARIA BARCIKOWSKA¹, MAREK KUJAWA², HENRYK WIŚNIEWSKI³

BETA-AMYLOID DEPOSITS WITHIN THE CEREBELLUM OF PERSONS OLDER THAN 80 YEARS OF AGE

¹ Department of Neuropathology, Medical Research Centre, Polish Academy of Sciences, Warsaw, ² Institute of Biostructure, School of Medicine, Warsaw, ³ New York State Institute for Basic Research in Developmental Disabilities, Staten Island, New York

The cerebellum, frontal cortex, hippocampal and parahippocampal regions of 100 patients older than 80 years, most of whom had died of stroke, were examined. Eighteen percent were diagnosed as clinically demented. On the specimens labeled previously with Thioflavin S and Bielschowsky method, immunohistochemical studies were performed with Fab (antigen-binding fragment) of the anti beta-amyloid antibody 4G8. Positive amyloid immunoreactivity was observed in the cerebrum in 71 of 100 cases, Cerebella of 31 subjects of 71 with cerebral amyloidosis also revealed amyloid deposits. They appeared in various morphological forms, such as diffuse plaques and focal subpial deposits, as well as classical and primitive neuritic plaques. Cases with amyloid in the cerebellum alone were not observed. Beta-amyloid deposits in the cerebellum were associated with a significant number of beta-amyloid plaques in the cerebrum, which showed other Alzheimer-type pathology, also in individuals without clinical symptoms of dementia. There was no correlation either between cerebellar amyloid deposits and clinical cerebellar symptoms or between the presence of diabetes mellitus, arterial hypertension, and neuropathological changes. A clear association of microglial cells with amyloid deposits in the cerebellum was demonstrated. In our experience, LN-1 and RCA-1 were not as suitable for formalin-fixed paraffin-embedded tissue, as was anti-ferritin. Negative staining for tau-1 and positive staining for anti-ubiquitin characterized neurites within primitive and classical plaques. No neurofibrillary pathology was detected in the cytoplasm of cerebellar neurons when we used anti tau-1 labeling.

Key words: *beta-amyloid protein, cerebellar amyloid, aging brain.*

Cerebellar amyloid deposits were first described by Barret in 1913. The diffuse type of cerebellar plaque in the molecular layer was found by von Braunmühl in 1954 when using silver impregnation. Recent reports indicate that amyloid deposits are frequently seen in the cerebellar cortex in Alzheimer's disease, but not in age-matched normal individuals (Aikawa et al. 1985; Azzarelli et al. 1985; Vakili, Muller 1987; Bruncher et al. 1989; Wiśniewski et al. 1989; Suenaga et al. 1990). According to the hypothesis of Selkoe (1989) the

amyloid within the cerebellum differs from amyloid deposits in the cerebrum. Selkoe (1989) proposed that cerebellar senile plaques are shaped not in a fibrillar, beta-pleated sheet form which cannot be detected by Congo red or Thioflavin S. They can be visualized only by Bielschowsky impregnation or by antibodies to beta-amyloid. Selkoe (1989) also did not observe either neurites within cerebellar amyloid deposits or microglial and astroglial cells.

According to Glenner (1990) amyloid deposits is composed primarily of twisted beta pleated sheet fibrils. Amyloid was isolated from meningeal vessels and purified. Amino acids sequence analysis (Glenner, Wong 1984) revealed a previously undescribed protein of 4.2 kilodaltons designated beta protein (A 4). The beta protein was initially reported to be composed of 28 amino acids (Wong et al. 1985). Antibodies raised to synthetic peptides comprising residues from 1-28 of beta-peptide were found by immunohistochemical methods to be localized in senile plaques of Alzheimer's disease throughout the brain.

The purpose of the present study was to determine whether the use of the highly specific immunomarker 4G8, fragment Fab (Wiśniewski et al. 1989) could confirm the above cited results and to evaluate the glial reaction to the presence of cerebellar amyloid in non-demented old individuals as well. Specific neuritic changes were also a matter of investigation.

MATERIAL AND METHODS

The object of this study were brains of 100 subjects (68 females and 32 males) who had died at an age exceeding 80 years (mean age 85.5). Most of the patients had been admitted to the Neurological Department, School of Medicine in Warsaw, with acute cerebrovascular failure. Among them, 18 cases were clinically assessed as demented before stroke, 15 patients suffered from diabetes and 27 from arterial hypertension. Autopsies of all cases were performed no later than 24 hours after death. Brains were fixed in 10% formalin and stored in this solution for at least 3 weeks. Gross neuropathological examination revealed thrombosis of cerebral artery as a cause of infarction in 53% of cases, embolus of brain vessel in 17%, hemorrhage in 16%, and subdural hematoma, tumor, or brain atrophy in 14%.

From each brain, samples were taken from the frontal cortex, hippocampal and parahippocampal areas, and cerebellar hemisphere at the level of nucleus dentatus. Serial sections (6 μm thick) from each paraffin block were labeled with routine and immunohistochemical stainings. All specimens were stained with Thioflavin S, and the number of plaques was semiquantitatively assessed per sq.mm to diagnose AD according to Khachaturian criteria (1985). For cerebellar sections the following methods were used: Bielschowsky impregnation, Congo red, and anti-beta-amyloid immunohistochemical staining.

Immunohistochemistry

Fourteen cases showing typical amyloid changes were selected for further investigations with sets of commercial and non commercial antibodies on serially cut material to compare adjacent sections stained by different antibodies. The commercial antibodies, used were: rabbit anti-ferritin, monoclonal GFAP, biotinylated RCA-1 (Dako), and LN 1 (ICN) and the rabbit anti-ubiquitin antibody (Sigma). The following non commercial antibodies were used, 4G8 Fab (Kim et al. 1988; Wiśniewski et al. 1989), anti-tau-1 (Binder et al. 1985) and MR 27. The latter was raised against amino acids 384-405 of the Kitaguchi sequence (Kitaguchi et al. 1988) and was a gift from Dr. P. Mehta.

Tissue sections were treated in 3% H₂O₂ in methanol and then blocked in 20% fetal calf serum. Primary antibody was added to the specimens, and they were incubated overnight at 4°C. Sections to be stained with 4G8 Fab were pretreated with 99% formic acid for 30 min, and those to be stained with tau-1 antibody, were incubated with alkaline phosphatase for 4 h at 37°C. The ABC method with extravidin was used for all immunostainings. The PAP method was exceptionally used for anti-ferritin. Diaminobenzidine was chosen as chromogen. Sections were counterstained with hematoxylin.

RESULTS

Amyloid deposits in the frontal cortex were found in 71 of cases, in the hippocampal and parahippocampal gyrus in 70 cases, and in the cerebellum in 31 cases. Among the 31 cases with the presence of amyloid within the cerebrum and cerebellum, 18 were clinically assessed as demented. However, 13 were diagnosed as normal for aged subjects.

Cerebellar amyloid deposits were always found in cases with cerebral beta-amyloid plaques within the neocortex and hippocampal area, with sufficient number of plaques to fulfill histological criteria for the diagnosis of Alzheimer's disease. However, there was no correlation between the presence and intensity of amyloid changes in the cerebellar cortex and dementia.

Using anti-beta-amyloid antibody with formic acid pretreatment, two general types of cerebellar amyloid deposits were revealed: focal and diffuse (Fig. 1). Diffuse deposits, were labeled by the 4G8 antibody and impregnated by Bielschowsky method as well. These amyloid deposits were not stained with Congo red, but in 28% of cases, they were visible with Thioflavin S staining. Diffuse deposits were discovered exclusively in the molecular layer. They usually had columnar or radial patterns of distribution along dendrites (Kosik et al. 1987). Some of them revealed a striking connection with blood vessels.

Focal amyloid formations were of the following types: a) subpial plaques (Fig. 2), b) perivascular (Figs 3, 4), c) primitive (Figs 1, 6) and classical plaques (Figs 4, 5). Subpial plaques were often present in pairs in the adjacent subpial

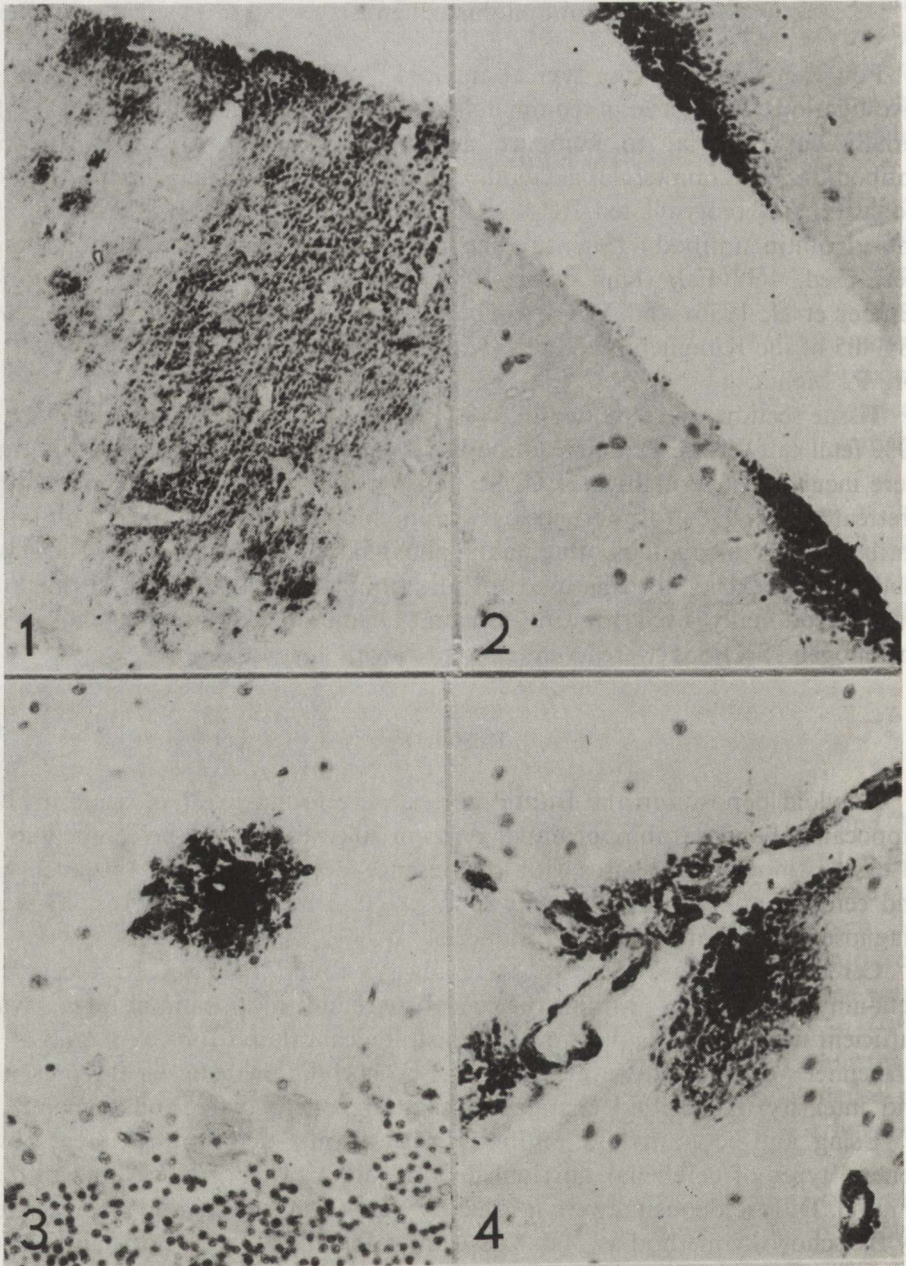


Fig. 1. Diffuse and primitive types of amyloid deposits (arrow) in cerebellar molecular layer. Immunostaining with 4G8 Fab (1:1000). $\times 450$

Fig. 2. Focal amyloid immunoreactivity in the subpial region of cerebellum. Immunostaining with 4G8 Fab (1:1000). $\times 450$

Fig. 3. Perivascular amyloid in the cerebellar granular layer. Immunostaining with 4G8 Fab (1:1000). $\times 450$

Fig. 4. Perivascular and classical cerebellar amyloid plaques. Immunostaining with 4G8 Fab (1:1000). $\times 450$

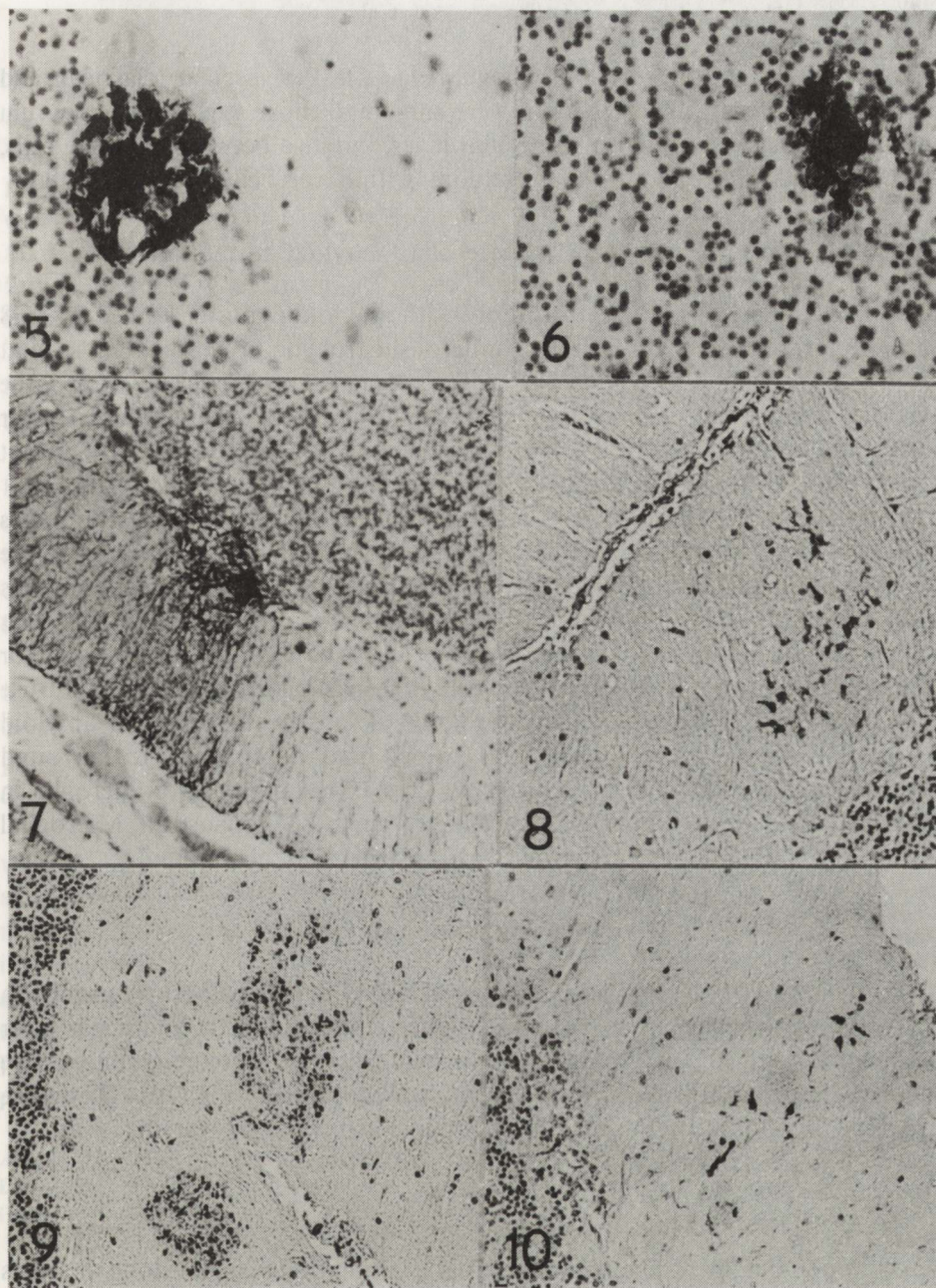


Fig. 5. Classical amyloid plaque in the Purkinje cell layer. Immunostaining with 4G8 Fab (1 : 1000). \times 450

Fig. 6. Primitive plaque in the cerebellar granular layer. Immunostaining with 4G8 Fab (1 : 1000). \times 450

Fig. 7. Astrocytic processes demonstrated by GFAP-immunostaining (arrow) in serially cut sections, showing the presence of astroglia processes within diffuse amyloid deposit. \times 450

Fig. 8. Anti-ferritin immunostaining revealed microglial cells (arrows) within 3 focal amyloid plaques (PAP, 1 : 50). \times 220

Fig. 9. Microglial cells (arrow) in the center of diffuse amyloid deposit. Anti-ferritin immunostaining (PAP, 1 : 50). \times 220

Fig. 10. Ubiquitin component in primitive and diffuse amyloid plaques. Immunostaining with anti-ubiquitin antibody (1 : 20). \times 220

regions, forming a mirror-like image (Fig. 2). Perivascular classical and primitive plaques in the cerebellum were similar to those seen in the cerebrum and mostly located within the molecular layer, but also between Purkinje cells, in the granular layer and rather seldom within cerebellar white matter.

Glia participation in cerebellar amyloid formation

Astroglia: Sections adjacent to those with amyloid deposits stained by 4G8 antibody, were labeled by GFAP. Numerous astrocytic processes were seen at the margin of amyloid changes (Fig. 7) and some processes penetrated the amyloid deposits. GFAP-positive cells were found also within the cerebellar cortex and white matter in the areas free of amyloid. Some deposits were not surrounded by astroglial cells.

Microglia: RCA-1, LN-1, anti-ferritin and MR-27 were the four antibodies used as markers for microglia. Rabbit anti-ferritin antibody appeared to be the best one for paraffin-embedded specimens (Figs 8, 9). Ferritin-positive cells were morphologically assessed as microglia. Delicate, ramified processes originating from the small cell body seemed to be highly characteristic for microglia. Ferritin-positive microglial cells were visualized in focal and diffuse deposits as well. Microglial cells were noted always in the center of amyloid deposits, contrary to astroglial ones, which had a tendency to surround amyloid plaques. The characteristic prevalence of the presence of microglia in the classic plaque (with neuritic component) has to be emphasized. Microglial cell reaction within the cerebellar white matter was also found.

Neuritic component

Tau-1 antibody revealed no PHF (paired helical filaments) positive profiles in any type of cerebellar amyloid deposits. Diffuse staining in the molecular layer was observed in 80% of cases with amyloid plaques. Anti-ubiquitin-positive neurites were found in all forms of beta-amyloid plaques (Fig. 10). They were visualized as numerous granular and rod-like structures of varying sizes.

DISCUSSION

Although detailed neuropsychological examination was not done, it seems possible to distinguish patients demented before the stroke on the basis of clinical history. Documented diagnosis of the psychoorganic syndrome seemed to be reliable enough. Our 18 patients with dementia in anamnesis and neuropathological Alzheimer's type changes could be assessed retrospectively as AD. However, the present study reveals that extensive amyloid deposits can be found in the cerebellum of nondemented old people: 13 cases with cerebellar amyloidosis and Alzheimer's type neuropathological changes in the cerebrum were considered not to exhibit symptoms of intellectual deterioration.

Cerebellar primitive, classical, and diffuse plaques were always found in association with amyloid deposits in the cerebrum. In other words, plaques in the cerebellum without the presence of cerebral plaques was not observed. This phenomenon suggests that amyloid deposition may appear in the cerebrum earlier than in the cerebellum. According to Azzarelli et al. (1985) and Pro et al. (1980), cerebellar amyloid deposits are frequently present in cases of familial type dementia with early onset. Diffuse amyloid deposits in the cerebellum, similarly as those found in the cerebral cortex, also showed poor Thioflavin S or Congo red staining or no such properties at all. The immunoreactivity of these deposits, like that of cerebral diffuse plaques, was enhanced by formic acid.

Anti-ferritin antibody showed the presence of microglial cells in all types of beta-amyloid plaques (Węgiel et al. 1990; Wiśniewski et al. 1990). However, some authors question the presence of microglia in the cerebellar plaques (Joachim et al. 1989; Yamaguchi et al. 1989), perhaps because of the difficulties in demonstrating this particular glial cell in formalin-fixed, paraffin-embedded samples.

It is of interest that astroglial cell participation in amyloid deposits within the cerebellum (but also cerebrum) is not uniform. Therefore, the cascade of events of amyloid fibrils production, their phagocytosis and astroglial cell participation in organizing amyloid deposits within the CNS still need to be elucidated.

Cerebellar and cerebral beta-amyloid neuritic and diffuse plaques do not vary much morphologically (Probst 1987; Joachim et al. 1989; Wiśniewski et al. 1989; Yamaguchi et al. 1989). The only difference we noted was that the neuritic component of cerebellar plaques does not show tau-1 or PHF immunoreactivity, as previously reported by Dickson et al. (1990) and Suenaga et al. (1990). However, anti-ubiquitin antibody revealed the presence of ubiquitin in every type of cerebellar plaque. Resistance of cerebellar cortex to PFH formation is well known, but the biochemical background of this resistance is not clear.

Acknowledgement. Supported in part by the NYS Office of Mental Retardation and Developmental Disabilities and Grand nos. PO1-AG 4220 and PO1 HD 22634 from the National Institutes of Health.

ZŁOGI BETA-AMYLOIDU W MÓZDŻKACH LUDZI POWYŻEJ 80 ROKU ŻYCIA

Streszczenie

Zbadano częstość występowania amyloidu w mózdku u 100 chorych zmarłych w większości przypadków z powodu udaru mózgu. U 18 z nich stwierdzono cechy otępienia przed wystąpieniem ostrego zespołu naczyniowego będącego przyczyną zgonu. W każdym przypadku pobrano skrawki z mózdku, kory czołowej, hipokampa i okolicy parahipokampalnej, które barwiono rutynowo

HE i tioflawiną S. W wybranych przypadkach zastosowano impregnację srebrową (Bielschowski) i wykonano barwienia immunohistochemiczne używając przeciwciał monoklonalnych: 4G8 Fab przeciwko beta-peptydowi, tau-1 przeciwko PHF oraz przeciwciał polyklonalnych przeciwko epitopom ubiquityny, przeciw GFAP, i ferrytynie, a także przeciw LN-1 i lektynie RCA-1.

Obecność amyloidu w mózgu stwierdzono w 71 przypadkach, spośród których 31 wykazywało także złogi amyloidu w mózdku w postaci amyloidu rozproszonego lub występującego ogniskowo, podoponowo lub w formie blaszek prymitywnych i klasycznych. Nie stwierdzono korelacji z klinicznie obserwowanym otępieniem, występowaniem objawów mózdkowych, cukrzycy i nadciśnienia tętniczego. Wykazano równocześnie współwystępowanie komórek mikrogleju barwiącego się przy użyciu przeciwciała przeciwko ferrytynie i złogów amyloidu. Wyniki naszych badań potwierdziły także pozytywne barwienie neurytycznych elementów blaszki amyloidowej dla przeciwciał przeciw ubiquitynie i negatywne dla anti-tau-1. W cytoplazmie neuronów mózdku nie stwierdzono zwyrodnienia nerwowo-włókienkowego.

REFERENCES

1. Aikawa H, Suzuki KI, Iwasaki Y, Izuka R: Atypical Alzheimer's disease with spastic paresis and ataxia. *Ann Neurol*, 1985, 17, 297–300.
2. Azzarelli B, Muller J, Ghetti B, Dyken M, Conneally PM: Cerebellar plaques in familial Alzheimer's disease (Gerstmann-Sträussler-Scheinker variant?). *Acta Neuropathol (Berl)*, 1985, 65, 235–246.
3. Barrett AM: A case of Alzheimer's disease with unusual neurological disturbances. *J Nerv Ment Dis*, 1913, 40, 361–374.
4. Binder LI, Frankfurter A, Rebhum LI: The distribution of tau in the mammalian central nervous system. *J Cell Biol*, 1985, 101, 1371–1378.
5. Braunnühl AU: Über eine eigenartige hereditäre familiäre Erkrankung des Zentralnervensystems. *Arch Psychiat Neurol*, 1954, 191, 419–449.
6. Bruncher JM, Gillain C, Baron H: Les plaques amyloides cerebelleuses dans la maladie de l'Alzheimer. *Acta Neurol Belg*, 1989, 89, 286–293.
7. Dickson DW, Wertkin A, Mattiace LA, Fier E, Kress Y, Davies P, Yen SH: Ubiquitin immunoelectron microscopy of dystrophic neurites in cerebellar senile plaques of Alzheimer's disease. *Acta Neuropathol (Berl)*, 1990, 79, 486–493.
8. Glenner GG: The nature and pathogenesis of Alzheimer's disease. In: *Molecular biology and genetics of Alzheimer's disease*. Eds: T. Miyatake, DJ Selkoe, Y Ihara. Elsevier, New York, 1990, pp 69–78.
9. Glenner GG, Wong CW: Alzheimer's disease: initial report of the purification and characterization of a novel cerebrovascular amyloid protein. *Biochem Biophys Res Comm*, 1984, 120, 885–890.
10. Joachim CL, Morris JH, Selkoe DJ: Diffuse senile plaques occur commonly in the cerebellum in Alzheimer's disease. *Am J Pathol*, 1989, 135, 309–319.
11. Khachaturian ZS: Diagnosis of Alzheimer's disease. *Arch Neurol*, 1985, 42, 1097–1105.
12. Kim KS, Miller DL, Sapienza VJ, Chen CM, Bai C, Grundke-Iqbal I, Currie JR, Wiśniewski HM: Production and characterization of monoclonal antibodies reactive to synthetic cerebrovascular amyloid peptide. *Neurosci Res Commun*, 1988, 2, 121–130.
13. Kitaguchi M, Takahashi Y, Tokushima Y, Shiojiri S, Ito H: Novel precursor of Alzheimer's disease amyloid protein shows protease inhibitory activity. *Nature*, 1988, 331, 530–532.
14. Kosik KS, Rogers J, Kowall NW: Senile plaques are located between apical dendritic clusters. *J Neuropathol Exp Neurol*, 1987, 46, 1–11.
15. Pro JD, Smith CH, Sumi M: Presenile Alzheimer disease: Amyloid plaques in the cerebellum. *Neurology*, 1980, 30, 820–825.
16. Probst A, Brunnschweiler C, Lautenschlager C, Ulrich J: A special type of plaque, possibly an initial stage. *Acta Neuropathol (Berl)*, 1987, 74, 133–141.

17. Selkoe DJ: Molecular pathology of amyloidogenic proteins the role of vascular amyloidosis in Alzheimer's disease. *Neurobiol Aging*, 1989, 10, 387–395.
18. Suenaga T, Hirano A, Llena JF, Ksiezak-Reding H, Yen SH, Dickson DW: Modified Bielschowsky and immunocytochemical studies on cerebellar plaques in Alzheimer's disease. *J Neuropathol Exp Neurol*, 1990, 49, 31–40.
19. Vakili St, Muller J: Juvenile Alzheimer's disease with cerebellar involvement. *Arch Pathol Lab Med*, 1987, 111, 480–482.
20. Węgiel J, Wiśniewski HM: The complex of microglial cells and amyloid star in three-dimensional reconstruction. *Acta Neuropathol (Berl)*, 1990, 81, 116–124.
21. Wiśniewski HM, Bancher C, Barcikowska M, Wen GY, Currie J: Spectrum of morphological appearance of amyloid deposits in Alzheimer's disease. *Acta Neuropathol (Berl)*, 1989a, 78, 334–347.
22. Wiśniewski M, Vorbrodt AW, Węgiel J, Moryś J, Lossinsky AS: Ultrastructure of the cells forming amyloid fibers in Alzheimer's disease and scrapie. *Am J Med Genet (Suppl)*, 1990, 7, 287–297.
23. Wiśniewski HM, Wen GY, Kim KS: Immunoreactivity of Fab of monoclonal antibodies to amyloid beta-peptide. *J Neuropathol Exp Neurol*, 1989b, 48, 352 (abstract).
24. Wong CW, Quaranta VW, Glenner GG: Neuritic plaques and cerebrovascular amyloid in Alzheimer disease are antigenically related. *Proc Natl Acad Sci USA*, 1985, 82, 8729–8732.
25. Yamaguchi H, Kirai S, Morimatsu M, Shoji M, Nakazoto Y: Diffuse type of senile plaques in the cerebellum of Alzheimer-type dementia demonstrated by beta protein immunostain. *Acta Neuropathol (Berl)*, 1989, 77, 314–319.

Correspondence address: dr M. Barcikowska, Department of Neuropathology, Medical Research Centre, PASci, 3 Dworkowa St, 00-784 Warsaw, Poland

WOJCIECH SPLIT¹, JADWIGA JANUSIK¹, JANUSZ ALWASIAK²,
WIELISŁAW PAPIERZ³, MARIA BARCIKOWSKA⁴, PAWEŁ P. LIBERSKI⁵

CREUTZFELDT-JAKOB DISEASE WITH TUBULOVESICULAR STRUCTURES: AN ULTRASTRUCTURAL STUDY

¹Department of Neurology, Regional Hospital, Zgierz, Poland, ²Department of Oncology, School of Medicine, Łódź, Poland, ³Laboratory of Neuropathology, Department of Pathological Anatomy, School of Medicine, Łódź, Poland, ⁴Department of Neuropathology, Medical Research Centre, Polish Academy of Sciences, Warsaw, Poland, ⁵Electron Microscopic Laboratory, Department of Oncology, School of Medicine, Łódź, Poland

Tubulovesicular structures (TVS) have been consistently observed in brain tissue of the transmissible spongiform virus encephalopathies such as natural and experimental scrapie, bovine spongiform encephalopathy and experimentally induced Creutzfeldt-Jakob disease (CJD). TVS were recently demonstrated in 3 cases of naturally occurring CJD. We report here the presence of TVS in another human brain with CJD, as detected in all 3 specimens by thin section electron microscopy. Their occurrence in all types of spongiform encephalopathies, irrespective of the affected host and the strain of infectious agent, emphasizes their biological significance.

Key words: Creutzfeldt-Jakob disease, tubulovesicular structures.

We report here the presence of tubulovesicular structures (TVS) in human brain affected with the Creutzfeldt-Jakob disease (CJD). So far, TVS have been consistently reported in all subacute spongiform viral encephalopathies (SSVE) such as natural and experimental scrapie (David-Ferreira et al. 1968; Bignami, Parry 1971; Narang 1973, 1988; Lamar et al. 1974; Baringer, Prusiner 1978; Baringer et al. 1979; Narang et al. 1980, 1987; Gibson, Doughty 1989; Liberski et al. 1988, 1989, 1990a), bovine spongiform encephalopathy (Liberski et al. 1990b), experimental (Lampert et al. 1971; Liberski et al. 1988, 1990a) and recently, natural CJD (Liberski et al. 1991, 1992a).

The presence of TVS in all SSVE, including human CJD, clearly suggests their biological significance and justified further studies.

MATERIAL AND METHODS

Case report

The patient was a 53-year-old female who was admitted in September 1991 to the Department of Neurology, Regional Hospital, Zgierz, with slowly progressive mental deterioration, headache and dizziness, and right-sided

numbness and weakness. She had also a one month history of a feeling of uncontrollable fear which appeared particularly during night-time. She lost her interest in family life, became apathetic, and showed memory and speech disturbances and insomnia. On admission, she exhibited mild right-sided pyramidal hemiparesis with central paresis of the right facial nerve. Dysarthria was also observed. A general slowing of her mental processes as well as severe cognitive impairment were apparent. CSF examination and CT scan were considered unremarkable. EEG tracing was recorded on a few occasions. In September 1991, it showed unspecific changes of numerous slow waves (1.5–3 Hz) lateralized to the right side and sharp waves on the left side. Two weeks later, biphasic slow waves and periodic sharp wave complexes synchronous with myoclonic jerks began to appear. In the following two months she rapidly deteriorated. There was increasing extrapyramidal rigidity, more pronounced at the right side. Myoclonus and seizures began to appear. The clinical diagnosis of Creutzfeldt-Jakob disease was suggested and antiviral therapy initiated (amantadine, isoprinosine, aciclovir) without any observable effect. There was also a rapid mental deterioration and she eventually lapsed into a coma and died 69 days after admission.

Neuropathological examination

Several brain samples were fixed in buffered formalin, embedded in paraffin and stained with hematoxylin and eosin and PAS. Immunohistochemistry with following antibodies was performed: against glial fibrillary acidic protein (GFAP, Dakopatts), prion protein (PrP) (two batches of polyclonal antibodies against scrapie-associated fibrils (SAF) purified from hamster brains infected with the 263K strain of scrapie virus and kindly supplied by Dr. Paul Brown, LCNSS, NIH, Bethesda, USA; and monoclonal antibodies against SAF purified from mouse brains infected with the ME7 strain of scrapie virus, supplied by Dr. Richard Kascak, IBR, New York, USA), and 4G8 (raised against a synthetic peptide comprising amino acids 17–24 of beta-A4 peptide, supplied by Dr. K. S. Kim, IBR, New York, USA). Sections to be stained with all anti-PrP and 4G8 antibodies were pretreated with formic acid as previously reported (Liberski et al. 1991).

Electron microscopy

Several brain samples were inadvertently fixed in buffered formalin for several hours, then smaller (1-mm³) samples were dissected, fixed in 2.5% buffered glutaraldehyde (pH 7.4) for 2 hours, rinsed in phosphate buffer, postfixed in 1% osmium tetroxide, dehydrated through a graded series of ethanols and propylene oxide and embedded in Epon 812. Ultrathin sections were stained with lead citrate and uranyl acetate, and the specimens were examined using a Zeiss EM109 transmission electron microscope.

RESULTS

Neuropathological examination confirmed clinical diagnosis of CJD. Spongiform changes (Fig. 1) were observed in the deeper cortical layers and several subcortical nuclei. Astrocytosis was prominent; particularly, GFAP

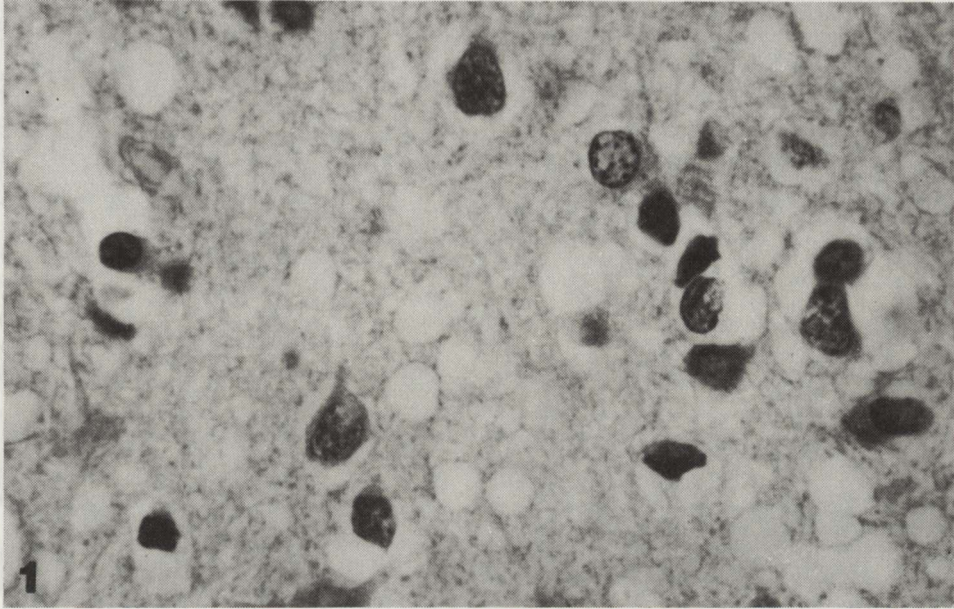


Fig. 1. Typical spongiform changes in cerebral cortex. HE. $\times 400$

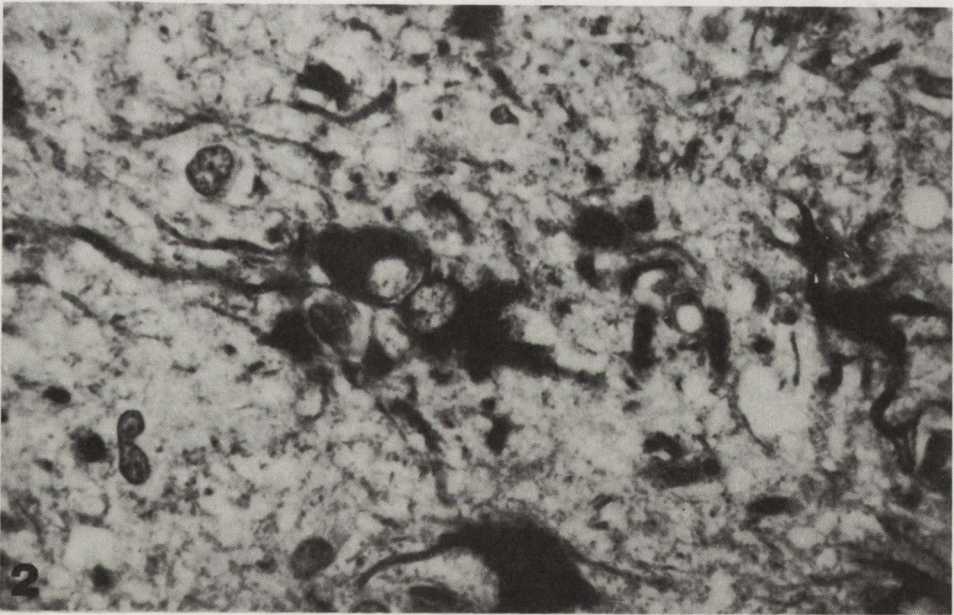


Fig. 2. Numerous immunopositive astrocytes in cerebral cortex. GFAP immunohistochemical staining. $\times 400$

immunohistochemistry revealed numerous gemistocytic astrocytes. Adjacent astrocytic nuclei suggested local mitoses (Fig. 2). PrP and beta-A4-immunohistochemistry failed to reveal any amyloid plaques.

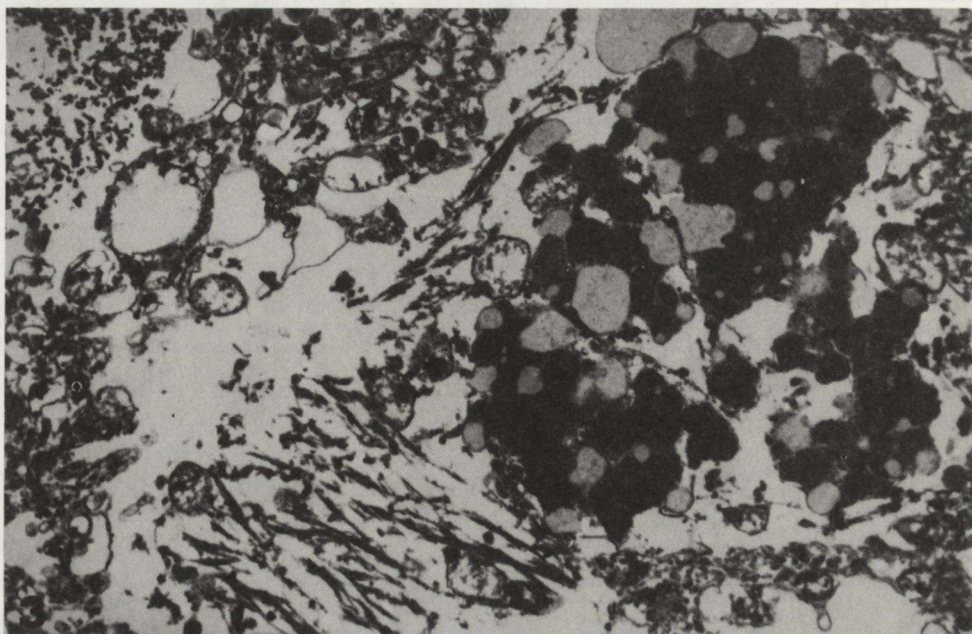


Fig. 3. An astrocyte containing abundant lipofuscin. $\times 12000$

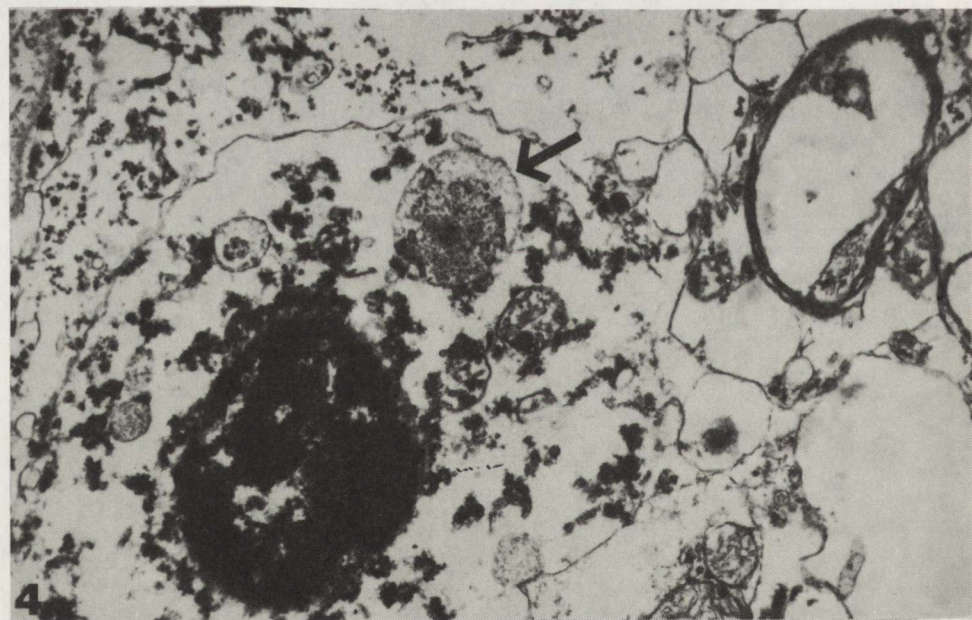


Fig. 4. An astrocyte containing autophagic vacuoles (arrow). $\times 12000$

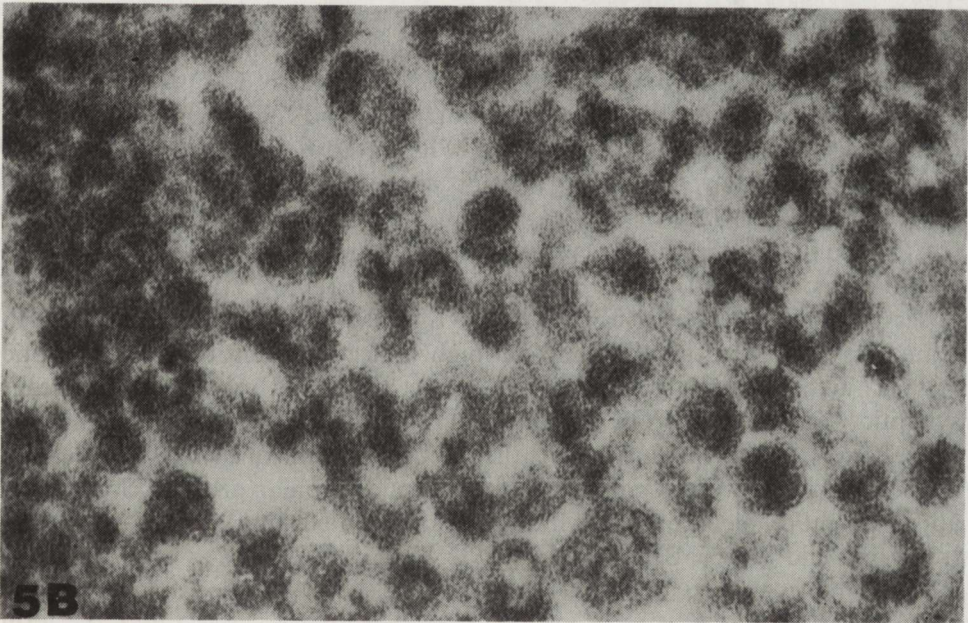
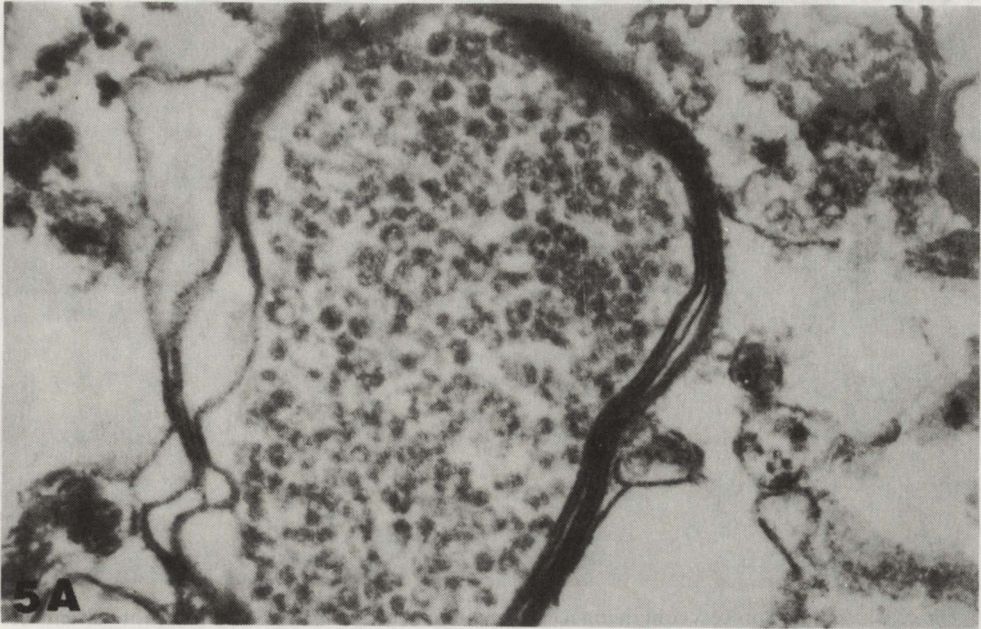


Fig. 5. Low (A) and high (B) power electron micrographs showing an axon containing tubulovesicular structures (asterisk) and synaptic terminal containing synaptic vesicles (SV). Note higher electron density, pleomorphism and smaller size of TVS in comparison with synaptic vesicles. (A) - $\times 12\,000$, (B) - $\times 85\,000$

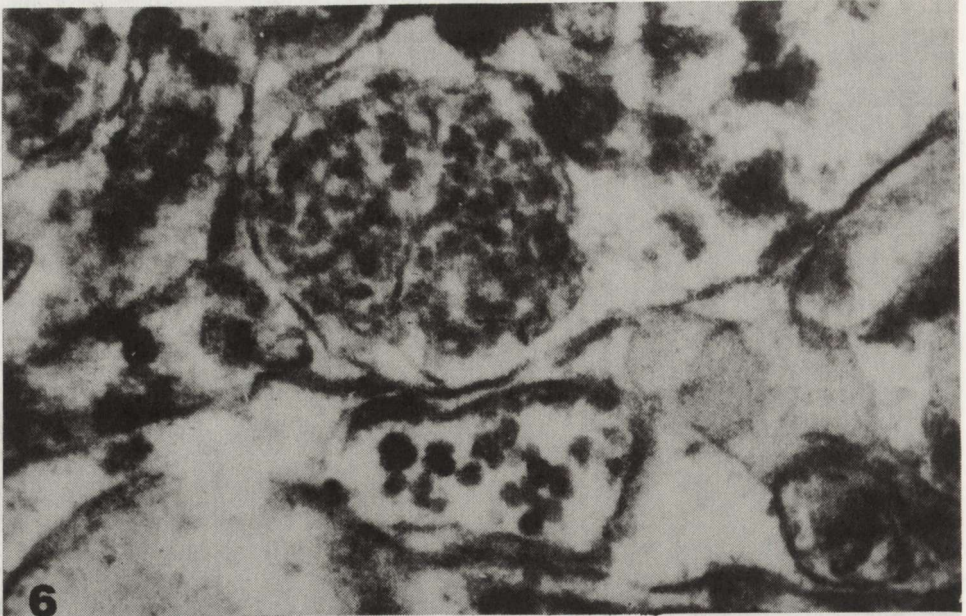


Fig. 6. Unidentified process containing membrane-bound abundant TVS (arrow). Note differences in electron densities and diameters of TVS in comparison with those of glycogen granules (open arrow). $\times 50\,000$

Electron microscopic examination, performed despite severe autolytic changes and fixation artifacts, revealed typical features of CJD — spongiform vacuoles containing curled membrane fragments and hypertrophic astrocytes containing large amounts of lipofuscin (Fig. 3). Several astrocytes contained large electron-dense vacuoles (Fig. 4) most consistent with autophagic vacuoles (Liberski et al. 1992b).

TVS-containing processes were extremely rare. Only a few of them were identified as distended pre- or postsynaptic terminals. Occasionally TVS were observed in myelinated axons (Fig. 5). TVS measured approximately 35 nm in diameter; they were smaller and of higher electron density than synaptic vesicles. TVS were easily differentiated from larger and more electron-lucent synaptic vesicles and from glycogen granules (Fig. 6) and multivesicular bodies. At higher magnification the pleomorphism of TVS was readily apparent (Fig. 5B). They appeared as circular or tubular profiles. Some TVS appeared more pleomorphic while others presented short “neck” budding from one end (Fig. 5B).

DISCUSSION

The tubulovesicular structures (designated also as scrapie-associated particles) are the only structures unique for all subacute spongiform virus encephalopathies (Gajdusek 1977). TVS were first described by David-Ferreira

and co-workers (1968) in NIH Swiss mice infected intracerebrally with the Chandler strain of scrapie virus as "particles and rods ranging in diameter from 320 to 360 Å". Interestingly, the rods were covered with spikes. It is very clear from the above-mentioned description and the following discussion that the reported size of TVS has been slightly different according to different investigators – but the factors linked to electron microscopic techniques, namely swelling or dehydration can account for this variation.

TVS were not found originally in samples from cases with CJD and at least one group of investigators *expressis verbis* denied their existence (Kim, Manuclidis 1986). However, TVS were found recently to be a consistent ultrastructural feature of well-fixed brain biopsies of patients with CJD (Liberski et al. 1991, 1992a). In this communication, analogously to the previous ones, we clearly demonstrated the presence of TVS in natural CJD. Furthermore, TVS have already been reported in experimental CJD in chimpanzees (Lampert et al. 1971) and in NIH Swiss mice infected intracerebrally or intraocularly with the Fujisaki strain of CJD virus (Liberski et al. 1988, 1990a). It seems, however, that in experimental CJD neurites containing TVS were more numerous than those reported here in natural disease. An explanation for this phenomenon will be offered later in the text.

In the natural diseases in ruminants, scrapie in sheep and bovine spongiform encephalopathy (BSE) in Fresian/Holstein cattle, TVS appeared as membrane-bound accumulations of round particles measuring 35 nm in diameter (Liberski et al. 1990a, b; 1992c). The electron-dense core could be demonstrated in some of them (Bignami, Parry 1971).

TVS have been reported in the majority of models of scrapie in rodents studied so far. Lamar et al. (1974) found TVS in postsynaptic processes of ICR mice inoculated intracerebrally or subcutaneously with the "Klenck" strain of scrapie virus isolated from a Suffolk ram. Spherical TVS reported by these investigators measured 30–35 nm in diameter; some of TVS, however, appeared as long rods. Interestingly, TVS could be found neither in spleens taken from scrapie-affected mice nor in brain cell cultures. It is noteworthy, that when one of us (P.P.L.) studied neuroblastoma cell cultures infected with scrapie virus (Caughey et al. 1989), TVS could not be found. The possible explanation for this phenomenon based on an estimation of the infectivity titer is provided later in the text.

Narang et al. (1980) extended these observations having reported TVS only in presynaptic terminals. In the cited experiment, TVS measured 76 nm in diameter. When stained with ruthenium red, TVS seemed larger, approaching 33 nm in diameter (Narang 1973). In Sprague-Dawley rats inoculated intracerebrally with the Chandler strain of scrapie virus, the TVS apparently appeared as tubular "cucumber-shaped particles" measuring approximately 20 nm in diameter and 60 nm in length, containing a 4 nm electron-dense core (Field, Narang 1972). Contrary to other reports, these structures were present not only in neuronal processes, but also in neuronal perikarya. In Swiss

mice inoculated with the Chandler strain of scrapie virus TVS were found in enlarged postsynaptic (dendrites) or unidentified neuronal processes (Baringer, Prusiner 1978; Baringer et al. 1979, 1981). Electron-dense spherical TVS measured 23 nm in diameter and frequently formed "paracrystalline" tubular or vermicellar arrays (Baringer et al. 1981). A tilting analysis of such arrays revealed a clear change in the apparent axis of tubular aggregates, suggesting that they resulted from overlapping spherical profiles. Baringer et al. (1981) constructed a topological model of TVS arrays which, when tilted, gave an image consistent with that observed by an electron microscope and supported the notion that tubular arrays consisted of round structures. Interestingly, when hamsters infected with the 263K strain of scrapie were examined, TVS were not detected initially (Baringer, Prusiner 1978; Baringer et al. 1979). This model of scrapie produces a higher titer of scrapie virus than any other and the negative findings were used to support the notion that TVS were not a significant ultrastructural feature of the disease, much less the infectious virus or an aggregate of it (Baringer, Prusiner 1978; Baringer et al. 1979). Subsequently, however, three groups of investigators reported TVS in hamsters infected with the 263K strain of scrapie virus. Narang et al. (1987) reported TVS measuring 22 to 24 nm in diameter but only in postsynaptic terminals. TVS were accompanied by larger vesicular profiles measuring 100–110 nm in diameter and a "smaller number of tubulofilamentous profiles" 200 nm long. As the latter structures were neither shown nor characterized it is impossible to judge their significance. Liberski et al. (1988, 1989, 1990a) identified TVS in the same hamster model in both postsynaptic and presynaptic terminals. Noteworthy, when the filed electron micrographs were searched for the presence of TVS, apparently not present at the time of publishing (Liberski 1987), they were easily identified. Thus, what is quite typical for electron microscopy, when a new finding is reported it often appears that the phenomenon has already been present but not recognized. Gibson and Doughty (1989) reported the most extensive survey of TVS in different experimental scrapie models in rodents and sheep. In agreement with Liberski et al. (1988, 1989, 1990a) these investigators found TVS in both pre- and postsynaptic terminals but postsynaptic terminals predominated (41 profiles out of 109 in postsynaptic as compared to 12 in presynaptic terminals). Gibson and Doughty (1989) reported the presence of dense "paracrystalline" arrays of TVS which were apparently absent in hamsters infected with the 263K strain of scrapie. TVS were most numerous in VL mice infected with the ME7 strain of scrapie virus followed by C3H mice infected with the 22C and 79A strains. Furthermore, when VM mice infected with the 87V strain of scrapie (a model which produces a large quantity of PrP amyloid deposits) were examined, numerous synaptic terminals containing TVS were found in the vicinity of amyloid plaques. TVS were also found in a Cheviot sheep inoculated with the ME7 strain of scrapie virus, but the number of affected processes was the lowest among the reported models.

The exact topology of TVS is not entirely clear. In most published electron micrographs TVS appeared as spheres measuring between 20 and 40 nm in diameter and our data correspond to those already published. Some investigators stressed that the tubular "arrays" of TVS are a spurious finding brought about by overlapping spherical profiles (Baringer, Prusiner 1978; Baringer et al. 1979, 1981). Recently however, Liberski et al. (1990a) clearly demonstrated short tubular forms of TVS, thus it became evident that TVS are pleomorphic structures existing in at least two forms — spheres and short tubules. It is also possible that the TVS circular profiles correspond to those of short tubules cut in transverse section. Some investigators strongly believe that this pleomorphism of TVS preclude them to represent a part of, or aggregate of the infectious scrapie virus. While we do not prejudge the true nature of TVS it is worth reminding the pleomorphism of other viruses — virions of hepatitis delta virus are heterogeneous and exist as spheres and short tubules (Purcell, Gerin 1990).

The nature and significance of TVS is unknown. Only limited data are available concerning the appearance of TVS during incubation time. In hamsters inoculated with the 263K strain of scrapie virus (Liberski et al. 1989, 1990a), TVS were initially observed as early as 3 weeks after intracerebral inoculation, but their number increased only with the onset of disease 9 to 10 weeks after inoculation. Noteworthy, vacuolation and astrocytosis were detected 8 weeks post inoculation and, thus, they followed the appearance of TVS. In Webster-Swiss mice TVS were found 12 and 16 weeks after intracerebral and intradermal (footpads) inoculation, respectively (Narang 1988). In NIH Swiss mice infected with the Fujisaki strain of CJD virus TVS were first seen 13 weeks after intracerebral inoculation and their numbers increased dramatically 18 weeks after inoculation, when the first signs of clinical disease were noted (Liberski et al. 1990a). Vacuolation and astrocytosis were detected at virtually the same time, and the increase in the number of processes containing TVS paralleled the increasing intensity of vacuolation and astrocytosis. TVS were approximately twice as abundant in terminally ill mice following intraocular inoculation as in mice following intracerebral inoculation (Liberski et al. 1990a). In contrast, the intensity of vacuolation and astrocytosis was not dependent on the route of inoculation.

Several conclusions can be drawn from these studies. TVS appeared early in the incubation period, preceding the onset of clinical disease. Furthermore, in scrapie-infected hamsters TVS preceded the appearance of other neuropathological changes. The approximately 1000-fold lower infectivity titer of the Fujisaki strain of CJD virus, compared to the 263K strain of scrapie virus, may have caused the delayed appearance of TVS in experimental CJD. The apparent correlation between the number of neuronal processes containing TVS and the infectivity titer may explain why in cell cultures infected with scrapie virus (titer: 1 LD₅₀ per 631 to 7943 neuroblastoma cells; Caughey et al. 1989) TVS could not be found and why their number in natural CJD (as

opposed to experimental CJD – Liberski et al. 1990a) and natural scrapie in sheep was so low (Gibson, Doughty 1989). Furthermore, it should be remembered that virus particles cannot be detected when the virus titer is lower than 10^6 infectious particles per 1 ml.

In conclusion, the presence of TVS in human CJD clearly demonstrated that TVS can be found in brain infected with every SSVE virus if examined properly. TVS, consistently found in all SSVE require further study, regardless whether they represent a virus, a part of the virus, an aggregate of it, or only a useful ultrastructural marker for the whole group of disorders.

Acknowledgements. Dr. P. P. Liberski is the recipient of a grant from the Polish Academy of Sciences (VIII/40). Dr. Richard K. Kimberlin is acknowledged for helpful criticism. Mr. R. Kurczewski, Ms. E. Nagańska, Ms. L. Romanska and Mr. K. Smoktunowicz are kindly acknowledged for skilful technical assistance.

CHOROBA CREUTZFELDTA-JAKOBA ZE STRUKTURAMI TUBULO-PĘCHERZYKOWYMI: BADANIA ULTRASTRUKTURALNE

Streszczenie

Struktury tubulo-pęcherzykowe (TVS) występują we wszystkich transmisyjnych encefalopatiach gąbczastych: w naturalnej i doświadczalnej scrapie, w encefalopatii gąbczastej bydła, w doświadczalnej chorobie Creutzfeldta-Jakoba (CJD). TVS wykazano niedawno w 3 przypadkach CJD u ludzi. W pracy przedstawiono kolejny przypadek CJD, w którym w badaniu mikroskopowo-elektronowym stwierdzono obecność TVS. Występowanie TVS we wszystkich postaciach encefalopatii gąbczastej, niezależnie od gospodarza i szczepu czynnika infekcyjnego przemawia za ich swoistością biologiczną.

REFERENCES

1. Baringer JR, Prusiner SB, Wong JS: Scrapie-associated particles in postsynaptic processes. Further ultrastructural studies. *J Neuropathol Exp Neurol*, 1981, 40, 281–288.
2. Baringer JR, Prusiner SB: Experimental scrapie in mice: ultrastructural observations. *Ann Neurol*, 1978, 4, 205–211.
3. Baringer JR, Wong J, Klassen T, Prusiner SB: Further observations on the neuropathology of experimental scrapie in mouse and hamsters. In: *Transmissible diseases of the nervous system*. Eds: SB Prusiner, WJ Hadlow. Academic Press, New York, 1979, vol 2, pp 111–121.
4. Bignami A, Parry HB: Aggregations of 35-nanometer particle associated with neuronal cytopathic changes in natural scrapie. *Science*, 1971, 171, 389–390.
5. Caughey B, Race RE, Ernst D, Buchmeier MJ, Chesebro B: Prion protein biosynthesis in scrapie-infected and uninfected neuroblastoma cells. *J Virol*, 1989, 63, 175–181.
6. David-Ferreira JF, David-Ferreira KL, Gibbs CJ, Jr, Morris JA: Scrapie in mice: ultrastructural observations in the cerebral cortex. *Proc Soc Exp Biol Med*, 1968, 127, 313–320.
7. Field EJ, Narang HK: An electron-microscopic study of scrapie in rat: further observations on “inclusion bodies”. *J Neurol Sci*, 1972, 17, 347–364.
8. Gajdusek DC: Unconventional viruses and the origin and disappearance of kuru. *Science*, 1977, 197, 943–960.

9. Gibson PH, Doughty LA: An electron microscopic study of inclusion bodies in synaptic terminals of scrapie-infected animals. *Acta Neuropathol (Berl)*, 1989, 77, 420–424.
10. Kim JH, Manuelidis EE: Serial ultrastructural study of experimental Creutzfeldt-Jakob disease in guinea pigs. *Acta Neuropathol (Berl)*, 1986, 69, 81–90.
11. Kingsbury DT, Smeltzer DA, Amyx HL, Gibbs CJ, Jr, Gajdusek DC: Evidence for an unconventional virus in mouse-adapted Creutzfeldt-Jakob disease. *Infect Immun*, 1982, 37, 1050–1053.
12. Lamar CH, Gustafson DP, Krasovich M, Hinsman EJ: Ultrastructural studies of spleens, brains, and brain cell cultures of mice with scrapie. *Vet Pathol*, 1974, 11, 13–19.
13. Lampert PW, Gajdusek DC, Gibbs CJ, Jr: Experimental spongiform encephalopathy (Creutzfeldt-Jakob disease) in chimpanzees. *J Neuropathol Exp Neurol*, 1971, 30, 20–32.
14. Liberski PP: Electron microscopic observations on dystrophic neurites in hamster brain infected with the 263K strain of scrapie. *J Comp Pathol*, 1987, 97, 35–39.
15. Liberski PP, Asher DM, Yanagihara R, Gibbs CJ, Jr, Gajdusek DC: Serial ultrastructural studies of scrapie in hamsters. *J Comp Pathol*, 1989, 101, 429–442.
16. Liberski PP, Budka H, Sluga E, Barcikowska M, Kwieciński H: Tubulovesicular structures in human and experimental Creutzfeldt-Jakob disease. *Europ J Epidemiol*, 1991, 7, 551–555.
17. Liberski PP, Budka H, Sluga E, Barcikowska M, Kwieciński H: Tubulovesicular structures in human and experimental Creutzfeldt-Jakob disease. *Acta Neuropathol (Berl)*, 1992a, 84, 238–243.
18. Liberski PP, Yanagihara R, Gibbs CJ, Jr, Gajdusek DC: Tubulovesicular structures in experimental Creutzfeldt-Jakob disease and scrapie. *Intervirology*, 1988, 29, 115–119.
19. Liberski PP, Yanagihara R, Gibbs CJ, Jr, Gajdusek DC: Appearance of tubulovesicular structures in experimental Creutzfeldt-Jakob disease and scrapie precedes the onset of clinical disease. *Acta Neuropathol (Berl)*, 1990a, 79, 349–354.
20. Liberski PP, Yanagihara R, Wells G, Gibbs CJ, Jr, Gajdusek DC: Ultrastructural neuropathology of bovine spongiform encephalopathy (BSE). VIIIth Internat Congress of Virology, Berlin, August 26–31, 1990b, Abstr P28–10, p 283.
21. Liberski PP, Yanagihara R, Gibbs CJ, Jr, Gajdusek DC: Neuronal autophagic vacuoles in experimental scrapie and Creutzfeldt-Jakob disease. *Acta Neuropathol (Berl)*, 1992b, 83, 134–139.
22. Liberski PP, Yanagihara R, Wells G, Gibbs CJ, Jr, Gajdusek DC: Comparative ultrastructural neuropathology of naturally occurring bovine spongiform encephalopathy and experimentally induced scrapie and Creutzfeldt-Jakob disease. *J Comp Pathol*, 1992c, 106, 361–381.
23. Narang HK: Ruthenium red and lanthanum nitrate a possible tracer and negative stain for scrapie “particles”? *Acta Neuropathol (Berl)*, 1973, 29, 37–43.
24. Narang HK: A chronological study of experimental scrapie in mice. *Virus Res*, 1988, 9, 293–306.
25. Narang HK, Asher DM, Pomeroy KL, Gajdusek DC: Abnormal tubulovesicular particles in brains of hamsters with scrapie. *Proc Soc Exp Biol Med*, 1987, 184, 504–509.
26. Narang HK, Chandler RL, Anger HS: Further observations on particulate structures in scrapie affected brain. *Neuropathol Appl Neurobiol*, 1980, 6, 23–28.
27. Purcell RH, Gerin JL: Hepatitis delta virus. In: *Virology (second edition)*. Eds: BN Fields, DM Knipe. Raven Press, New York, 1990, vol 2, pp 2275–2287.

Correspondence address: prof. P. P. Liberski, Electron Microscopic Laboratory, Department of Oncology, 4 Paderewskiego St, 93-509 Łódź, Poland

MILENA LAURE-KAMIONOWSKA, MARIA DAŃBESKA

DAMAGE OF MATURING BRAIN IN THE COURSE OF TOXOPLASMIC ENCEPHALITIS

Laboratory of Developmental Neuropathology, Medical Research Centre, Polish Academy of Sciences, Warsaw

The aim of the study is to present the damaging influence of toxoplasmic encephalitis on newborn brains. The material consisted of six cases of toxoplasmosis who died during the first months of life. The neuropathological picture indicated indirectly the mechanism of spread of the inflammatory-necrotic process. In the first stage of pathologic process intensive inflammatory infiltrations in the periventricular white matter were seen. In the next stage the necrotic changes involved the majority of the hemispheric white matter. Further development of the disease transformed the brain hemispheres into thin-walled sacs composed of meninges and remnants of the nervous system. Finally, the inflammatory process resulted in hydranencephaly. Proliferation of subependymal glia evident in all cases and blocking the pathways of the cerebro-spinal fluid circulation, may have played a role in this process.

Key words: *toxoplasmic encephalitis, newborn's brain, hydranencephaly.*

The problem of fetal brain damage in the course of a congenital inflammatory process is still open. Fortunately a diminishing incidence of these diseases hampers the observation of pathological changes in immature brains. Toxoplasmosis seem to be one of the most representative disease in this group. Therefore we decided to analyze neuropathologically the sequelae of infection by *Toxoplasma gondii* in a group of newborn's brains obtained during the last twenty years.

MATERIAL AND METHODS

The material consists of six cases of congenital toxoplasmosis deceased during the first months of life. The summary of their clinicopathological data is listed in Table 1. The brains were fixed in formalin, blocks of tissue from their various parts were embedded in paraffin and the section were stained with hematoxylin and eosin, cresyl violet, luxol fast blue, PAS and Holzer methods.

Table 1. Clinicopathological data

Case	Sex	Survival	Clinical data	General autopsy
1 (32/84)	F	few hours	Normal pregnancy	Pneumonia
2 (18/84)	F	1 month	Normal pregnancy Hydrocephalus Encephalomyelitis	Pneumonia Otitis media
3 (45/80)	M	2 weeks	Normal pregnancy	Pneumonia
4 (90/73)	M	4 months	Normal pregnancy Hydrocephalus	Pneumonia
5 (161/63)	F	10 days	Normal pregnancy Toxoplasmosis seropositive Hydrocephalus	Cachexia
6 (19/63)	F	2 months	Premature — 35 Hbd Fever of mother in 6th month of pregnancy Hydrocephalus	Erythropoiesis in spleen, liver, lungs

RESULTS

In the first two cases (cases 1 and 2) neuropathological examination of the brain showed widespread inflammatory lesions localized mainly in the periventricular white matter (Fig. 1). Diffuse infiltrations, mainly lymphoplasmatic,

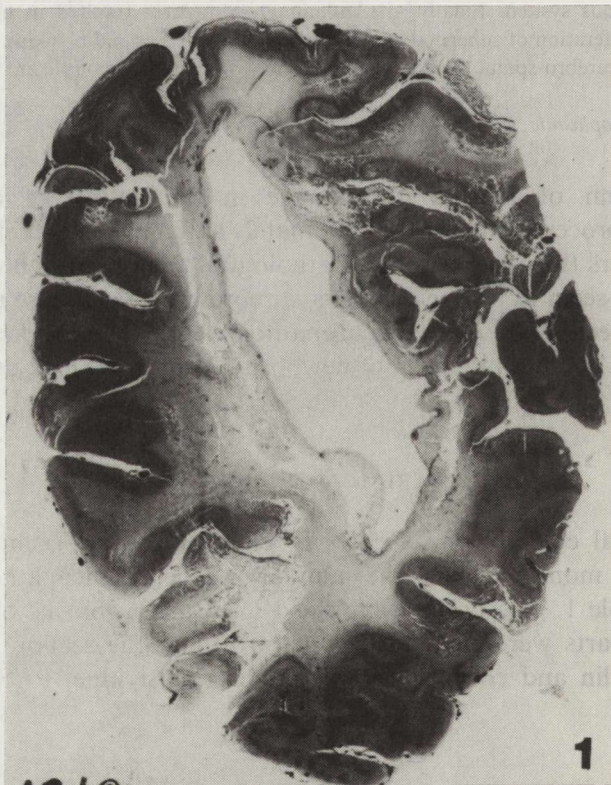


Fig. 1. Brain hemisphere with periventricular inflammatory lesions. HE. Glass magnification

were observed around the ventricles (Fig. 2). Terminal toxoplasmic cysts were found among the inflammatory changes, in the edematous white matter (Fig. 3). Only minimal perivascular infiltrations were seen in the subcortical white

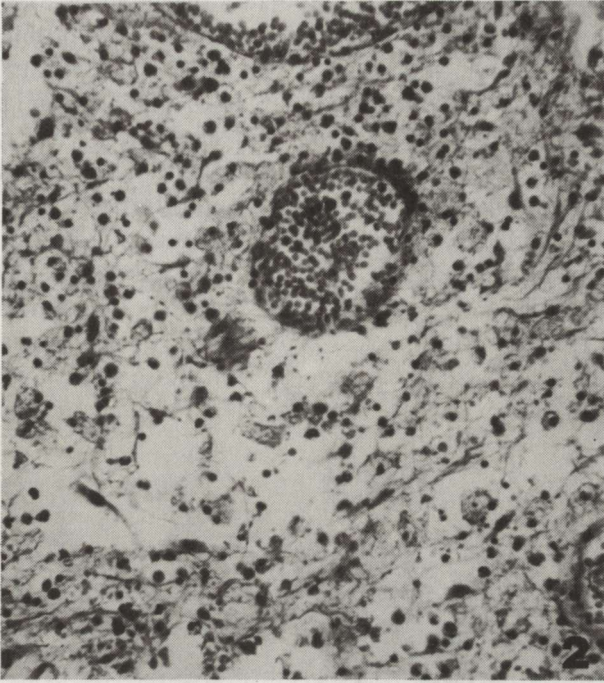


Fig. 2. Leukomalacia, macrophages, inflammatory cells and glial elements in disintegrated periventricular white matter. HE. $\times 100$

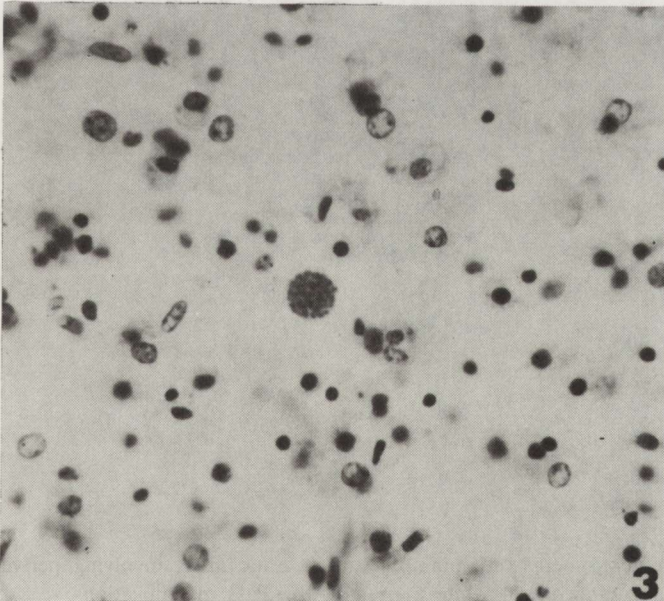


Fig. 3. Terminal toxoplasmic cyst in edematous white matter. PAS. $\times 400$

matter. In the cortex laminar necrosis was present. The subtentorial structures were less affected, nevertheless some microglial nodules and perivascular infiltrates were observed in medulla oblongata. The meninges showed intensive inflammatory infiltration with lymphocytes, plasmocytes, polymorphs and macrophages. The ventricular system was dilated and proliferation of the subependymal glia around the whole ventricular system was observed.

In cases 3 and 4 there were diffuse areas of intensive inflammatory and necrotic changes involving periventricular and subcortical white matter (Fig. 4). Large foci of necrosis led to destruction of the tissue. They were surrounded by microglial and lymphoplasmatic inflammatory infiltrations. Microglial proliferation was diffuse or in the form of reactive nodules. Calcium deposits were seen within the necrotic changes. Proliferation of the vessels around necrotic areas was observed (Fig. 5). In the basal ganglia, brain stem and cerebellum the structural abnormalities were less pronounced, but microglial nodules and perivascular lymphocytic infiltrates appeared in those structures. In the cortex neuronal loss was diffuse. In case 4 micropolygyria of the occipital cortex was



Fig. 4. Cerebral hemisphere. Inflammatory and necrotic areas involving periventricular and subcortical white matter. PAS. Glass magnification

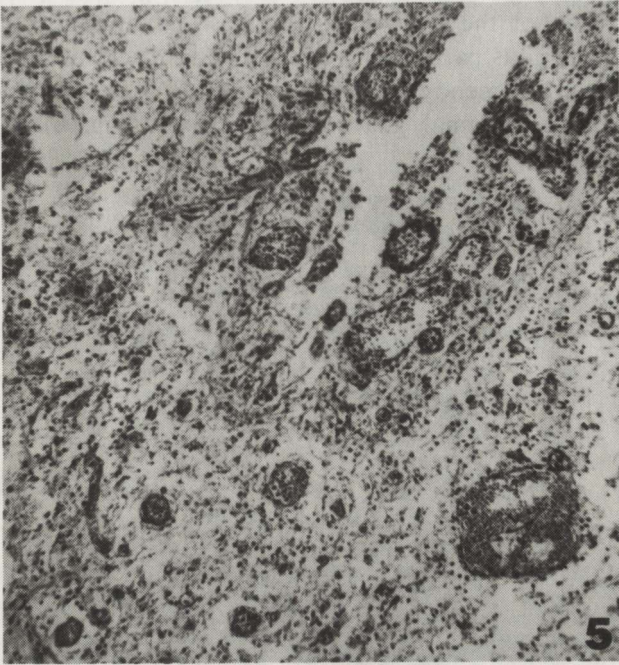


Fig. 5. Proliferation of vessels around necrotic area. HE. $\times 60$

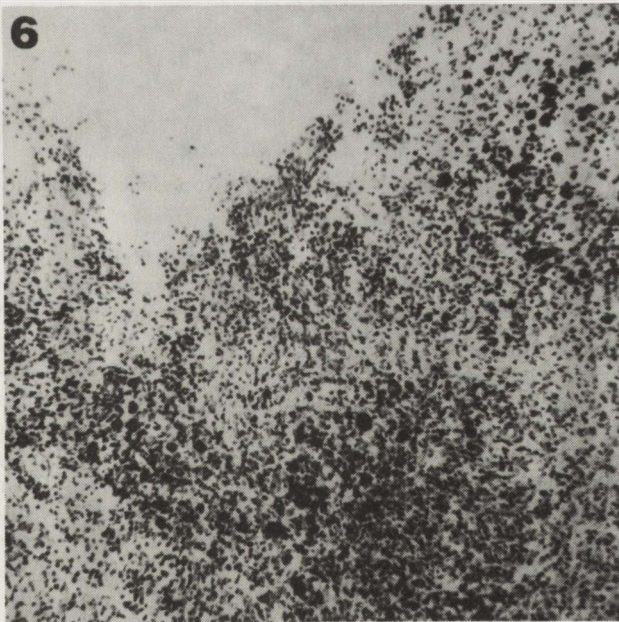


Fig. 6. Inflammatory changes and subependymal glia proliferating into the lateral ventricle. Cresyl violet. $\times 60$

found. The diffuse inflammatory-necrotic process was accompanied by inflammatory infiltration of the overlying meninges. Toxoplasmic terminal cysts were numerous in various parts of the brain. The ventricles were enlarged. The extensive loss of the ependymal cells lining all the ventricles and the proliferation of subependymal glia were noticeable (Fig. 6).



Fig. 7. Hydranencephaly in the case of toxoplasmic encephalitis

Table 2. Summary of neuropathological findings

Cases	Cerebral hemispheres		Subtentorial structures	Ventricular system
	White matter	Cortex		
1-2	Periventricular widespread inflammatory lesions	Laminar necrosis	Microglial nodules	Dilatation. Proliferation of subependymal glia
3-4	Diffuse necrosis Inflammatory infiltrations	Diffuse neuronal damage	Glial nodules. Perivascular infiltrations	Enlargement of ventricles. Proliferation of subependymal glia
5-6	Cerebral hemispheres changed into baloon-like structures with thin walls formed of glial and mesodermal elements		Microglial nodules	Glial proliferation closing the aqueduct

In cases 5 and 6 neuropathological examination revealed the presence of only basal ganglia instead of hemispheres. They were covered by a thick layer of proliferating glia. In the place of the hemispheres there remained a balloon-like structure with thin walls formed of glial tissue and mesodermal fibers (Fig. 7). Subtentorial structures were normal. The intensive subependymal glial proliferation closed the aqueduct. In the brain stem and basal ganglia several toxoplasmic cysts were found. Slight perivascular and meningeal infiltrates presented remnants of the inflammatory process. The infiltrates included mainly macrophages and some lymphocytes and plasmocytes. A summary of the neuropathological findings is presented in Table 2.

DISCUSSION

The presented six cases of congenital toxoplasmosis illustrate the various degrees of damage of newborn brain from moderate to very severe. They allow to follow the development of damage of the maturing nervous tissue and to speculate about the pathomechanism of this process.

In the first stage intensive inflammatory changes were localized mainly in the periventricular white matter. Then the inflammatory and necrotic lesions involved the majority of the white matter, not only periventricular, but also subcortical. Further development of this process transformed the brain hemispheres into sacs composed of meninges and remnants of the nervous tissue, they presented a classical picture of hydranencephaly.

The topography and severity of the brain lesions in the first two stages of the disease were similar to those observed in experimental studies on animals (Beverley, Henry 1971; Kittas et al. 1984). The surroundings of the ventricles were the most severely damaged area of the brain. Lymphoplasmic infiltrates were often observed in the vicinity of the ventricles. The cerebellum was only minimally involved, even in the later stages of the disease. In our cases the earliest changes were found mostly around the lateral ventricles, and the subtentorial structures were spared. A tendency to necrotic changes is known as characteristic for immature nervous tissue (Dąmbska 1965). On the other hand, proliferation of the subependymal tissue leading to a blockade of the cerebrospinal fluid (CSF) circulation seems to play the role of an additional factor in the widespread lesions of the cerebral hemispheres. Obstructive hydrocephalus was observed in congenital toxoplasmosis by Altshuler (1973). Some ependymal defects may occur in the normal fetal brain in the late second and early third trimester of gestation (Dobbing et al. 1983), but the intensity of reactive changes, particularly the proliferation of subependymal glia observed in our cases, exceeded this type of changes. It seems abundant enough to block the normal pathways of CSF circulation. Both inflammatory necrosis and impairment of CSF flow can participate in the pathomechanism of hydranencephaly, which has been described already in the

course of congenital toxoplasmosis (Francois 1963; Altshuler 1973; Dąbska et al. 1965, 1983).

We present our material as a morphological illustration of the consecutive steps of the pathological process leading to this final stage.

USZKODZENIA DOJRZEWAJĄCEGO MÓZGU W PRZEBIEGU WRODZONEJ TOKSOPLAZMOZY

Streszczenie

W pracy przedstawiono kolejne etapy uszkodzenia rozwijającego się układu nerwowego w przebiegu wrodzonej toksoplazmozy. Materiał stanowi 6 przypadków zmarłych w pierwszych miesiącach życia. Badanie neuropatologiczne ujawniło pośrednio mechanizm rozwoju procesu zapalno-martwicze. W pierwszym stadium stwierdzono duże nacieki zapalne w okołokomorowej istocie białej. W następnym stadium zmiany martwicze obejmowały większość istoty białej półkul mózgu. Dalszy rozwój choroby prowadził do zmiany półkul mózgu w cienkościenny worek o ścianach złożonych z opon i resztek tkanki nerwowej. W końcu proces zapalny doprowadzał do hydranencefalii. Rozrost gleju podwyściółkowego, wyraźny we wszystkich przypadkach, blokujący krążenie płynu mózgowo-rdzeniowego wydaje się odgrywać istotną rolę w tym procesie.

REFERENCES

1. Altshuler G: Toxoplasmosis as the cause of hydranencephaly. *Am J Dis Child*, 1973, 125, 251–252.
2. Beverley JKA, Henry L: Histopathological changes caused by congenital toxoplasmosis in mice. *Lyon Med*, 1971, 225, 883–887.
3. Dąbska M: Acute inflammatory necrosis as a factor of destruction of nervous tissue in the fetus (in Polish). *Neuropatol Pol*, 1965, 4, 367–372.
4. Dąbska M, Kraśnicka Z, Michałkiewicz R: Hydranencephaly in the course of congenital toxoplasmosis (in Polish). *Neuropatol Pol*, 1965, 3, 49–58.
5. Dąbska M, Laure-Kamionowska M, Kozłowski P: Meningoencephalitis in newborns and infants as the cause of the central nervous system injury during its development. *Neuropatol Pol*, 1983, 21, 45–54.
6. Dobbing EC, Chi JG, Gilles FH: Developmental changes in ventricular epithelia. In: *The developing human brain*. Eds: FH Gilles, A Leviton, EC Dobbing. J Wright, PSG Inc, Boston, Bristol, London, 1983, pp 113–116.
7. Francois J: *La toxoplasmose et ses manifestations oculaires*, vol 1, Masson, Paris, 1963.
8. Kittas S, Kittas C, Paizi-Biza P, Henry L: A histological and immunohistochemical study of the changes induced in the brains of white mice by infection with *Toxoplasma gondii*. *Br J Exp Pathol*, 1984, 65, 67–74.

Authors' address: Laboratory of Developmental Neuropathology, Medical Research Centre, PASci, 3 Pasteura St, 02-093 Warsaw, Poland

HALINA KROH

ANAPLASTIC TEMPORAL LOBE GANGLIOGLIOMA. CASE REPORT

Department of Neuropathology, Medical Research Centre, Polish Academy of Sciences, Warsaw
and Department of Neurosurgery, School of Medicine, Warsaw

Clinical, histological and histochemical features of anaplastic temporal ganglioglioma in a 30-year-old woman are described. Short clinical course (preoperative 2 years, postoperative 6 months), anaplastic features of glial astrocytic component with scarce GFAP and negative vimentin immunostaining indicate aggressive character of the tumor. Ganglionic component is confirmed by the strong Con A affinity and discrete FN and NSE immunostaining.

Key words: *ganglioglioma, anaplastic astrocytes, lectins, immunocytochemistry.*

Gangliogliomas in adults in contrast to children cases are rare and their incidence has been estimated around 0.1–0.5 per cent of all primary CNS tumors (Jänisch et al. 1988). In Polish literature the description of ganglioglioma tumors belongs to exceptions (Matyja et al. 1992).

The scope of this paper is the presentation of a tumor of mixed neuronal and glial elements which fulfills the criteria required by Russel and Rubinstein (1989), but in some particulars differs from most reported cases.

CASE REPORT

A 30-year-old female, married, one child, was admitted to the Neurosurgery Department, suffering of olfactory delusions which had occurred at various rates every day for 2 years and were followed a year prior to admission by spells of taste delusion. Lately the patient experienced transient disturbances of visual acuity. Since temporal epilepsy was diagnosed, the patient was treated with anticonvulsant drugs. CT examination performed at that time was negative, when repeated before admission showed a tumor in left temporal lobe. Past medical history of the patient was irrelevant. Neurological examination: visual acuity bilaterally normal, fundus oculi normal, palsy of left *n.*

oculomotorius, visual field with homonymous quadrant hemianopia. Apart from the above symptoms no abnormal neurological signs were noted. Angiography of left carotid artery showed an expansive process deep in the temporal lobe structures which caused an elevation of temporal arteries, tension of anterior choroid artery and of lenticulo-striatae arteries. Late phase of angiography showed tumoral blush in the area of the internal cerebral vein. CT presented a well contrast-enhanced tumor containing multiple calcifications, located deep in left temporal lobe, 32 × 50 mm in diameter. The tumor infiltrated from the left the perisellar cisternae, pressed anterior horn of the left lateral ventricle and the III ventricle. Other parts of the ventricular system remained narrow, without dislocation. Operation: Left frontal-temporal craniectomy revealed an ischemic, swollen temporal lobe and elevated Sylvian fissure. Resection was performed 4 cm from temporal pole. In the line of resection 1.5 cm deep a pathological tissue of hard, rubbery consistence was found. Evacuation of neoplastic tissue had to be limited to the intratumoral part because the tumor spread towards posterior and medial structures and infiltrated the Sylvian fissure.

The patients postoperative deterioration lasted a few days, but was followed by recovery, without amelioration of III n.palsy. Control CT after 2 weeks revealed remnants of deep parts of the tumor pressing on perisellar cisternae, lateral and III ventricle as well as some peritumoral edema. Two weeks later patient started radiotherapy Co 60.500c Gy/t (brain) and 1.000c Gy/t (tumor area). Three months later the patient's condition deteriorated, she developed right-sided hemiparesis. Control CT confirmed the localization of tumor remnants, widened ventricular system, its slight dislocation towards the right indicating progression of the process. Six months later the patient was admitted to the Intensive Care Unit, she could not walk and swallow, psychic disturbances occurred. The patient died 6 months after the operation. Autopsy was not performed.

MATERIAL AND METHODS

Four blocks of neoplastic tissue selected from different areas of the removed tumor were processed for light microscopy after formalin fixation. The paraffin sections from each block were stained with hematoxylin-eosin, Nissl and Gomori methods. Mirror sections were used for immunocytochemical investigations of glial fibrillary acidic protein (GFAP) with polyclonal antibody (Daco) at a concentration of 1:500 by the Avidin-Biotin-Complex method (ABC), neurofilaments (NF) with monoclonal antibody (Daco) by an alkaline phosphatase-antialkaline phosphatase method (APAAP), concentration 1:1000, neuron-specific enolase (NSE) by the ABC method, at

concentration 1:3000, vimentin with polyclonal antibody (Daco) by ABC method, concentration 1:50. Besides, direct reactions with the lectin *Concavalia ensiformis* (Con A) labeled with peroxidase (Sigma) solution 20 µg/ml and *Arachis hypogaea* (Peanut agglutinin, PNA) labeled with peroxidase (Sigma), solution 15 µg/ml were performed (Figols et al. 1991).

RESULTS

The general appearance of neoplastic tissue was monotonous. Dominant feature was a marked cellular density varying from field to field being denser beneath the infiltrated arachnoidea. The main isomorphous component were small cells with clear, chromatin-dotted nuclei, without visible cytoplasm, resembling anaplastic glial cells (Fig. 1). The cells were negative for PNA, NF, NSE and vimentin reaction. Among these small not reacting glial cells were dispersed similar cells but exhibiting Con A and GFAP-immunostaining, less numerous in dense areas. Larger, GFAP-positive astrocytes of reactive type, also binuclear, with distinct but scarre processes, were present in the tumor (Fig. 2) and in submeningeal gliosis (Fig. 3). The latter cells displayed strong Con A binding (Fig. 4), some were vimentin-positive. Necrotic foci were absent, whereas occasional mitotic figures could be found. Numerous small calcospherites were confined to perivascular spaces or scattered in the stroma. Small, thin-walled blood vessels presented a scanty amount of reticulin fibers exclusively in the vascular walls. Thin vascular sprouts in and around the main tumoral area exhibited endothelial vimentin immunostaining. Occasionally, the vessels showed discrete mononuclear cuffings.

The tumor contained in places dispersed nerve cells, in others there were larger clusters of ganglion cells (Fig. 5). The ganglion cells were of various size and shape, from elongated to round or oval. They were characterized by light nuclei often located excentrically, with prominent nucleoli and varying amount of cytoplasm presenting some Nissl substance in hilar part of axons. Binucleated neurons appeared occasionally (Fig. 5). Many neurons showed perinuclear satellitosis (Fig. 6). The large tumoral neurons presented a distinct cytoplasmic affinity to Con A (Figs 7, 8) corresponding to that in non-affected cortex. Discrete NF immunostaining was visualized in perikarya and axons of some tumoral neurons and in some neurons at the periphery of infiltrated tissue. Axonal staining was much more intensive than perikaryal, inside and outside the neoplastic tissue. NSE staining hardly visible could be observed only in some ganglion cells including the axonal hilus. Results of other stainings (PNA, vimentin) were negative.

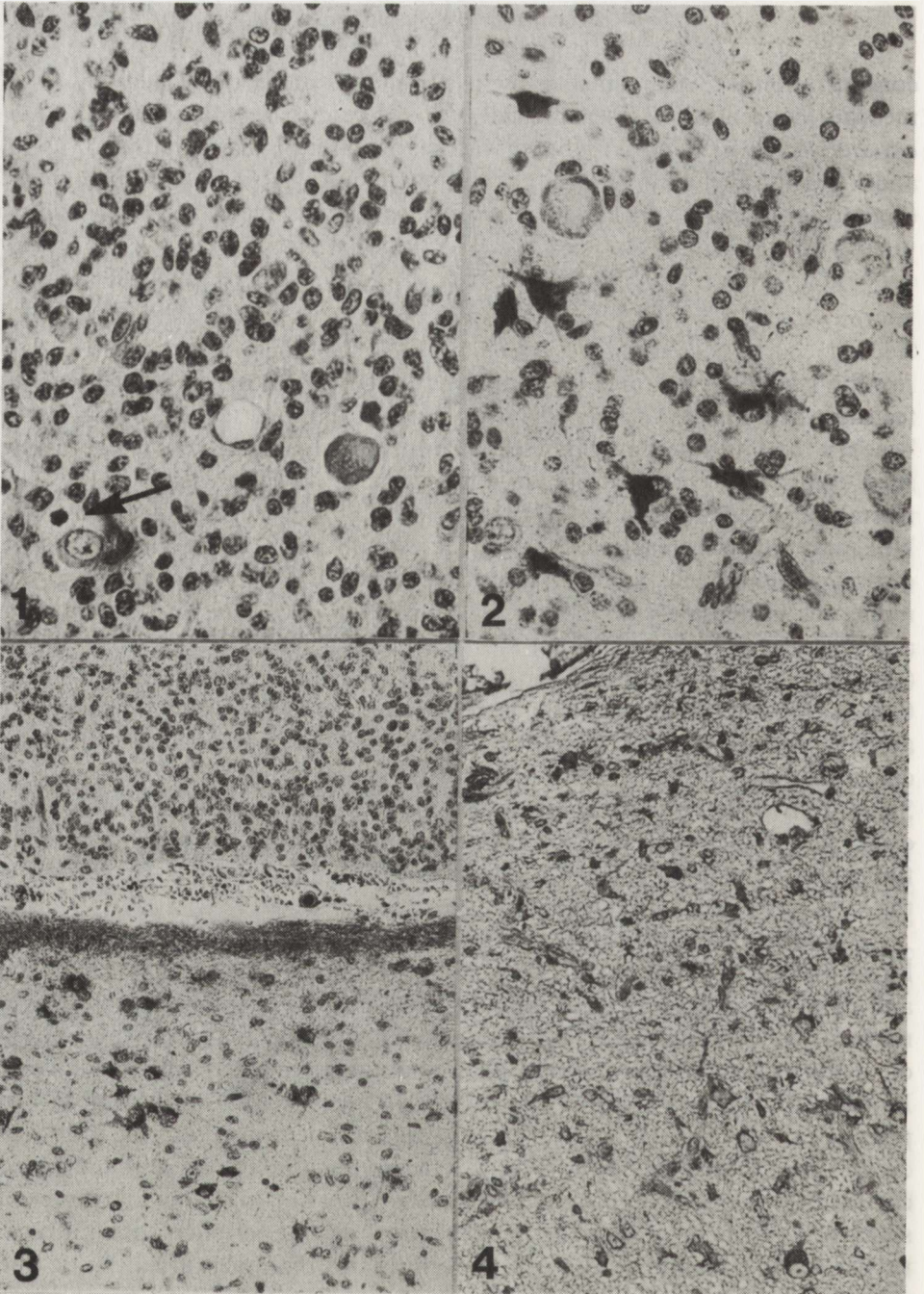


Fig. 1. Dense neoplastic glial infiltration with two ganglion cells and mitotic figure (arrow). HE. $\times 400$

Fig. 2. GFAP-immunostained reactive astrocytes among unstained glial and ganglionic component of neoplastic infiltration. $\times 400$

Fig. 3. Negative neoplastic infiltration above the sulcus, below GFAP-immunostained reactive astrocytes and submeningeal fibrous gliosis. $\times 120$

Fig. 4. Moderate glial response in upper cortical layers. Cytoplasm of neurons and astroglia binds Con A lectin. $\times 300$

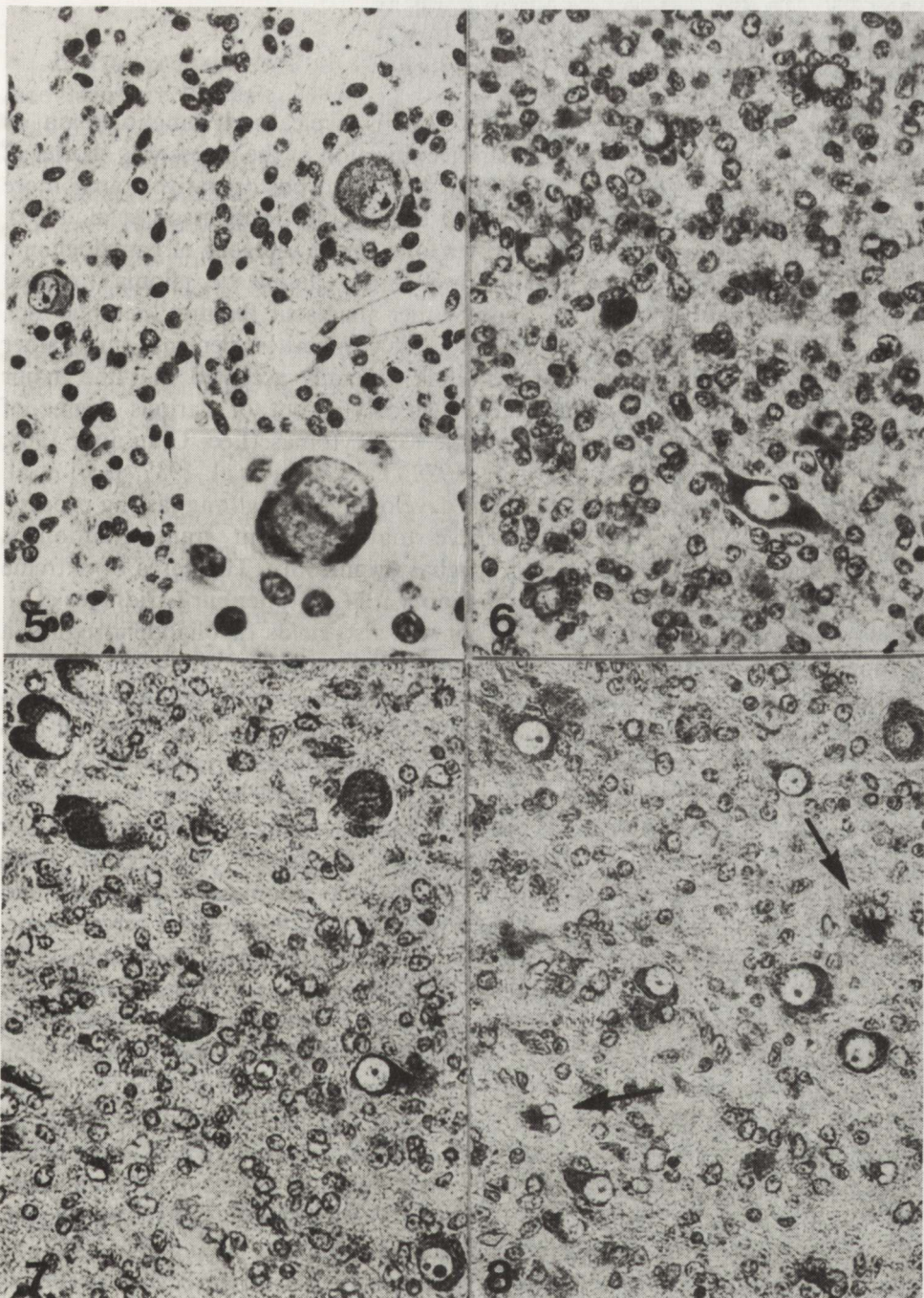


Fig. 5. Ganglion cells with excentric nuclei and prominent nucleoli. Cresyl violet. $\times 400$. Insert: ganglion cell in division. $\times 1000$

Fig. 6. Agglomeration of ganglion cells in dense part of tumor. Neoplastic perineuronal satellitosis. Strong binding of Con A by ganglion cells. $\times 400$

Fig. 7. Agglomeration of ganglion cells of various size and shape. Excentric nuclei. Ganglion cell in right lower corner contains two nucleoli. Strong affinity of Con A to ganglion cell and axon. $\times 400$

Fig. 8. Agglomeration of various size ganglion cells with prominent nuclei and nucleoli. Strong affinity of Con A to ganglion cells, their axons and to some astrocytic cells also binuclear (arrows). $\times 400$

DISCUSSION

Clinical history of the presented case is typical of ganglioglioma as concerns age and site, but the preoperative duration of the illness was shorter (2 years) than reported (Russel, Rubinstein 1989) and postoperative course more aggressive than usually observed (Henry et al. 1978, Johannsson et al. 1981). Histological features of the tumor correspond to the category of ganglioglioma whose main component is that of moderately anaplastic glioma (marked cellularity and mitoses) but deprived of other anaplastic features (necrotic foci, polymorphy, vascular changes). It contains calcospherites, element found rather in well-differentiated gangliogliomas. It is generally accepted that the major component of most gangliogliomas is astrocytic but of various degree of differentiation from common high grade astrocytomas (Lee, Glausauer 1968; Rubinstein, Herman 1972; Cox et al. 1972; Takahashi et al. 1987; Hori et al. 1988) to less frequent anaplastic forms developing during long-lasting process. Russel and Rubinstein (1962) believe that malignant transformation is uncommon and concerns the cells of glial origin only. The cases of extreme malignancy won the name of ganglioglioblastoma (Stoltenburg-Didinger et al. 1989). Occasionally gangliogliomas contain also fields of oligodendroglioma (Johannssen et al. 1981) or spongioblastic cells (Steezman, Winer 1961). As an exception, a malignant ganglioglioma with glial oligodendrogliomatous component was reported (Russel, Rubinstein 1989). Some authors observed also non-tumorous hamartomatous elements and neurofibrillary tangles (Hori et al. 1988). The anaplastic character of the glial component in the presented case can be confirmed by the lack of GFAP immunostaining as observed in earlier studies on astrocytomas (van der Meulen et al. 1978; Velasco et al. 1980; Tascos et al. 1982). Immunoreactive are some neoplastic astrocytes and reactive astrocytes embedded in neoplastic tissue and those in the subpial zone. The striking lack of GFAP expression in neoplastic cells distinguishes the presented tumor from many recently investigated cases (Roessmann et al. 1983; Trojanowski et al. 1984; Kawai et al. 1987; Takahashi et al. 1987, 1989; Cras et al. 1988; Hori et al. 1988), just as does the lack of vimentin expression in glial neoplastic elements which are supposed to coexpress intermediate filaments in reactive and neoplastic astrocytes independently of the degree of their differentiation (Herpers et al. 1986). The lack of both types of intermediate filaments in neoplastic cells suggests either a very low degree of differentiation of the astrocytic component or any other than astrocytic glial component. Lack of PNA binding is observed in oligodendrogliomas (Wang et al. 1989), in particular in undifferentiated ones as well as in anaplastic astrocytomas (Figols et al. 1991, 1992). Absence of Con A binding by the majority of glial neoplastic elements is in agreement with the previous observations (Figols et al. 1991) of the binding disability of undifferentiated astrocytes of anaplastic astrocytomas, though contradictory to results of Wang et al. (1989). However, the disparity of histological and immunohistochemical picture observed in other CNS neoplasms should be remembered (Hubbard et al. 1989).

In concordance with other reports the minor cellular component of the neoplasm are the ganglion cells aggregated or scattered, occasionally binucleated. Courville (1956) explains the phenomenon of multinucleated neuronal elements at the periphery of gliogenic tumors as engulfed neurons undergoing degeneration and at this stage stimulated by the adjacent tumor to abortive nuclear division. Other authors underline an anaplastic process concerning only the gliogenous component of the tumor, whereas the ganglionic component might be of hamartomatous origin (Russel, Rubinstein 1962; Rubinstein, Herman 1972). Our material presents well-preserved ganglion cells differing only by size. They display high binding of a Con A, similar to that of the neurons outside the neoplastic infiltration (Schwechheimer et al. 1984). Ganglion cells cytoplasm in the tumor area immunostain for NF weaker than their processes. Strong immunoreaction of neuronal processes contrary to that of cytoplasm of well differentiated neoplastic ganglion cells has been explained by a low content of intermediate filaments in the perikaryon and low degree of cellular maturation (Roessmann et al. 1983; Azarelli et al. 1991). However, a strong perikaryal and axonal reaction for NF in anaplastic and well-differentiated gangliogliomas has also been reported (Trojanowski, Lee 1983; Stoltenburg-Didinger et al. 1989). Scarce NSE activity was demonstrated in some ganglion cells. Variable positivity in tumors of neuroblastic origin was reported (Carlei et al. 1984) not only of ganglion cells, but of neoplastic astrocytes (Cras et al. 1988) and normal and neoplastic oligodendroglia, even in reactive astrocytes (Nakagawa et al. 1986).

ANAPLASTYCZNY GANGLIOGLIOMA PŁATA SKRONIOWEGO. OPIS PRZYPADKU

Streszczenie

Przypadek dotyczy 30-letniej kobiety, u której po 2 latach objawów z płata skroniowego usunięto subtotalnie ganglioglioma. Mimo następczej radioterapii stan się pogarszał i zgon nastąpił po upływie pół roku. Komponent glejowy guza stanowiły komórki pochodzenia astrocytarnego. Znaczna gęstość komórkowa, figury podziału i wyniki badań immunohistochemicznych (przewaga komórek GFAP-ujemnych, brak barwienia wimentyny i odczynu PNA) wskazują na znaczną anaplazję nowotworu potwierdzoną agresywnym przebiegiem pooperacyjnym.

Komponent neuronalny guza tworzyły komórki zwojowe silnie wiążące Con A i śladowo NF i NSE-immunobarwliwe.

REFERENCES

1. Azarelli B, Luerssen T, Wolfe T: Intramedullary secretory gangliocytoma. *Acta Neuropathol (Berl)*, 1991, 82, 402–407.
2. Carlei F, Polak J, Ceccamea A, Marangos P, Dahl D, Cocchia D, Michetti F, Lezoche E, Speranza V: Neuronal and glial markers in tumours of neuroblastic origin. *Virch Arch (Pathol Anat)*, 1984, 404, 313–324.

3. Cox J, Zimmermann H, Houghton V: Microcystic ganglioglioma treated by partial removal and radiation therapy. *Cancer*, 1982, 50, 473–477.
4. Courville C: Multinucleation of cortical nerve cells at margin of malignant glioma. *J Neuropathol Exp Neurol*, 1956, 15, 369–376.
5. Cras P, Martin J, Gheuens J: γ -enolase and glial fibrillary acidic protein in nervous system tumors. *Acta Neuropathol (Berl)* 1988, 75, 377–384.
6. Figs J, Cervós-Navarro J, Cruz-Sanchez F: Peanut agglutinin (PNA): a reliable differentiation marker in human oligodendrogliomas. *Brain Tumor Pathol*, 1992, in press.
7. Figs J, Madrid J, Cervos-Navarro J: Lectins as differentiation markers of human gliomas. *Histol Histopath*, 1991, 6, 79–85.
8. Henry J, Heffner R, Earle K: Gangliogliomas of CNS: a clinico-pathological study of 50 cases. *J Neuropathol Exp Neurol*, 1978, 37, 626, abstract.
9. Herpers M, Ramaekers F, Aldeweireldt J, Moesker O, Slooff J: Co-expression of glial fibrillary acidic protein- and vimentin-type intermediate filaments in human astrocytomas. *Acta Neuropathol (Berl)*, 1986, 70, 333–339.
10. Hori A, Weiss R, Schaake T: Ganglioglioma containing osseous tissue and neurofibrillary tangles. *Arch Pathol Lab Med*, 1988, 112, 653–655.
11. Hubbard J, Scheithauer B, Kispert D, Carpenter S, Wick M, Laws E: Adult cerebellar medulloblastomas: the pathological, radiographic and clinical disease spectrum. *J Neurosurg*, 1989, 70, 536–544.
12. Jänisch W, Schreiber D, Güthert H: *Neuropathologie-Tumoren der Nervensystems*. VEB G Fischer, Jena, 1988, pp 188–192.
13. Johannsson J, ReKate H, Roessmann U: Gangliogliomas: pathological and clinical correlation. *J Neurosurg*, 1981, 54, 58–63.
14. Kawai K, Takahaschi H, Ikuta F, Tanimura K, Honda Y, Yamazaki H: The occurrence of catecholamine neurons in a parietal lobe ganglioglioma. *Cancer*, 1987, 60, 1532–1536.
15. Lee J, Glasauer F: Ganglioglioma: light and electron microscopic study. *Neurochirurgia*, 1968, 11, 160–170.
16. Matyja E, Kuchna I, Ząbek M: Cerebral ganglioglioma with long history and unusual prominence of the mesenchymal elements. *Neuropatol Pol*, 1992, 30, 165–171.
17. van der Meulen, Houthoff J, Ebels E: Glial fibrillary acidic protein in human gliomas. *Neuropathol Appl Neurobiol*, 1978, 4, 177–190.
18. Nakagawa Y, Perentes E, Rubinstein L: Immunohistochemical characterization of oligodendrogliomas: an analysis of multiple markers. *Acta Neuropathol (Berl)*, 1986, 72, 15–22.
19. Roessmann U, Velasco M, Gambetti P, Autilio-Gambetti L: Neuronal and astrocytic differentiation in human neuroepithelial neoplasms. *J Neuropathol Exp Neurol*, 1983, 42, 113–121.
20. Rubinstein L, Herman M: A light- and electron-microscopic study of a temporal-lobe ganglioglioma. *J Neurol Sci*, 1972, 16, 27–48.
21. Russel D, Rubinstein L: Ganglioglioma: a case with long history and malignant evolution. *J Neuropathol Exp Neurol*, 1962, 21, 185–193.
22. Russel D, Rubinstein L: *Pathology of tumours of the nervous system*. V Edition E Arnold, London, Melbourne, Auckland, 1989, pp 289–306.
23. Schwechheimer K, Weiss G, Möller P: Concanavalin A target cells in human brain tumors. *J Neurol Sci*, 1984, 63, 393–401.
24. Steegmann T, Winer B: Temporal lobe epilepsy resulting from ganglioglioma. *Neurology*, 1961, 11, 406–412.
25. Stoltenburg-Didinger G, Kaden B, Patt S: Ganglioglioblastoma. *Clin Neuropathol*, 1989, 8, 209, abstract.
26. Takahashi H, Ikuta F, Tanaka R: Ultrastructural alterations of neuronal cells in a brain stem ganglioglioma. *Acta Neuropathol (Berl)*, 1987, 74, 307–312.
27. Takahashi H, Wakabayashi K, Kawai K, Ikuta F, Tanaka R, Takeda N, Washiyama K: Neuroendocrine markers in central nervous system neuronal tumors (gangliocytoma and ganglioglioma). *Acta Neuropathol (Berl)*, 1989, 77, 237–243.

28. Tascos N, Parr J, Gonatas N: Immunocytochemical study of the glial fibrillary acidic protein in human neoplasms of the central nervous system. *Hum Pathol*, 1982, 13, 454–458.
29. Trojanowski J, Lee V: Anti-neurofilament monoclonal antibodies: reagents for the evaluation of human neoplasms. *Acta Neuropathol (Berl)*, 1983, 59, 155–158.
30. Trojanowski J, Lee V, Schlaepfer W: An immunohistochemical study of human central and peripheral nervous system tumors using monoclonal antibodies against neurofilaments and glial filaments. *Hum Pathol*, 1984, 15, 248–257.
31. Velasco M, Dahl D, Roessmann U, Gambetti P: Immunohistochemical localization of glial fibrillary acidic protein in human glial neoplasms. *Cancer*, 1980, 45, 484–494.
32. Wang X, Kochi N, Tani E, Kaba K, Matsumoto T, Shindo H: Lectin histochemistry of human gliomas. *Acta Neuropathol (Berl)*, 1989, 79, 176–182.

Author's address: Department of Neuropathology, Medical Research Centre, PASci, 3 Dworkowa St, 00-784 Warsaw, Poland

PRZEMYSŁAW NOWACKI, DOROTA DOLIŃSKA, KRYSZYNA HONCZARENKO,
ANDRZEJ POTEMKOWSKI

IMPAIRMENT OF VERTEBRAL CANAL NERVOUS STRUCTURES AFTER INTRATHECAL PROPHYLAXIS IN NON-HODGKIN'S LYMPHOMAS

Department of Neurology and Department of Hematology, School of Medicine, Szczecin, Poland

Neuropathological analysis of spinal cord and spinal roots as well as spinal leptomeninges after intrathecal methotrexate (MTX) therapy was performed in 44 cases of non-Hodgkin's lymphomas of high malignancy. It was shown that MTX applied according to the program applied as a prophylaxis against lymphomatous infiltrations in the central nervous system, caused demyelination of spinal roots and fibrosis of leptomeninges and their blood vessels. However, it does not affect spinal cord structures. Described morphological changes remained clinically mute, therefore they do not seem counterindicate prophylactic intrathecal MTX application.

Key words: *non-Hodgkin's lymphomas, methotrexate therapy, spinal root damage.*

Methotrexate (MTX), folic acid anti-metabolite has been used for treatment of leukemias, lymphomas and some solid tumors since 1953 (Bleyer 1978). Because of poor penetration of the drug into the cerebrospinal fluid, it was administered intrathecally in 1958 (Young, Posner 1980). Ever since MTX was applied for treatment and prophylaxis of central nervous system (CNS) leukemias and lymphomas. A reversible and irreversible effects upon the CNS may occur following intrathecal, intravenous, intracarotid and intraventricular administration (Shapiro et al. 1975; Bleyer, Dedrick 1977; Freeman et al. 1977; Johnson et al. 1984). Papers concerning these problems describe usually cases with clinical manifestation of nervous system impairment, especially cerebral white matter (Silverstein 1986; Poskitt 1988; Robbins 1988; Yim et al. 1991), and spinal cord (Saiki, Thompson 1972; Martins et al. 1990, von der Weid et al. 1991).

In some cases neuropathological investigations have revealed hemorrhagic changes in the vertebral canal, within the spinal cord and cerebral hemispheres, calcifications and necrosis of intracerebral blood vessels (Young, Posner 1980). However, the above-mentioned neurological abnormalities and structural changes appear very seldom if we consider the widespread usage of intrathecal MTX (IT-MTX) to protect the CNS against leukemia and lymphoma.

It seemed interesting to find, whether any neuropathological changes develop after IT-MTX administration in patients without clinical manifestation due to side effects of such applied drug. We also tried to answer whether IT-MTX administration was hazardous from the clinical view point in patients with high grade non-Hodgkin's lymphomas.

MATERIAL AND METHODS

The neuropathological investigations were carried out in 44 patients ranging in age from 17 to 75 years (mean 50.3), deceased due to non-Hodgkin's lymphomas (HGNHL). In 37 cases lymphoblastic, in 5 immunoblastic, in 2 centroblastic lymphoma were diagnosed. The material was divided into two groups. Group I consisted of 23 cases treated with MTX administered intrathecally (12 mg/m² of body surface) and Fenicort 25 mg. The total dose of MTX given to one patient ranged from 20 to 380 mg (on the average 180 mg). The period between the last IT-MTX injection and the patient's death ranged from 2 to 30 days. To group II were included 21 cases untreated with IT-MTX. All patients in both groups were treated with polychemotherapy according to protocols: CBVPM/AVBP (6–8 cycles) or CHOP (5–7 cycles). The global dose of cytostatics in subsequent cycles was as follows: CBVPM (cyclophosphamide 1200 mg/m², bleomycin 75 mg, vincristine 4 mg, prednisone 560 mg, methotrexate 3 mg/kg); AVBP (hydroxyrubicin 90 mg/m², vincristine 4 mg, bleomycin 30 mg, prednisone 560 mg); CHOP (cyclophosphamide 750 mg/m², hydroxyrubicin 50 mg/m², vincristine 2 mg, prednisone 500 mg). Stage IV of the HGN-HL was diagnosed in all patients, however, the vertebral canal nervous structures were not infiltrated by lymphoma.

For neuropathological investigation the spinal cord from the cervical, thoracic and lumbal regions, was taken. Ventral and dorsal spinal roots from C2–C4 region and from cauda equina in the neighbourhood of IT-MTX injection were taken as well. The material was stained with hematoxylin-eosin, cresyl violet, PAS and according to Heidenhain, Holmes, Bielschowsky, as well as van Gieson methods.

The results were statistically analysed by chi-square test.

RESULTS

Neuropathological changes within the spinal roots (Fig. 1)

Group I

In 70% of cases myelin destruction of spinal roots was observed. The areas of complete or almost complete demyelination located among regions of markedly swollen and usually pale myelin sheaths occurred in 29.5% of cases (Fig. 2). Almost in one half of them the demyelinated areas were chiefly observed within the roots of cauda equina. Focal demyelination (Fig. 3)

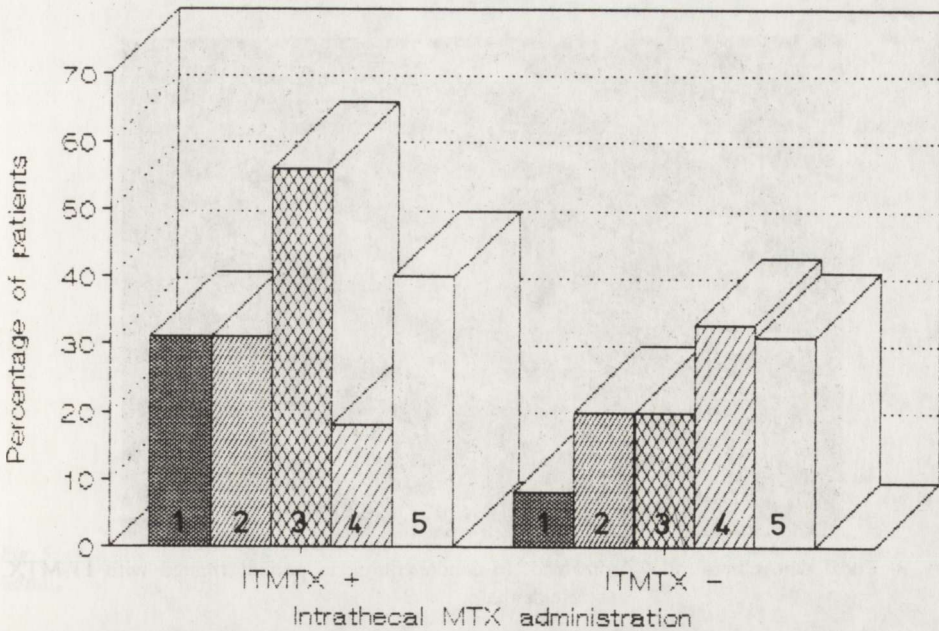


Fig. 1. Intrathecal MTX administration and degenerative changes in the spinal roots: 1-extensive demyelination (ED), 2-focal demyelination (FD), 3-extensive myelin swelling (EMS), 4-focal myelin swelling (FMS), 5-axonal changes (AC).

Dependence between ED + FD + EMS and FMS in group with ITMTX + and ITMTX - are statistically significant (chi-square = 5.56, $p < 0.025$)

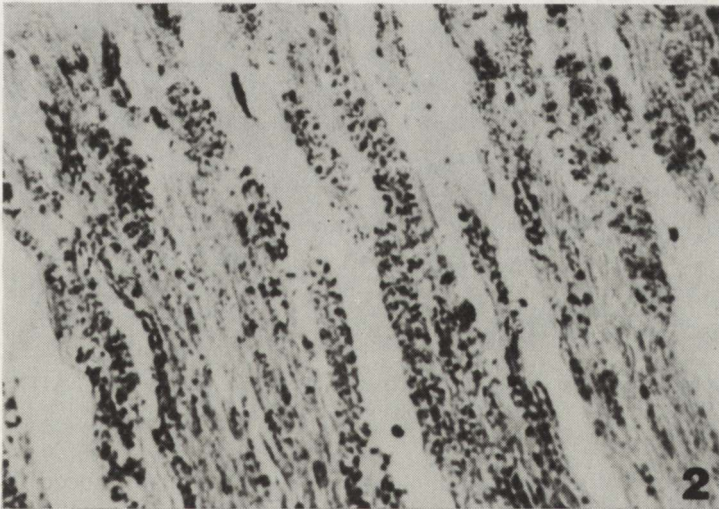


Fig. 2. Demyelination of spinal root in the vicinity of IT-MTX injections. Heidenhain $\times 240$

occurred in 29.5% of cases, in the cauda equina roots more intensively as compared with other regions. Distinct, usually focal myelin swelling (Fig. 4) was found in 54.5% of cases. The phenomenon was noted in all investigated

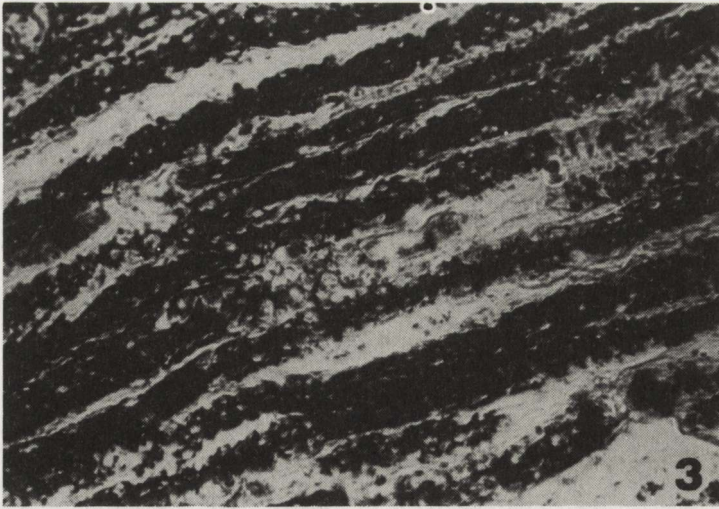


Fig. 3. Focal demyelination of spinal root in cauda equina in patient treated with IT-MTX. Heidenhain. $\times 240$

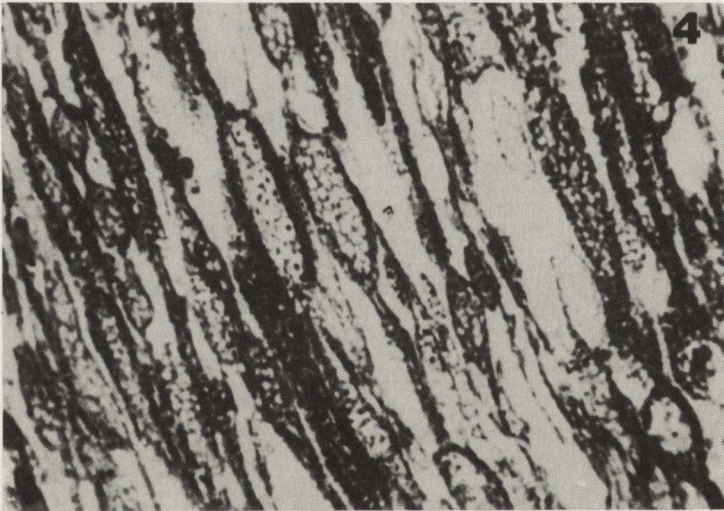


Fig. 4. Distinct focal myelin swelling of spinal root in the vicinity of IT-MTX injections. Heidenhain. $\times 240$

regions, however, within the cauda equina it was more pronounced than in the remaining areas; 16% of cases demonstrated only minimal swelling of myelin sheaths.

Axonal damage occurred in 34% of cases mainly in thick nerve fibers. Axons were moderately swollen and slightly rarefied (Fig. 5). The intensity of axonal changes was similar both in the cervical and caudal regions.

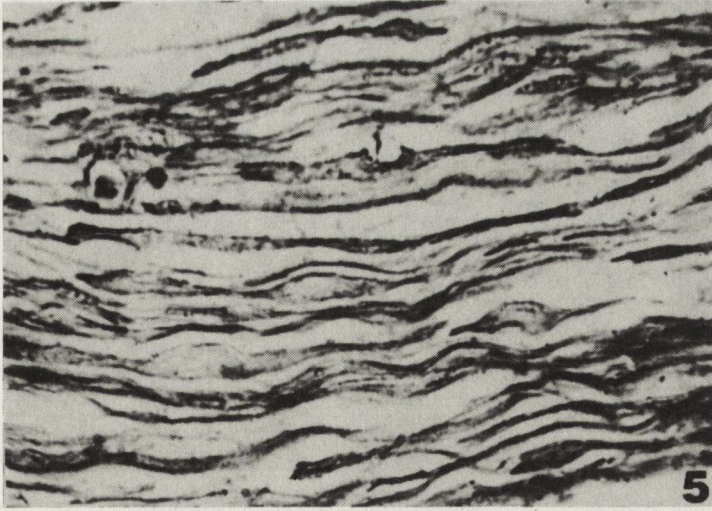


Fig. 5. Slight rarefaction and moderate swelling of axons in spinal root of cauda equina after IT-MTX administration (myelin changes in the same case were shown on Fig. 2). Bielschowsky. $\times 240$

Group II

Myelin damage developed in 50% of cases. In 8% it consisted of extensive demyelination. In 18% focal demyelination and also in 18% distinct myelin swelling were observed. 29.5% of the cases included in this group exhibited focal swelling of myelin sheaths. There were no significant differences between the above-mentioned myelin changes within the cervical and the caudal roots.

In this group, 29.5% of cases showed a minimal loss of axons and their local swelling. The intensity of axonal changes was similar in all investigated regions.

Changes within the spinal leptomeninges

Group I

In general, changes were observed in 70% of cases. The leptomeninges were thickened (reaching 200 μm in thickness) and underwent fibromatous changes. In 36% of cases vessels with greatly thickened and fibrous walls occurred within the meninges (Fig. 6). The weak local inflammatory reaction consisting of lymphocytes and monocyto-macrophages was present also in 36% of cases. Leptomeningeal changes were seen both in the cervical, thoracic and lumbo-sacral parts of the spinal cord.

Group II

The leptomeninges were thickened in 29.5% of cases (rarely achieved 200 μm in thickness). Of the cases included to this group, 18% had single vessels with fibrous walls (40–50 μm in thickness). Slight lymphocytic and fibroblastic reaction was also observed in 18% of cases.

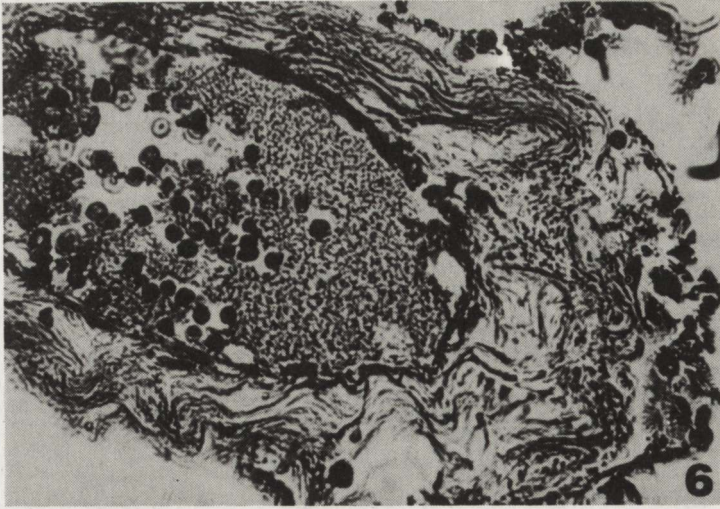


Fig. 6. Leptomeningeal vessel with thickened fibrotic wall in patient treated with IT-MTX. Van Gieson. $\times 240$

Neuropathological changes in the spinal cord

There were no significant neuropathological changes within the spinal cord either in cases of groups I or II. In the majority of cases, there developed only small myelin swelling in the dorsal and lateral tracts. Spinal gray matter and blood vessels were microscopically intact.

Intrathecal MTX administration and clinical complications

In patients included to group I, 205 intrathecal MTX injections were globally applied. After 7.1% of injections a typical "post-puncture" syndrome developed (headache, nausea, vertigo in vertical position). After another 1.8% of injections minimal neck stiffness was observed. The symptoms disappeared spontaneously after 5–6 days.

Both in patients of groups I and II (80.5% and 75.9%, respectively) weakening of tendon reflexes developed during systemic chemotherapy, especially after CBVPM/AVBP protocol (89.7% of patients), less frequently after CHOP schedule (69%). Disturbances in tendon reflexes were observed irrespective of IT-MTX prophylaxis.

DISCUSSION

In patients with IT-MTX administered the most pronounced changes were observed within the spinal roots. There was focal demyelination, less frequently extensive one. It seemed to be due to segmental myelin swelling which appeared to be the first reaction after IT-MTX injection. Neuropathological changes within the spinal roots were mostly of demyelinating nature, much less axonal. More visible and frequent myelin lesions, especially located in cauda

equina denote the toxic influence of IT-MTX on myelin sheaths. Studies of Werner et al. (1988) confirm such a viewpoint. MTX acts by inhibition of DNA synthesis and cellular replication, thus, can also impair Schwann cells.

It is difficult to prove whether axonal changes are secondary to myelin damage or depend rather on the toxic effect of systemic chemotherapy consisting of schedules with vincristine, which have been applied in our patients. Vincristine has been shown to produce axonal damage, and consequently, the well known peripheral neuropathy.

Perhaps low doses of MTX given repeatedly are more dangerous than a single high dose of the drug (Phillips 1986). The former management may inhibit myelin regeneration. Our patients received IT-MTX once a month, and during the second and fourth cycle of CBVPM once a week. Thus the spinal roots were chronically subjected to the toxic influence of MTX. Nevertheless, we did not observe "onion bulbs" — the neuropathological evidence of alternating de- and remyelination (Dyck 1975; Kamen 1986). Indeed, in some patients who received the highest total IT-MTX dosage, the demyelinative changes were more distinct than in the remaining persons, but the role of cumulation of IT-MTX in the development of spinal root neuropathological changes requires further investigations. Up till now this theory was based on experimental trials (Ramadan et al. 1988) and has not been verified in human pathology.

In patients with IT-MX administration fibrous changes within the spinal leptomeninges and their vessels were more frequent and conspicuous than in other patients, so it is possible that some cases with headache, vomiting, nausea, vertigo and meningismus after IT-MTX injection are rather due to chemically evoked meningitis (Dameshek, Gunz 1983) than to cerebrospinal fluid hypotonia.

The fact that myelin impairment within the spinal roots and fibrous changes in the spinal leptomeninges were also observed in cases without IT-MTX application confirm the role of other factors in the development of the mentioned changes such as systemic chemotherapy, malnutrition, metabolic and immunological disturbances. We have not observe significant changes in the spinal cord either in patients with or without IT-MTX administration. It depends may be on the resistance of spinal tissues to IT-MTX action. It is not unlikely that the leptomeninges effectively protect the spinal cord against the toxicity of the drug. The occasionally described acute spinal cord necrosis after IT-MTX (Kumar et al. 1989) develops perhaps owing to a drug-dependent lesion of blood vessels in the neighbourhood of MTX application.

Finally, it should be emphasized that only in 9% out of 205 lumbar punctures performed in our patients, transient slightly conspicuous neurological signs were seen. The diminution of tendon reflexes as a clinical manifestation of peripheral neuropathy should be attributed to the neurotoxicity of IT-MTX and systemic chemotherapy as well.

CONCLUSIONS

1. Methotrexate given intrathecally to protect the central nervous system against lymphomatous infiltrations either causes or intensifies spinal roots demyelination and fibrous changes in spinal leptomeninges.

2. The above mentioned neuropathological changes do not indicate limitation of intrathecal application of methotrexate in prophylaxis of CNS lymphoma.

USZKODZENIE STRUKTUR NERWOWYCH KANAŁU KRĘGOWEGO
W NASTĘPSTWIE PROFILAKTYKI DOKANAŁOWEJ W CHŁONIAKACH
ZŁOŚLIWYCH NIEZIARNICZYCH

Streszczenie

Na podstawie badań neuropatologicznych, przeprowadzonych u 44 chorych zmarłych z powodu chłoniaków nieziarniczych o wysokiej złośliwości, autorzy przeanalizowali zmiany w korzeniach rdzeniowych, oponach miękkich i rdzeniu kręgowym po dokanałowym stosowaniu metotreksatu. Badania wykazały, że metotreksat podawany według schematów przyjętych w zapobieganiu naciekom chłoniakowym w ośrodkowym układzie nerwowym wywołuje demielinizację korzeni rdzeniowych oraz zwłóknienie opon miękkich rdzenia i ich naczyń. Nie wpływa natomiast na rdzeń kręgowy. Opisanym zmianom nie towarzyszą objawy kliniczne, które ograniczałyby wykorzystanie tej drogi podawania leku.

REFERENCES

1. Bleyer WA: The clinical pharmacology of methotrexate. *Cancer*, 1978, 41, 36–51.
2. Bleyer WA, Dedrick RL: Clinical pharmacology of intrathecal methotrexate. *Cancer Treat Rep*, 1977, 61, 703–708.
3. Dameshek W, Gunz P: *Leukemia*, Grune, Stratton, New York, London, Paris, 1983.
4. Dyck PI: Pathologic alterations of the peripheral nervous system of man. In: *Peripheral neuropathy*, Eds: PI Dyck, PK Thomas, EH Lambert, Saunders, Philadelphia, London, Toronto, 1975.
5. Freeman AJ, Wang JJ, Sinks LE: High-dose methotrexate in acute lymphoblastic leukemia. *Cancer Treat Rep*, 1977, 61, 727–731.
6. Johnson GJ, Oken MM, Anderson JR, O'Connell MJ, Glick J: Central nervous system relapse in unfavourable histology non-Hodgkin's lymphoma: Is prophylaxis indicated? *Lancet*, 1984, 8404, 685–687.
7. Kamen BA: Methotrexate, folate and the brain. *Neurotoxicology*, 1986, 7, 209–216.
8. Kumar L, Rajkumar T, Raghunath-Rao D, Usha-Devi J, Sagar T, Shanta V: Intrathecal methotrexate toxicity. *J Assoc Physicians (India)*, 1989, 37, 351–353.
9. Martins A, Bartsch Ch, Gander H: Acute respiratory failure after intrathecal methotrexate administration. *Pediatr Hematol Oncol*, 1990, 7, 189–192.
10. Phillips P: Acute high-dose methotrexate neurotoxicity in the rat. *Ann Neurol*, 1986, 20, 583–589.
11. Poskitt K: Methotrexate leukoencephalopathy mimicking cerebral abscess on CT brain scan. *Childs Neurol Syst*, 1988, 4, 119–121.
12. Ramadan A, Badr W, Ali A: The effect of methotrexate on small intestine of the mouse. I A macroscopic study. *Folia Morphol*, 1988, 36, 68–78.

13. Robbins T: Toxicity, pathological effects and antineoplastic activity of non-toxic dose of 5-fluorouracil in combination with methotrexate. *Anticancer Res*, 1988, 8, 43–49.
14. Rubinstein L: Tumors of the central nervous system. Armed Forces Institute of Pathology, Washington, 1972.
15. Saiki J, Thompson S: Paraplegia following intrathecal chemotherapy. *Cancer*, 1972, 29, 70–74.
16. Shapiro W, Young D, Mehda B: Methotrexate distribution in cerebrospinal fluid after intravenous, ventricular and lumbar injection. *N Engl J Med*, 1975, 293, 161–166.
17. Silverstein F: A model of methotrexate encephalopathy: neurotransmitter and pathologic abnormalities. *J Child Neurol*, 1986, 1, 351–357.
18. von der Weid N, Crousaz H, Beck D, Denonna T, Miklossy J, Janzer R: Acute fatal myeloencephalopathy after combined intrathecal chemotherapy in a child with acute lymphoblastic leukemia. *Med Pediatr Oncol*, 1991, 19, 192–198.
19. Werner R: Paraplegia and quadriplegia after intrathecal chemotherapy. *Arch Phys Med Rehabil*, 1988, 69, 1054–1056.
20. Yim Y, Mahoney D, Oshman D: Hemiparesis and ischemic changes of the white matter after intrathecal therapy for children with acute lymphocytic leukemia. *Cancer*, 1991, 67, 2058–2061.
21. Young D, Posner J: Nervous system toxicity of the chemotherapeutic agents. In: *Handbook of clinical neurology*, vol 39, part II, P Vinken, G Bruyn (ed), North Holland Publishing Comp, Amsterdam, New York, Oxford, 1980.

Authors' address: Department of Neurology, Medical School, 1 Unii Lubelskiej St, 71–344 Szczecin, Poland

Zakład Narodowy im. Ossolińskich – Wydawnictwo. Wrocław 1993.
Objętość: ark. wyd. 10; druk 9; A,-12.
Wrocławska Drukarnia Naukowa. Zam. 63/93.

<http://rcin.org.pl>

CONTENTS

I. Hausmanowa-Petrusewicz: Role of electromyography in the diagnosis of motor neuron disorders	187
A. Fidziańska, H. Drac, Z. Glinka: Inclusion body myositis (IBM). Morphological study	199
R. Gadamski, M. J. Mossakowski: Asymmetric damage of the CA1 sector of Ammon's horn after short-term forebrain ischemia in Mongolian gerbils	209
R. Gadamski, H. Kroh: Immunoreactivity of astroglia in the hippocampus of the Mongolian gerbil during short survival following brief ischemia	221
E. Matyja, E. Kida: Hippocampal damage <i>in vitro</i> after different periods of oxygen deprivation	231
M. Dąbska, D. Maślińska, I. Kuchna: Astrogliosis in the temporal lobe of newborn infants who died in the perinatal period	245
J. Rafałowska, D. Dziewulska, S. Krajewski: The breakdown process of human brain infarction in middle-aged and senile cases	255
M. Ryba, M. Walski, K. Iwańska, K. Głowicki, M. Pastuszko: The possible role of endothelium in prevention of rebleeding in experimental subarachnoid hemorrhage (SAH)	263
A. Taraszewska, I. B. Zelman: Ultrastructural pattern of brain aging in normal rabbit and in pt mutant	271
M. Barcikowska, M. Kujawa, H. Wiśniewski: Beta-amyloid deposits within the cerebellum of persons older than 80 years of age	285
W. Split, J. Janusik, J. Alwasiak, W. Papierz, M. Barcikowska, P. P. Liberski: Creutzfeldt-Jakob disease with tubulovesicular structures: an ultrastructural study	295
M. Laure-Kamionowska, M. Dąbska: Damage of maturing brain in the course of toxoplasmic encephalitis	307
H. Kroh: Anaplastic temporal lobe ganglioglioma. Case report	315
P. Nowacki, D. Dolińska, K. Honczarenko, A. Potemkowski: Impairment of vertebral canal nervous structures after intrathecal prophylaxis in non-Hodgkin's lymphomas	325